Modeling the Adsorption of Weak Organic Acids on Goethite

The Ligand and Charge Distribution model

Promotor: prof. dr. W.H. Van Riemsdijk
hoogleraar in de bodemscheikunde en chemische bodemkwaliteit

Co-promotor: dr. ir. J.C.L. Meeussen
stafmedewerker van de afdeling water en milieu van Alterra bv

Samenstelling promotiecommissie:

dr. R.N.J. Comans	Energieonderzoek Centrum Nederland, Petten
prof. dr. P. van Cappellen	Universiteit Utrecht
dr. ir. L.K. Koopal	Wageningen Universiteit
prof. dr. D.L. Sparks	University of Delaware, USA
prof. dr. ir. S.E.A.T.M. van der Zee	Wageningen Universiteit

J.D. Filius

Modeling the Adsorption of Weak Organic Acids on Goethite
The Ligand and Charge Distribution model

Proefschrift

ter verkrijging van de graad van doctor
op gezag van de rector magnificus
van Wageningen Universiteit,
prof. dr. ir. L. Speelman,
in het openbaar te verdedigen
op maandag 1 oktober 2001
des namiddags te 16.00 uur in de Aula.

CIP-DATA KONINKLIJKE BIBLIOTHEEK, DEN HAAG

Filius, J.D.

Modeling the adsorption of weak organic acids on goethite. The ligand and charge distribution model. / Jeroen Filius - [S.l.:s.n.]

Thesis Wageningen University, The Netherlands. – With ref. – with summary in Dutch

ISBN 90-5808-454-x

Subject headings: adsorption / organic acids / goethite / transport / modeling

Printing: Grafisch bedrijf Ponsen & Looijen, Wageningen

Abstract

Filius, J.D., 2001. **Modeling the adsorption of weak organic acids on goethite. The ligand and charge distribution model.**

Doctoral thesis, Wageningen University, The Netherlands, 183 pages.

A detailed study is presented in which the CD-MUSIC modeling approach is used in a new modeling approach that can describe the binding of large organic molecules by metal (hydr)oxides taking the full speciation of the adsorbed molecule into account. Batch equilibration experiments were performed using the iron (hydr)oxide goethite to determine the adsorption of a series of weak organic acids (e.g. lactic acid, oxalic acid, malonic acid, phthalic acid, citric acid, and fulvic acid). In order to develop the new modeling approach, the binding of weak organic acids with a well-defined structure and charging behavior is first described using the classical CD-MUSIC model approach. The adsorption can be described accurately with a limited number of surface species, which differ in the degree of protonation and in the number of inner sphere and outer sphere complexes formed between the reactive groups of the organic molecule and the oxide surface. For the formation of inner and outer sphere complexes, a constant distribution of charge over the solid/water interface is assumed. With the same charge distribution for inner and outer sphere complexes, the adsorption of fulvic acid is described with the CD-MUSIC model using a small set of discrete surface species. This approach is not fully satisfactory since it does not take the full speciation of the adsorbed weak organic acids into account as can be inferred from spectroscopic data. In order to take the full possible speciation of the adsorbed organic molecule into account, a new model concept was developed. In the ligand and charge distribution (LCD) model concept, the number of inner sphere, outer sphere, and proton complexes of the reactive groups of one adsorbed organic molecule is calculated using the NICCA equation. From the resulting speciation of the adsorbed molecule, the main input parameters of the CD-MUSIC model are obtained. The new model concept is successfully tested on the adsorption and infrared data of benzenecarboxylic acid adsorption on goethite by Boily et al. (2000a,b). The LCD model was extended for the surface complexation of the phenolic groups in order to describe the previously determined data of fulvic acid adsorption by goethite. Simultaneously, the concentration, pH, and salt dependency of the fulvic acid adsorption are described well. Furthermore, the co-adsorption of protons upon the adsorption of fulvic acid by goethite is

predicted accurately. The developed model approach offers new insights in the fundamental understanding of ion adsorption under natural conditions.

Stellingen

1. A realistic representation of the surfaces of natural particulate matter requires a heterogeneous multisite model (Davis, 1982).

2. Wie het proton niet eert, begrijpt niet hoe een ion aan een natuurlijk oppervlak adsorbeert. (Dit proefschrift)

3. Iemand die zich niet laat leiden door de verwondering hoort niet thuis in het wetenschappelijk onderzoek.

4. Een goede wetenschapper vindt nooit wat hij of zij zoekt.

5. Wat ons begrenst, is de onbegrensdheid van de effecten van ons handelen. (Anders, 1987).

6. Na atleten, wielrenners, voetballers en zelfs korfballers hebben binnenkort de moderne wetenschappers doping nodig om optimaal te kunnen presteren.

7. Het plezier bij het bereiken van een doel is groter naarmate de weg er naar toe intenser is geweest.

8. Eenheid moet je ontdekken - eenheid mag je niet afdwingen.

Stellingen behorende bij het proefschrift:

"Modeling the adsorption of weak organic acids on goethite. The ligand and charge distribution model"

J.D. Filius, Wageningen, 1 oktober 2001.

Contents

1

General Introduction

1.1 Introduction

Organic matter in soils plays a very important role in determining soil quality, both from the point of view of soil fertility as well as of eco-toxicology. The bioavailability and transport of contaminants and nutrients is largely affected by the presence of natural organic matter (NOM). NOM strongly binds contaminants and cationic nutrients. When the organic matter is immobile (SOM; solid organic matter), it can retard the transport of the contaminants and nutrients significantly (Tipping *et al.*,1983; McKnight *et al.*, 1992; Boekhold *et al.*, 1993; Murphy *et al.*, 1994). Dissolved organic matter (DOM) enhances the mobility of heavy metals and xenobiotics because the DOM can act as a carrier to which the contaminants are bound. Therefore, the solubility of organic materials largely determines the migration behavior of contaminants.

The solubility of NOM is mainly determined by two processes; *e.g.*, coagulation and adsorption by reactive surfaces. Coagulation is the process in which colloidal particles come together and form a complex with a larger mass. In case the mass of the complex formed is too large, the complex is no longer stabile in solution and will precipitate. Furthermore, the DOM content in soil solutions is affected by the adsorption on metal(hydr)oxide surfaces. During adsorption, the organic matter is bound by the oxide surfaces due to chemical and/or electrostatic bonds.

Adsorption of organic matter by oxide surfaces not only affects the transport of DOM and bound contaminants and cationic nutrients, it also affects the availability of some anionic nutrients in soils. The adsorption of oxyanions like phosphate and sulfate is reduced due to the competition of organic matter for the same sites on the oxide surface. In soils, well-defined small organic acids may also be present because they may be released by plant roots and microorganisms. In the presence of these small organic acids, an increase in the mobilization of phosphate has been observed for soils with a high content of Fe and Al (hydr)oxides on which phosphate was sorbed (Earl *et al.*, 1979; Hue, 1991; Gerke, 1992).

In order to give an accurate prediction of the bioavailability and migration of contaminants and nutrients through the soil, it is important to gain more quantitative insight into the solubility and speciation of the organic materials in soils. For such an important challenge, a fundamental understanding of the adsorption behavior of organic matter by oxide surfaces is required before significant progress can be made.

The adsorption of NOM by oxide surfaces is a complicated process for several reasons. 1) The oxide surface and the NOM molecules both have a charge that is dependent on pH and ionic composition of the soil solution; 2) NOM molecules are compared to simple electrolyte ions relatively large molecules of which the charge is not located in one point but is distributed over the whole molecule; 3) the NOM is a mixture of molecules with a varying number of reactive groups. Figure 1.1 shows schematically the sorption reaction of a relatively simple NOM molecule by an oxide surface.

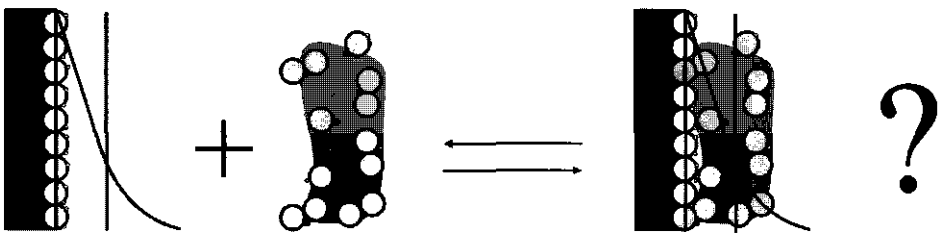

Fig. 1.1 The problem

In the figure, the circles represent oxygen atoms, the black dots represent the carbon atoms, and the very small blank dots represent the hydrogen atoms. From the figure, it becomes clear that the adsorption of NOM by an oxide surface is a very complicated process. The oxygen groups of the oxide surface and the organic molecule can bind protons. The degree of protonation of the reactive oxygen groups determines the electrical charge of the oxide surface and of the organic molecule. Note that the charge of the oxide surface is located in a plane, whereas the charge of the organic molecules is distributed in space. The charge of the oxide surface causes an electrostatic potential profile near the surface. In figure 1.1, this is indicated by the decreasing line near the oxide surface. As the potential decreases with increasing distance from the surface, the location of the charge of the bound organic molecules with respect to the surface determines the strength of the electrostatic interactions between the surface and the organic molecule.

The right hand side of figure 1.1 shows a possible configuration of a weak organic acid molecule adsorbed by an oxide surface. Some of the reactive groups are orientated towards the surface, whereas others are more orientated towards solution. The surface-orientated groups may have a strong interaction with the surface due to chemical interactions. For the solution-orientated groups it is impossible to have any chemical interactions with the

reactive surface groups. However, as in solution, these groups may have interactions with protons. Due to the specific interactions of the surface orientated groups and the protonation of the solution-orientated groups, there is a very wide range of possible configurations of the adsorbed organic molecules. The number of possible configurations of an adsorbed organic molecule can be calculated according to: $(x)^n$, in which x is the number of modes that the reactive groups of the organic molecule can form, and n is the number of reactive groups per molecule. When we assume that the reactive groups of the organic molecule that is depicted in figure 1.1 can be bound by the reactive surface groups, can become protonated, and can remain deprotonated, the number of possible configurations is given by $(3)^8$. A simple organic molecule as depicted in figure 1.1 can already form > 5000 possible configurations.

The aim of this thesis is to develop a modeling approach that includes the adsorption of organic molecules in speciation calculations. The adsorption of several organic molecules, varying in size and number of reactive groups, by one particular iron (hydr)oxide, *e.g.* goethite, is studied and described with surface complexation models. In this introduction we give a short overview of the basic characteristics of goethite and organic matter found under natural conditions. Further, the approach and outline of the present research is given.

1.2 Metal (hydr)oxide surfaces

Iron (hydr)oxides are the most abundant metal (hydr)oxides present in soil systems. The crystalline iron (hydr)oxide goethite is chosen as a model substance for a detailed study on the chemical interactions between organic molecules and the goethite surface.

The goethite surface that is depicted in figure 1.1 shows a large number of surface oxygen groups (oxygen, hydroxyl, and water groups). Those oxygen groups differ in the number of bonds with the underlying Fe^{3+} ions in the goethite crystal. A distinct amount of charge of the Fe^{3+} ion is attributed to the surface oxygen groups. According to the Pauling bond valence rule (Pauling, 1929), the Fe^{3+} ion in hexa-coordination with oxygens (as is found in the bulk of the goethite crystal) attributes half a unit charge to the surface oxygen groups per Fe-O bond. As the surface oxygens are singly, doubly, or triply coordinated to the Fe^{3+} ion the surface oxygen groups are of the type $FeOH^{0.5-}$, Fe_2OH^0, $Fe_3O^{0.5-}$ respectively. The charge of the $FeOH^{0.5-}$ and $Fe_3O^{0.5-}$ groups can become reversed by the adsorption of a proton. The proton affinities of the various types of groups differ.

The protonation of the reactive oxygens is strongly dependent on pH and ionic strength. At high pH, the bound protons on average don't fully compensate the negative charge of the reactive oxygen groups. Therefore, the goethite surface is negatively charged at high pH. At low pH, the charge of the bound protons overcompensates on average the charge of the reactive oxygen groups. So, at low pH, the surface is positively charged. The pH at which the net charge of the surface is zero in the absence of chemically bound ions other than OH^- and H^+ is called the pristine point of zero charge (ppzc).

The net charge of the surface (charge of the oxygen groups plus the adsorbed protons) at either side of the ppzc is neutralized by accumulation and depletion of electrolyte ions in the diffuse double layer (ddl). The electrolyte ions approach the surface to a distance approximately equal to the size of a water molecule. Stern (1924) accounted for the distance of closest approach by introducing a layer that is free of charge in an indifferent electrolyte solution. This layer is called the Stern layer.

1.3 Natural organic matter (NOM)

Natural organic matter consists of a mixture of molecules with an ill-defined structure. The reactivity of the functional groups present in these molecules depends on their type and their environment in the organic molecule. The bulk of the reactive groups in these molecules are carboxyl (R-COOH) and hydroxyl groups (R-COH). However, nitrogen or sulfur containing groups are also found to be present in the ill-defined organic molecules. As a result, the exact structures of these humic substances are not known, and the molecules can be considered as heterogeneous ligands.

The NOM mixture can be divided into three fractions on the basis of their solubility. Humic acid (HA) is soluble at pH 7, but is precipitated at low pH (pH 1), fulvic acid (FA) is soluble over the entire pH range, whereas humine remains insoluble. Here, we will focus on the soluble fractions of the natural organic matter (NOM); HA and FA. Figure 1.2 shows some characteristics of these larger organic molecules.

The molecular weight of most fulvic acids ranges from 500-1500 g/mol. Humic acids are larger and have a molecular weight of 1500 up to $>10^5$ g/mol. Note that for polydisperse materials like natural organic matter it is only possible to determine average weight values. The very high molecular weights are probably not due to single HA molecules but due to aggregates, which can easily form.

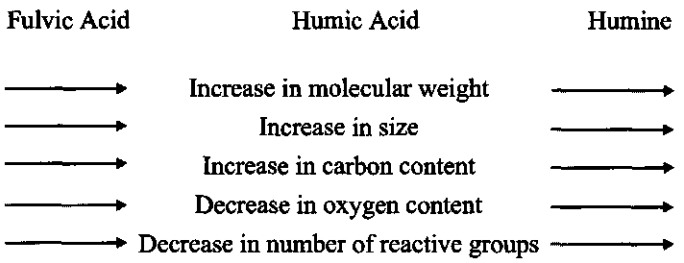

Fig. 1.2 Chemical properties of different NOM fractions. Adapted from Stevenson (1984).

Elemental analyses of FA and HA shows a higher C- and N-content for HA molecules, whereas the O-content of HA is lower than for FA. The higher O/C ratio for FA indicates that FA molecules contain more reactive groups per gram carbon than HA. Therefore FA can exhibit a higher charge density than HA. The charging behavior and metal binding properties of FA and HA can be determined from proton and metal ion titration experiments. The proton and metal binding by humic substances is discussed intensively in literature (Ephraim *et al.*, 1986; Benedetti *et al.*, 1995; Christensen *et al.*, 1998; Kinniburgh *et al.*, 1999).

Compared to simple electrolyte ions or oxyanions, FA and HA are relatively large. The shape of the molecules is poorly known. A commonly proposed shape for the larger humic materials is the random coil structure. A random coil flexes and winds randomly. This results in a molecule that is roughly enclosed by a sphere. The size and shape of the sphere is affected by the negative electrostatic charge of the molecules and therefore dependent on pH and ionic strength. Under neutral or alkaline conditions, the charged reactive groups of the organic molecules will repel each other. Therefore, the molecule will have an expanded configuration. In case the charge of the reactive groups is neutralized by the complexation of protons or metal ions, the reactive groups no longer repel each other and the organic molecules will have a more condensed configuration.

Fulvic acids are considerably smaller than humic acid. Swelling and shrinking of the FA molecules is therefore limited. Lead *et al.* (2000) suggested, based on fluorescence correlation spectroscopy, that the hydrodynamic diameters for Suwannee River Fulvic Acid (SRFA) and Suwannee River Humic Acid (standard FA and HA of the International Humic Substances Society) are 1.5 and 1.7 nm respectively. Note that the value found for SRFA is in

close agreement with the suggested diameter of de Wit *et al.* (1993a) based on the optimum values for the spherical double layer model.

1.4 Modeling the adsorption of organic acids by goethite

Modeling the adsorption of natural organic matter by oxide surfaces is a major challenge. To date, only a few attempts have been made to include organic matter in speciation calculations (Karltun, 1998; Evanko and Dzombak, 1999; Vermeer *et al.*, 1998). Note that all these studies were published in the period of this thesis work.

A chemically and physically realistic surface complexation model takes the following factors into account:

- pH and ionic strength of the solution, the total concentration of the aqueous ion of interest, and the solid-solution ratio.
- The speciation of the organic ion in solution and possible changes in the speciation during adsorption
- The intrinsic nature of the surface, *e.g.* the surface charge as a function of pH, the ddl properties, and the number and nature of reactive surface sites.
- The type of complexes formed between the organic ion and the reactive groups of the goethite surface.
- The effects of other ions in solution that may form solution complexes with the organic ion that can adsorb.
- The competitive and cooperative adsorption of ions for the same reactive sites on the goethite surface.

Note that the effects of the presence of oxyanions and metal ions during the adsorption of organic molecules are outside the scope of this thesis. However, a prerequisite for a new model approach is that it can be extended easily for the description of the adsorption of organic molecules under more complex conditions as can be found in nature.

1.4.1 CD-MUSIC model

A wide variety of thermodynamic models describing the adsorption of ions by oxide surfaces has been developed, all based on the pioneering work of Gouy, Chapman, Stern

Stumm, Schindler, Posner, Quirk, Yates, Grahame, Parks, de Bruyn, Davis and Leckie. Most of these models assume that the adsorbing ion can be treated as point charges. Figure 1.1 shows a possible configuration of an adsorbed organic molecule. From this figure, we concluded that the charge of the organic molecule cannot be considered to be a point charge. A charge distribution over the solid/water interface has to be applied in order to be able to model the binding of organic molecules in a chemically and physically realistic way. The CD-MUSIC model of Hiemstra and Van Riemsdijk (1996) is the only thermodynamic surface complexation model that accounts for a distribution of the charge of an adsorbed molecule over several electrostatic planes. The model uses the surface structure, the structure of the adsorbed complexes, and the structure of the electrostatic profile near the surface as the basis for the description of ion adsorption by oxide surfaces. The CD-MUSIC model is based on the one-pK approach in which the protonation of the different oxygen surface groups is described by a single protonation reaction. The difference in reactivity of the various oxygen groups present on the goethite surface is taken into account in the model. The CD-MUSIC model is taken as a staring point to develop models for the description of the binding of organic molecules by oxide surfaces as studied in this thesis.

1.4.2 NICCA-Donnan model

For small, well-defined weak organic acids (*e.g.*, lactic acid, oxalic acid, citric acid, etc.), the speciation in solution is commonly described with discrete ion binding reactions. However, both electrostatics and chemical heterogeneity affect the binding of protons and metal ions by larger, ill-defined weak organic molecules with much more reactive groups. Several studies have shown that protonation and metal binding by these large molecules can only be described using a distribution of affinity constants. The NICCA-Donnan model is a site-binding model that takes heterogeneity, competition, and electrostatics into account explicitly using an intrinsic affinity distribution. In this thesis, the NICCA-Donnan model is used to describe the charging behavior of large, ill-defined weak organic acids in solution.

1.4.3 Charge distribution

In the CD-MUSIC approach, the distribution of the charge of the organic molecule over the solid/water interface is one of the most prominent features. Rietra *et al.* (1999)

showed that the charge distribution is directly related to the pH dependency of the ion binding. As for organic molecules, the charge is associated with the reactive groups of the organic molecules, the spatial distribution of the reactive groups becomes important. In this thesis, we distinguish between groups that coordinate with reactive surface groups and non-coordinated groups that are orientated towards solution. The reactive groups that bind to the surface can form inner and outer sphere complexes. Depending on the type of complex formed, the coordinated reactive groups distribute their charge over the interface.

The charge distribution of the individual reactive group involved in the two types of complex formation can best be studied using small, well-defined weak organic acids with a known configuration of the adsorbed molecule. For example, oxalic and phthalic acid contain just two carboxylic groups. Citric acid contains three carboxylic groups and one hydroxyl group. The affinity of those acids to take up protons is explicitly known. Due to the relatively small number of reactive groups of the well-defined acids, the number of possible surface configurations is limited. Furthermore, for some small acids, the configuration of the adsorbed molecules is studied using infrared (IR) spectroscopy (Cornell and Schindler, 1980; Yost *et al.*, 1990; Tejedor-Tejedor *et al.*, 1992; Boily *et al.*, 2000a,b). When the configuration of the adsorbed molecule is fixed, the charge distribution of the individual reactive groups that coordinate with reactive surface groups can be fitted. The relative presence of the inner and outer sphere complexes and their specific charge distribution determine the pH dependency of the binding. Therefore, we will study the adsorption of well-defined weak organic acids in order to find the charge distribution of the inner and outer sphere complexes.

1.4.4 Surface speciation

A physically and chemically realistic model accounts for the full speciation (or configuration) of the adsorbed organic molecules. This speciation is strongly dependent on pH, ionic strength, and surface loading. As stated before, the organic molecule depicted in figure 1.1 can be present in more than 5000 different surface species (configurations) and is therefore unmanageable for speciation calculation. In order to establish the coordination modes of weak organic acids bound by oxide surfaces, *in situ* IR spectroscopy has recently been used (Tejedor-Tejedor *et al.*, 1992; Boily *et al.*, 2000a,b). However, IR spectroscopy yields information about the local environment of the individual groups of the organic acid rather than about the adsorption configuration of the complete organic molecule. Note that IR

spectroscopy can at best supply statistical information about the fraction of organic groups that forms a certain type of complex (inner sphere, outer sphere, or protonation).

The model developed in this thesis calculates the speciation of the organic molecules (both in solution and adsorbed by the surface) using a more statistical approach. The speciation of the organic molecules is calculated using a continuous distribution of affinity constants for the protonation and surface complexation reactions of the reactive organic groups. For this purpose, the NICCA equation is applied. The distribution of the organic molecules over the solution and the surface is calculated using the CD-MUSIC model. Note that this more statistical approach corresponds very well with the type of information obtained from IR spectroscopy.

1.5 This thesis

In this thesis, the larger ill-defined organic molecules are represented by the FA fraction of the NOM. The use of FA has the advantage that the variation in molecular weight of the molecules is relatively small. Therefore, it can be assumed that the FA consists of one type of molecules with an average molecular weight. The number of reactive groups in a FA molecule is small enough to describe the charging behavior of FA in the classical discrete way. However, the number of reactive groups is also large enough to describe the charging of the FA molecules with a continuous affinity distribution type of modeling approach.

During the period of the thesis research, a lot of work was published on the binding of organic matter by oxide surfaces. Moreover, also insight in the relation between ion binding and modeling with the CD-MUSIC model and NICCA model increased in the period the thesis was written (see also the year of publication of cited references). Due to the exploratory nature of the model development and the new results published in literature, the assumptions made in the different chapters are not always consistent. Most alternative assumptions were used to simplify the model approach as they were seen to fit at the particular stage in the investigation.

1.6 Outline

The adsorption of small well-defined weak organic acids by goethite is studied in chapter 2. The aim of this chapter is to find trends in the adsorption behavior of individual

carboxylic groups of the acids. We will focus on the charge distribution of the individual reactive groups of the organic molecule over the solid water interface. This charge distribution is very important for the description of the pH dependence of the adsorption (Rietra *et al.*, 2000). The charge distribution of individual groups can be obtained from an accurate description of the adsorption of organic molecules with a limited number of reactive groups

In chapter 3, the transport of malonate in a silica-goethite system is studied. The chapter forms an intermezzo in which the modeling efforts from chapter 2 are applied to transport phenomena.

After this intermezzo, the thesis continues in chapter 4 with the modeling of FA adsorption by goethite. The insights obtained from the discrete modeling approach for the adsorption of the small weak organic acids by goethite (chapter 2) are applied to describe the binding of larger, less well-defined organic molecules, in this case fulvic acid.

In chapters 5 and 6, the large number of possible configurations of the adsorbed organic molecules is taken into account using a more statistical approach. In chapter 5, the ligand and charge distribution (LCD) model approach is developed for the adsorption of well-defined weak organic acids. In chapter 6, the LCD model is extended and applied to the FA adsorption data presented in chapter 4. The new model approach is used to predict the co-adsorption of protons at very low FA adsorption levels.

2

Adsorption of small weak organic acids on goethite: Modeling of mechanisms

Abstract— The adsorption of lactate, oxalate, malonate, phthalate, and citrate have been determined experimentally as function of concentration, pH, and ionic strength. The data have been described with the CD-MUSIC model of Hiemstra and Van Riemsdijk (1996) which allows a distribution of charge of the organic molecule over the surface and the Stern layer. Simultaneously, the concentration, pH, and salt dependency as well as the basic charging behavior of goethite could be described well. On the basis of model calculations, a distinction is made between inner and outer sphere complexation of weak organic acids by goethite. The results indicate that the affinity of the organic acids is dominated by the electrostatic attraction. The intrinsic affinity constants for the exchange reaction of surface water groups and organic acids, expressed per bond, increases with increasing number of reactive groups on the organic molecule. Ion pair formation between non-coordinated carboxylic groups of adsorbed organic acids and cations of the background electrolyte proved to be important for the salt dependency. The knowledge obtained may contribute to the interpretation of the binding of larger organic acids like fulvic and humic acids.

Jeroen D. Filius, Tjisse Hiemstra, and Willem H. van Riemsdijk
Journal of Colloid and Interface Science **195**, (1997), 368-380

2.1 Introduction

The interaction of natural organic acids with mineral surfaces is an important phenomenon in environmental systems and is studied extensively over the last two decades (Parfitt *et al.*, 1977c; Tipping, 1981; Gu *et al.*, 1994; Leenheer *et al.*, 1995a and 1995b). Natural organic matter consists of a mixture of well- and ill-defined organic acids. The structure and chemical behavior of the ill-defined organic acids are very complex. The functional groups of ill-defined large organic molecules (carboxylic and phenolic groups) can also be found in smaller, well-defined organic acids. Recently, several studies were done with small organic acids with better-known structure and chemical behavior (Kummert and Stumm, 1980; Bowden *et al.*, 1980; Zhang *et al.*, 1984; Balistrieri and Murray, 1986; Mesuere and Fish, 1992; Ali and Dzombak, 1996). It was found that there are important similarities in sorption mechanisms of humic substances and simple weak organic acids (Gu *et al.*, 1994). The results suggest that by studying well-defined weak organic acids a better understanding of the interactions of ill-defined organic acids with mineral surfaces can be gained. The knowledge obtained may also be of importance in understanding the effects of organic acid binding on the dissolution kinetics of metal(hydr)oxides and the change in geochemical processes, colloidal stability, and the sorption characteristics of silicate, iron and aluminum oxide surfaces (Tipping and Cooke, 1980; Zinder *et al.*, 1986; Benett *et al.*, 1988).

This study focuses on the binding of well-defined weak organic acids by goethite. Detailed molecular information about the adsorption mechanisms of weak organic acids has become available from conventional infrared spectroscopy (IR) (Parfitt *et al.*, 1977a,b and c) and recently from *in situ* Fourier transform infrared spectroscopy (*in situ* FTIR) studies (Tejedor-Tejedor *et al.*, 1992; Yost *et al.*, 1990; Biber and Stumm, 1994).

Ions can be bound by mineral surfaces by different mechanisms. Often, a distinction is made between so-called inner sphere complexes (the ligand is coordinated to the metal atom of the surface) and outer sphere complexes (the ligands weakly interact with surface groups without formation of common ligands). The difference between inner and outer sphere complexation is illustrated in figure 2.1. It is widely believed that organic acids can form inner spheres complexes (figure 2.1a) with the goethite surface via ligand exchange (Parfitt *et al.*, 1977a and 1977b; Sigg and Stumm, 1980; Ali and Dzombak, 1996). However, some FTIR and

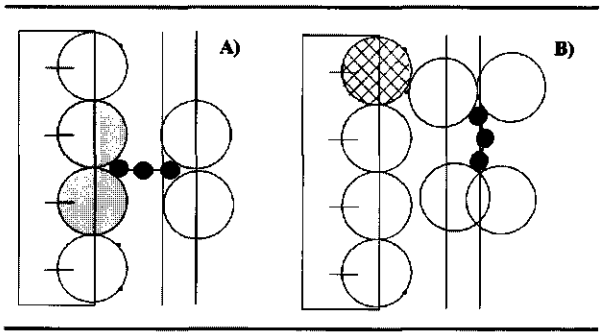

Fig. 2.1: Illustration of the differences between inner and outer sphere complex formation, using malonate as example. Inner sphere complexes are in general characterized by direct coordination of one or more oxygen atoms to the surface metal ion. In figure 2.1a these oxygens are indicated by shading. The other oxygens of the malonate are not located in the metal oxide surface. Outer sphere complexes are characterized by interaction of the organic anion with surface water or hydroxyl groups without the formation of common ligands, *i.e.* no oxygen atoms of the anion will be present in the surface layer (figure 2.1b). The charge of the organic acid is divided over the three electrostatic planes.

adsorption modeling points to the formation of outer sphere complexes (Mesuere and Fish, 1992; Nilsson *et al.*, 1996).

The position of adsorbed organic molecules in the mineral-water interface (figure 2.1) illustrates that the charges of the adsorbed molecules are spatially distributed (*i.e.*, the charge is distributed over more than one electrostatic plane). This concept of charge distribution (CD) has recently been formulated in the multi site complexation (MUSIC) model (Hiemstra and Van Riemsdijk, 1996).

The aim of this study is to interpret the binding of weak organic acids on the basis of the CD-MUSIC model concept. The organic acids used in this study are lactic acid, oxalic acid, malonic acid, phthalic acid, and citric acid (see table 2.1). The modeling results will be related to IR spectroscopy data from literature as much as possible. Figure 2.2 shows schematically the binding structures of the organic acid as proposed in literature. The IR spectra of lactic, oxalic, and citric acid have been measured with conventional methods (Parfitt *et al.*, 1977a,b and c; Cornell and Schindler, 1980), whereas the data for phthalic acid come from *in situ* FTIR studies (Tejedor-Tejedor *et al.*, 1992; Gu *et al.*, 1994; Nilsson *et al*,

1996). Most IR spectroscopy data suggest that organic acid binding is due to formation of inner sphere complexes.

Table 2.1

Structures, protonation constants and Na^+ pair formation constants of various organic anions in order of the number of reactive groups[a].

Organic acid	Abbrev	Structure	log $K_{H,1}$	Log $K_{H,2}$	log $K_{H,3}$	log K_{Na}
Lactic acid	LactH	H_3C-CHOH-COOH	3.86			
Oxalic acid	Ox	HOOC-COOH	4.27	1.25		
Malonic acid	Mal	HOOC-CH_2-COOH	5.70	2.85		0.74
Phthalic acid	Phth	HOOC-C_6H_4-COOH	5.40	3.14		0.70
Citric acid	CitH	HOOC-CH_2-COH(COOH)-CH_2-COOH	6.40	4.80	3.10	0.70[b]

[a] Data are from Martell and Smith (1977).

[b] T = 25°C, I = 0.1 M

2.2 Model description

Various models have been used to describe the adsorption of organic ions on mineral surfaces (Kummert and Stumm, 1980; Balistrieri and Murray, 1987; Lovgren, 1991; Mesuere and Fish, 1992). In general these models comprise several formation reactions of surface species in combination with an electrostatic model accounting for the influence of surface charge. A proper model should describe simultaneously a series of related phenomena. Not only should the basic charge of the mineral surface and the concentration, pH, and salt dependency of a particular ion be described, the description should also be in line with surface structural information gained from spectroscopy and the fact that only a part of the organic molecule is incorporated in the surface structure (*i.e.*, the ion is not treated as a point charge). In addition, it also should be constrained by the given chemical composition of the mineral structure. At present, the CD-MUSIC model seems most promising because it emphasizes the importance of the surface structure and of the charge distribution at the interface. We therefore use the CD-MUSIC model in this study to describe the organic anion adsorption. A short description of important characteristics will be given.

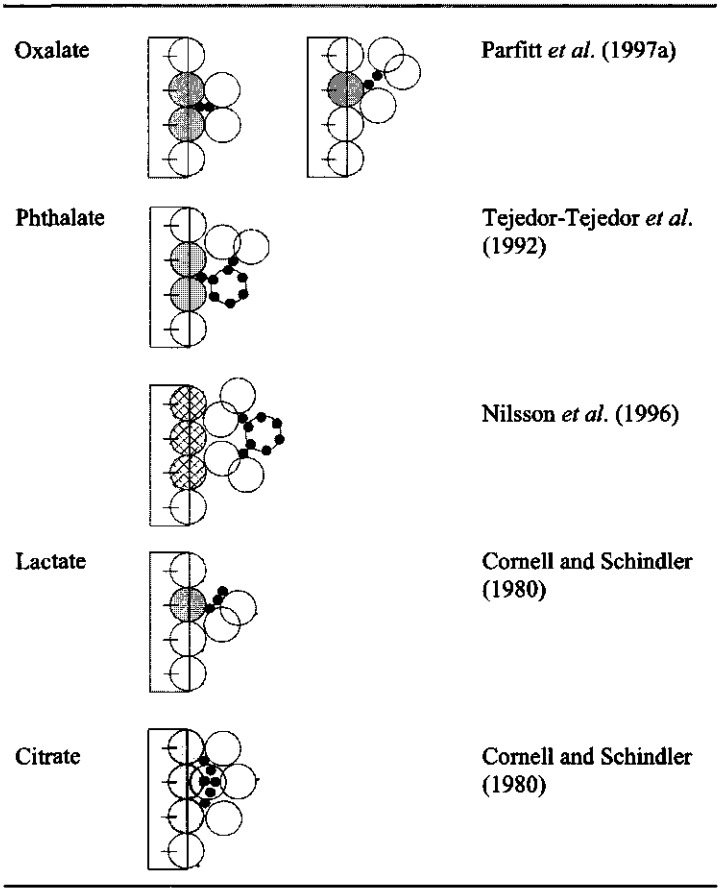

Fig. 2.2: Schematic surface structures of bound organic anions as proposed in literature. All structures are inner sphere structures except the phthalate structures of Nilsson *et al.* (1996).

The chemical composition of the goethite surface is based on the morphology and crystallographic structure of goethite. The dominant crystal face in our goethite preparation is the 110 face (Venema et al, 1996; Hiemstra and Van Riemsdijk, 1996). The 021 face is found on the head ends of the needle-shaped crystals. There are singly, doubly, and triply coordinated surface groups, meaning that the surface oxygens are bound to respectively one, two, or three Fe^{3+} ions in the goethite.

The principle of electroneutrality implies that in the bulk mineral structure the charge of the Fe^{3+} ion is compensated by the charge of the surrounding oxygens. An equal distribution of charge of the Fe^{3+} ion over the six surrounding oxygens yields $+^1/_2$ valence

units (vu) per bond. Pauling (1929) introduced this concept. The charge of an oxygen ion is -2 vu. Depending on the number of bonds with Fe^{3+} ions, the oxygens in the surface are charged differently. The charge of the singly coordinated surface oxygens is $-2 + {}^{1}/_{2} = -1{}^{1}/_{2}$ vu. In the pH range of interest, these surface oxygens are protonated by at least one proton, *i.e.* the charge is $-2 + {}^{1}/_{2} + 1 = -{}^{1}/_{2}$ vu ($FeOH^{-0.5}$). On the basis of the proton affinity of this surface site, it can be shown that the hydroxyl groups can react with an additional proton forming a singly coordinated water group with a charge of $+{}^{1}/_{2}$ vu. The doubly coordinated oxygens have a charge of –1 vu. These groups bind only one proton over a wide pH range of 2 to 12 (Fe_2OH^0) and are then uncharged, *i.e.*, the groups are considered to be not reactive for protons within this pH range (Hiemstra *et al*, 1996). The triply coordinated surface oxygens have a charge of $-{}^{1}/_{2}$ vu ($Fe_3O^{-0.5}$), and it has been argued that a nett amount of only one-third of the triply coordinated surface groups is reactive for protons (Hiemstra and Van Riemsdijk, 1996; Hiemstra *et al.*, 1996). On the basis of the relative presence of the 110 and 021 faces, the site density of singly and triply coordinated surface groups is estimated to be 3.45 and 2.7 sites/nm^2 respectively.

On the basis of the analysis above, the charging of the goethite particles can be described with the protonation reactions of singly and triply coordinated groups according to:

$$-FeOH^{0.5-} + H^{+} \Leftrightarrow -FeOH_2^{0.5+}; \qquad \log K_{H1}, \qquad [2.1]$$

$$-Fe_3O^{0.5-} + H^{+} \Leftrightarrow -Fe_3OH^{0.5+}; \qquad \log K_{H2}. \qquad [2.2]$$

The proton affinity constants were recently evaluated on the basis of the undersaturation of the surface oxygen (Hiemstra *et al.*, 1996), indicating some differences between both affinity constants. However, in this paper we will follow the simplifications of Hiemstra and Van Riemsdijk (1996), in which the logarithm of both affinity constants are set equal to the priston point of zero charge (ppzc) of the goethite.

The primary charging behavior of the goethite can be described assuming, in addition, ion pair formation located at the head end of the diffuse double layer (ddl) and assuming a charge-free Stern layer between the surface and the head end of the ddl. The Stern layer has a capacitance that is found by fitting the model to the charging curves of the goethite.

The starting point in modeling is the reaction equation describing the binding of the organic acid by the surface. The basic reaction equation for the formation of an outer sphere complex is:

$$-FeOH^{0.5-} + nH^{+} + L^{m-} \Leftrightarrow -FeOH_{(1+n)}L^{(0.5-n+m)-} \quad [2.3a]$$

in which n is 0 or 1 and m is the charge of the completely deprotonated organic anion. The overall charge of the adsorbed complex ((0.5-n+m)-) can be distributed over the three electrostatic planes taken into account in the CD-MUSIC model (see figure 2.1).

In the CD approach, the charge of the proton is fully attributed to the surface oxygen, although H bonds may transfer charge between for instance the oxygens of the surface and water molecules in solution (Hiemstra *et al.*, 1996). This simplification is allowed as long as the strength of the H bonds is not changed in the adsorption process. According to Brown (1978), the H bond involved in organic complexes can be stronger than the H bond between water molecules. In that case, it implies that extra charge is transferred from the surface to the 1-plane due to a stronger H bond between the organic molecule and the surface water or hydroxyl group. In the present study, we therefore allow the transfer of proton charge between the surface and the 1-plane in case of organic outer sphere complexation. Furthermore, it is assumed that outer sphere complexes will only be formed with singly coordinated $FeOH_2^{+0.5}$ groups.

Besides outer sphere complexes, also inner sphere complexes may form. Inner sphere complexes are formed via ligand exchange with one or more singly coordinated reactive groups (see figure 2.1). The reaction equation can be formulated as:

$$n\,(-FeOH^{0.5-}) + n\,H^{+} + L^{m-} \Leftrightarrow -Fe_nL^{(m+0.5n)-} + n\,H_2O \quad [2.3b]$$

Note that there is no difference between equation [2.3a] and equation [2.3b] in a thermodynamic sense if n = 1 at a constant activity of water. The activity of the surface groups is set equal to their mole fraction as has been done by Hiemstra and Van Riemsdijk (1996).

The distinction between inner sphere or outer sphere complex formation follows from the interpretation of the differences in the location of charge. If the charge of a carboxylate group (COO^{-1}) is equally distributed over both carboxylate oxygens, then each oxygen carries half a unit charge. In case of inner sphere complex formation, the oxygen is placed in the surface. There it is neutralized by the Pauling charge of a Fe-O bond (+0.5 vu). In this case, the charge is fully neutralized and equally distributed over the ligands, which is favorable for adsorption. The total change in charge of the surface plane can be calculated on the basis of

the number of common oxygens, each contributing -0.5 vu, and the number of protons that react with the surface hydroxyl to form the water that is subsequently released.

The model calculations were carried out with the computer program ECOSAT (Keizer and Van Riemsdijk, 1995).

2.3 Materials and Methods

2.3.1 Preparation of goethite

Goethite batches were prepared by titrating 5 L of 0.5 M $Fe(NO_3)_3 \cdot 9\ H_2O$ with 2.5 M NaOH, at a rate of 9 mL/min, to a pH of 12. The suspension was aged for 4 days at 60°C and subsequently dialyzed with distilled demineralized (DD) water (Hiemstra *et al.*, 1989b). The specific surface areas of the goethite batches used were determined by BET_N_2 adsorption and are listed in table 2.2.

Table 2.2

Pristine Point of Zero Charge and the specific surface Area of the goethite batches used.

Goethite	I	II	III
PPZC	9.3	9.2	9.3
A (m^2/g)	96.8	88.9	117

The ppzcs of the goethite batches (table 2.2) were determined from the intersection points of the charging curves, obtained with potentiometric titrations of goethite at three different ionic strengths (Venema *et al.*, 1996).

2.3.2 Adsorption experiments

Adsorption was determined in batch experiments. The added amounts of organic acid solution and goethite suspension and the total volume of the batch were determined by weighing. The extent of adsorption was calculated from the difference of the initial and final concentration of organic acid after equilibration. All solutions used were made with DD water. The chemicals used were of the grade p.a.

The adsorption envelopes of the different organic acids were determined in the same experimental setup. The adsorption envelopes were determined in a pH range from 3 to 7.5. Small volumes of 0.01 M organic acid were added to goethite suspensions (12 g/L) in 0.1 or 0.01 M $NaNO_3$. Differences in pH were obtained by adding small volumes of 0.1 M NaOH or 0.1 M HNO_3. After shaking in an end-over-end shaker for at least 24 hours, the samples were centrifuged at 22,000 *g* and the pH of the supernatant was measured. The organic acid concentration in the supernatant was measured with a total organic carbon (TOC) analyzer after the supernatant was acidified.

For citric acid, adsorption isotherms were determined at pH 4, 7, and 9. Small volumes of citric acid were added to goethite suspensions in 0.1 M $NaNO_3$. The suspensions were adjusted to the required pH by adding small doses of NaOH or HNO_3. After being left for 8 hours, the pH of the samples was readjusted. Total citrate in solution was determined enzymatically (Boehringer Mannheim). Nicotinamide adenine dinucliotide (NADH) spectra were measured spectrophotometrically at 340 nm. From the difference in NADH concentration between sample and blank, the amount of citrate in solution could be calculated.

No evidence for microbiological degradation was found in the blanks.

2.4 Results

2.4.1 Effect of pH

Figure 2.3 shows the adsorption envelopes of lactic, oxalic, malonic, phthalic, and citric acid. The adsorption envelopes of all the acids were investigated in goethite suspension of 12 g/l in 0.1 or 0.01 M $NaNO_3$, and two different initial organic acid concentrations (0.2 and 2 mM). Striking is the low adsorption of lactic acid compared to the other organic acids. This was also found by Balistrieri and Murray (1986) who investigated the binding of several weak organic acids by goethite in seawater.

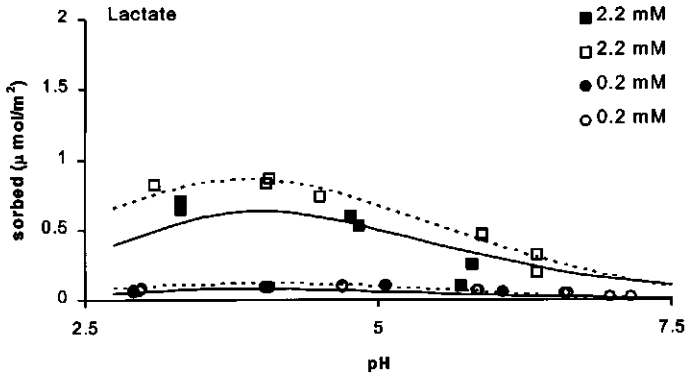
Lactate
2.2 mM
2.2 mM
0.2 mM
0.2 mM
sorbed (µ mol/m²)
2
1.5
1
0.5
0
2.5
5
7.5
pH

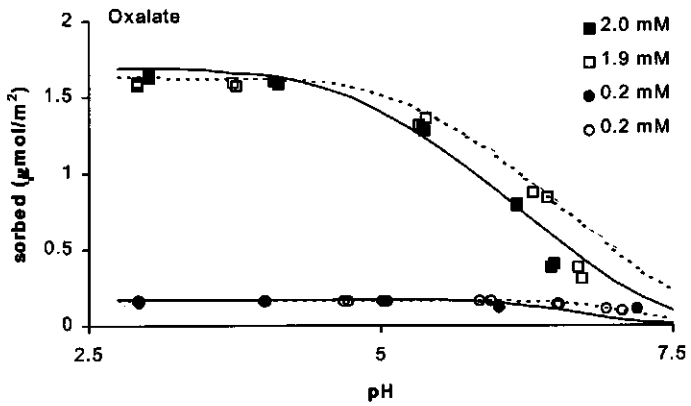
Oxalate
2.0 mM
1.9 mM
0.2 mM
0.2 mM
sorbed (µmol/m²)
2
1.5
1
0.5
0
2.5
5
7.5
pH

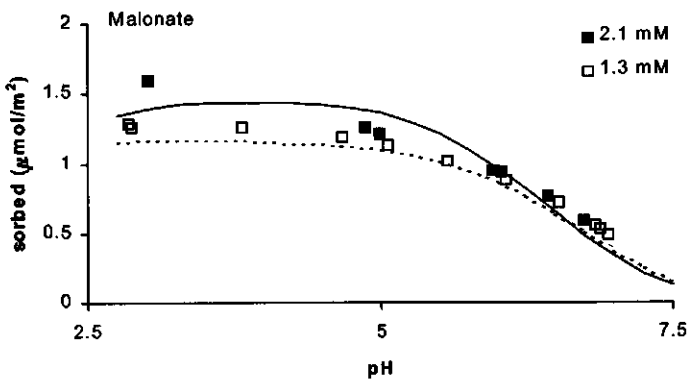
Malonate
2.1 mM
1.3 mM
sorbed (µmol/m²)
2
1.5
1
0.5
0
2.5
5
7.5
pH

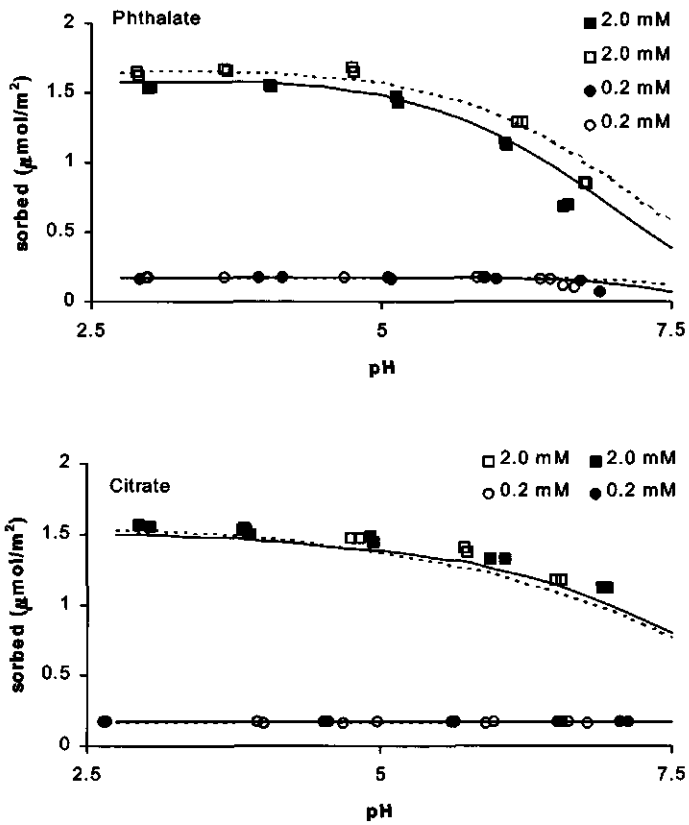

Fig. 2.3 Adsorption envelopes of lactate, oxalate, malonate, phthalate, and citrate determined in 0.01 M (open symbols and dotted lines) and 0.1 M $NaNO_3$ (solid symbols and solid lines) at a goethite suspension density of 12 g/L (goethite II for malonate; rest goethite I).

At pH values above the PPZC of goethite, both the charge of the goethite surface and the charge of the organic acid are negative. At these pH values, extrapolation of the data in figure 2.3 suggest that there is no interaction between the goethite surface and organic anions, which indicates that the chemical affinity of organic anions for the goethite surface is relatively small. At pH values just below the PPZC (surface and organic anion are now oppositely charged), only little interaction between the organic anions and the surface can be observed. At these pH values, the adsorption increases linearly with decreasing pH due to the increasing surface charge of goethite. In this pH range, the highest adsorption is found for

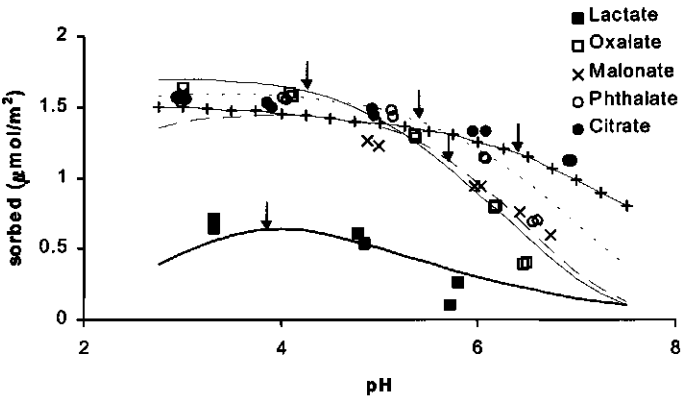

Fig. 2.4 Adsorption envelopes of 2 mM lactate, malonate, oxalate, phthalate and citrate determined in 0.1 M $NaNO_3$ at a goethite suspension of 12 g/L (goethite II for malonate; rest goethite I). The arrows indicate the log K value of the strongest acidic carboxylic group. At pH 7.5 the order of the model lines from top to bottom is citrate, phthalate, malonate, oxalate, and lactate.

citrate, the anion with the highest charge (-3), followed by the three anions with two deprotonated carboxyl groups (-2). Lactate (-1) shows the weakest adsorption. This is illustrated in figure 2.4. This behavior points to a strongly electrostatic binding nature. The increase in adsorption with decreasing pH continues until the organic anion in solution becomes protonated and the charge of the anion diminishes. As a result of the protonation, the adsorption envelope will be less steep and an adsorption maximum may occur. This effect is most clearly visible for model calculations of lactate. The lactate molecules in solution are predominantly uncharged below pH 3.86.

In figure 2.4, the $\log K_{H1}$ values of the first protonation step of the anions are indicated by arrows. The figure shows that maxima in the envelopes are found at pH values just below $\log K_{H1}$. A relation between $\log K_{H1}$ of weak acids and the optimum pH of adsorption has been found by Hingston *et al.* (1967).

2.4.2 Effect of ionic strength

The adsorption of organic acids is dependent on the ionic strength. At a low initial organic acid concentration (0.2 mM), this is only apparent at high pH. At high initial organic

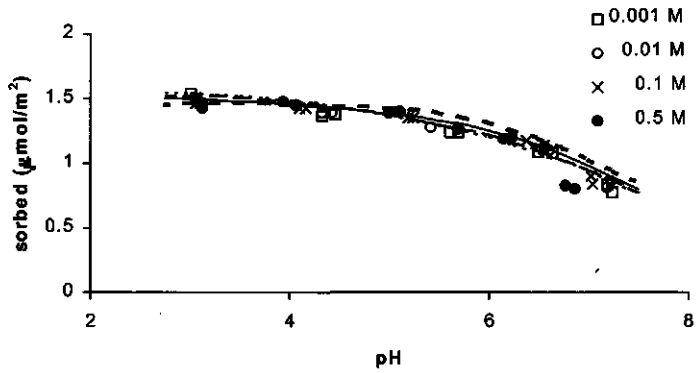

Fig. 2.5 Adsorption envelopes for 2 mM citrate in a goethite I suspension density of 12 g/L at four different ionic strength values. The lines are model calculations.

acid concentration (2 mM), an increase of the level of adsorption at low pH is observed in most cases. This is consistent with the work of Mesuere and Fish (1992), who found suppressed sorption of oxalate and chromate with increasing ionic strength. Citric acid, however, shows a somewhat different behavior. Even at high total concentrations, the adsorbed amount at low pH is hardly affected by the salt level, reflecting a stronger binding and minimizing the charge of the ddl. Figure 2.5 shows the absence of a clear effect on the adsorption of citric acid over a large range of ionic strength values (0.001-0.5 M). Calculations show that the small ionic strength effects on the citrate adsorption can be explained being due to the low positive particle charge at high surface coverage of the goethite, leading to a sharp diminished ddl. At both low and high pH (but below the ppzc), even charge reversal may occur at high surface coverages, the goethite surface can become negatively charged.

2.4.3 Effect of total organic acid concentration

The adsorption of lactic, malonic, and citric acid was studied in more detail. Figure 2.6 shows the adsorption isotherms of these three organic acids for different pH values. As the equilibrium concentrations increase, the adsorption of citric acid first reaches a plateau while the adsorption of malonic and lactic acid still gradually increases. At low concentrations, the slope of the isotherms can be correlated with an increasing number of

carboxylic groups per molecule. This might be explained on the basis of an increased number of reactive groups involved in the binding between organic anion and the surface. This results in a higher electrostatic energy and a higher chemical interaction energy.

2.4.4 Modeling the sorption data

Mechanistic modeling requires the introduction of the basic physical chemical surface characteristics. In table 2.3 and 2.4, the reaction equations and parameters are given. The charging curves of our goethites (data not shown) were in essence the same as those given by Hiemstra and Van Riemsdijk (1996). The site densities of both singly and triply coordinated groups are obtained from electron microscopy studies and crystal morphology. The log K_H

Table 2.3

Reaction equations for singly ($FeOH^{1/2-}$) and triply ($Fe_3O^{1/2-}$) coordinated surface groups.

[1]	$FeOH^{1/2-} + H^+$	$\Leftrightarrow$	$FeOH_2^{1/2+}$	K_H
	$Fe_3O^{1/2-} + H^+$	$\Leftrightarrow$	$Fe_3OH^{1/2+}$	K_H
[2]	$FeOH^{1/2-} + Na^+$	$\Leftrightarrow$	$FeOH^{1/2-}\text{-}Na^+$	K_{Na}
	$Fe_3O^{1/2-} + Na^+$	$\Leftrightarrow$	$Fe_3O^{1/2-}\text{-}Na^+$	K_{Na}
[3]	$FeOH^{1/2-} + H^+ + NO_3^-$	$\Leftrightarrow$	$FeOH_2^{1/2+}\text{-}NO_3^-$	K_{NO3}
	$Fe_3O^{1/2-} + H^+ + NO_3^-$	$\Leftrightarrow$	$Fe_3OH^{1/2+}\text{-}NO_3^-$	K_{NO3}

Table 2.4

Basic model parameters for the goethite surface.

site $density_{singly}$	3.45	nm^{-2}
site $density_{triply}$	2.7	nm^{-2}
$\log K_{H,\ singly} = \log K_{H,\ triply}$	9.2	
$\log K_{Na}$	-1.0	
$\log K_{NO3}$	8.2	
Stern layer capacitance, C	0.9	$F\ m^{-2}$
inner layer capacitance, C_1	1.1	$F\ m^{-2}$
outer layer capacitance, C_2	5.0	$F\ m^{-2}$

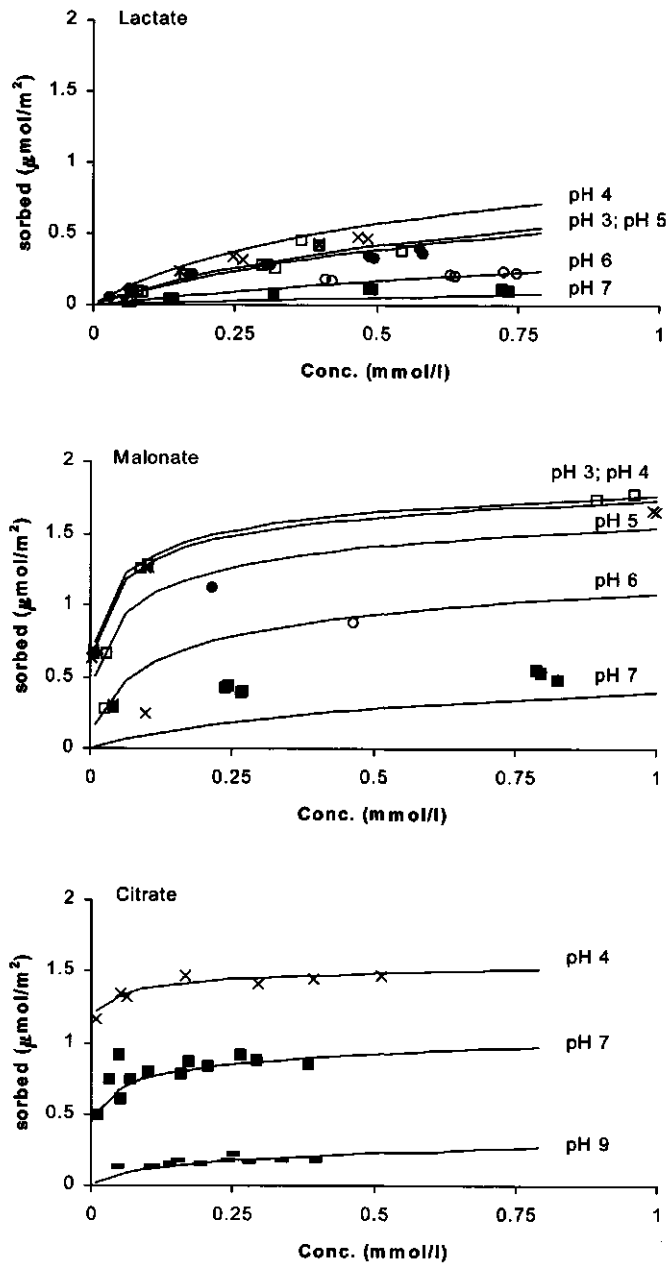

Fig. 2.6 Adsorption isotherms of lactate (goethite I) and malonate (goethite II) determined in 0.01 M $NaNO_3$ and citrate (goethite III) in 0.1 M $NaNO_3$. The lines indicate model calculations.

values are taken directly from the PPZC of our goethites. The values for the pair formation constants for Na and NO_3 and inner layer and outer layer capacitances are taken from Hiemstra and Van Riemsdijk (1996). The inner and outer layer capacitances are related to the overall Stern layer capacitance by $1/C = 1/C_1 + 1/C_2$. The coefficients used for describing the charging behavior of the goethite are fixed while the organic acid binding data are modeled.

The reaction equations describing the binding of organic molecules by the surface (equations [2.3a] and [2.3b]) are the starting point in the modeling. The stoichiometry coefficients of the corresponding formation reactions are given in table 2.5 together with the logarithm of the formation constants. Furthermore, the overall changes of charge in the different electrostatic planes (Δz_i) are given.

Table 2.5

Speciation table used in modeling the adsorption of lactate, oxalate, malonate, phthalate and citrate on goethite.

		Species	logK	FeOH	H	anion	Na	Δz_0	Δz_1	Δz_2
1	Oxalate	Fe_2-Ox	18.00	2	2	1	0	1.00	-1.00	0
2	Phthalate	Fe_3-Phth	28.40	3	3	1	0	1.80	-0.80	0
3	Malonate	Fe_2-Mal	17.80	2	2	1	0	1.00	0	-1.00
4		Fe_3-Mal	26.70	3	3	1	0	1.80	-0.30	-0.50
5		Fe_2-Mal-Na	19.80	2	2	1	1	1.00	0	0
6	Lactate	Fe-LactH	8.40	1	1	1	0	0.80	-0.80	0
7		Fe-LactH-Na	11.10	1	1	1	1	0.80	-0.80	1.00
8		Fe_2-Lact	9.35	2	1	1	0	0.70	-0.70	0
9	Citrate	Fe_3-CitH	29.75	3	3	1	0	1.80	-0.80	-1.00
10		Fe_3-CitH-H	34.40	3	4	1	0	1.80	-0.30	-0.50
11		Fe_3-CitH-Na	31.00	3	3	1	1	1.80	-0.80	0
12		Fe_3-Cit-Na	23.90	3	2	1	1	1.80	-0.80	-1.00
13		Fe_4-CitH	39.80	4	4	1	0	2.60	-0.60	-1.00

Note. The coefficients Δz_i express the change of charge in electrostatic layer i due to ion adsorption. The values of these coefficients are calculated according to the scheme given in table 2.6.

Table 2.6

Calculation scheme of coefficients for the change in charge in table 2.5.

$$\Delta z_0 = p.z_O + q.z_H - r.\Delta s_{O\bullet\bullet\bullet H}$$

$$\Delta z_1 = s.z_O + r.\Delta s_{O\bullet\bullet\bullet H}$$

$$\Delta z_2 = t.z_O + u.z_H + v.z_{Na}$$

Note. Δz_i: change of charge in plane i; $\Delta s_{O\bullet\bullet\bullet H}$: change of charge due to change in strength of H bonds; z_O, z_H and z_{Na}: chare of respectively carboxylate or hydroxylate oxygens, protons and sodium ions; *p, q, r, s, t, u, v*: coefficients corresponding to the various quantities. Note that z_O is -0.5 in case of a carboxylate oxygen and -1 in case of a hydroxylate oxygen.

The changes of charge are calculated according to the equations given in table 2.6. These equations can be formulated on the basis of the type and number of bonds (*p, r*) between oxygen atoms of the organic molecule and the surface, the number of oxygens of carboxylate groups in the 1- or 2-plane (*s, t*), the number of adsorbed protons in each electrostatic plane (*q, u*), and the number of sodium ions in the 2-plane. The surface groups can form hydrogen bonds with water molecules. In these bonds the surface groups can act as the proton donor or as the proton acceptor. Surface groups can also form H bonds with the organic molecules. In case of an H bond between a surface group and a carboxylate group, the surface group is the proton donor. In case of H bond formation between a surface group and an organic hydroxyl group, the surface group is the proton acceptor. The H bonds between surface groups and reactive groups of the organic molecule are assumed to be stronger than the H bonds between surface groups and water molecules. In table 2.6, $\Delta s_{O\bullet\bullet\bullet H}$ is the change in charge replacing an H bond between the surface and a water molecule for an H bond between the surface and an organic anion. The value for $\Delta s_{O\bullet\bullet\bullet H}$ is found by curve fitting. In case the surface group acts as the proton donor, the values of $\Delta s_{O\bullet\bullet\bullet H}$ found for the different species were all approximately 0.2 vu per H bond. This value is therefore taken throughout this article. In case the surface groups acts as the proton acceptor, the value for $\Delta s_{O\bullet\bullet\bullet H}$ is set at 0.8 vu.

As an example we will discuss the various parameter values used for the tridentate citrate surface species with an H bond and complexed sodium (number 11 of table 2.5 and figure 2.7). The reaction equation of the formation of this surface species can be written as:

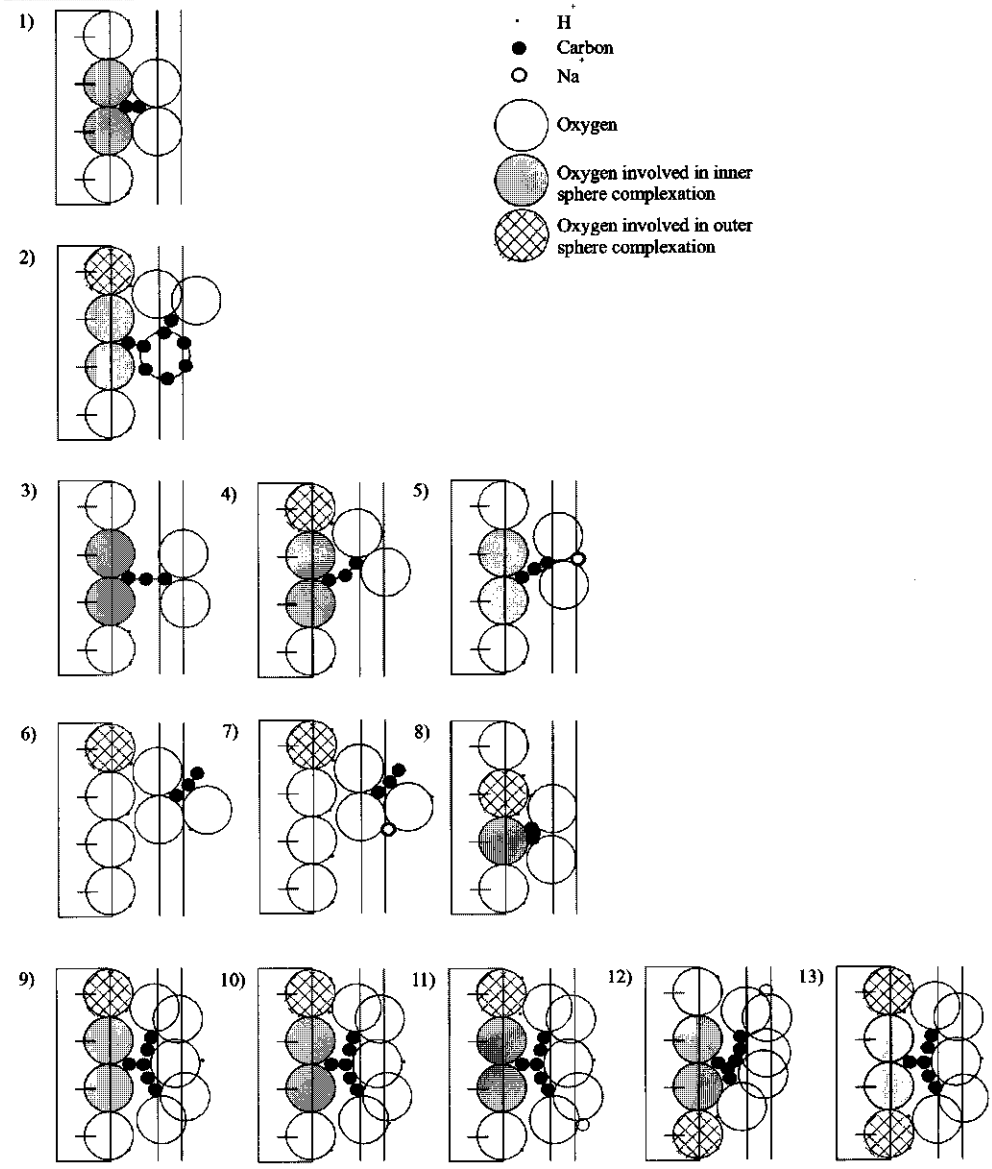

Fig. 2.7 Schematic representation of the surface species used in modeling the adsorption of the different organic anions.

$$3\ (\text{-FeOH}^{0.5\text{-}}) + 3\ H^{+} + \text{CitH}^{3\text{-}} + Na^{+} \Leftrightarrow (\text{-Fe}_3\text{OH}_2\text{ -CitH-Na})^{0.5\text{-}} + 2\ H_2O;\ \log K_{\text{Fe3-CitH-Na}} \quad [2.4]$$

Three surface groups are involved in the formation of this surface species together with three protons, one citrate ion, and one sodium ion. The citrate surface complex has two carboxylate oxygens involved in inner sphere complex formation ($p = 2$). Two oxygens of one carboxylate group are situated in the 1-plane ($s = 2$), of which one forms an outer sphere complex ($r = 1$). The value of q is 3 because three surface hydroxyls are protonated in equation [2.4]. Furthermore, two oxygens of the third carboxylate group are situated in the 2-plane ($t = 2$). The carboxylate group in the 2-plane forms an ion pair with a sodium ion, therefore $v = 1$.

The description of the data with the CD-MUSIC model was optimized by trial and error, aided by plots of the data. The surface species considered are as much as possible in correspondence with results from spectroscopic studies. However, the interpretation of spectroscopic results is not always straightforward and insights in the actual structure of these surface species is at the moment still limited. The datasets for lactic acid, malonic, acid and citric acid cover a broad range of conditions. Several surface species are required to obtain a satisfactory description. The use of several species leads to an increase of the number of parameters and makes it less likely that a unique solution of the parameter set can be obtained. The datasets for oxalate and phthalate are relatively small. A good description was obtained assuming only one surface species. The lines in figures 2.3 – 2.6 represent the model description of the organic anion binding. The effect of pH, ionic strength, and total concentration are described well.

2.5 Discussion

Table 2.5 shows the surface species used in modeling. The modeling of the various species will be discussed in more detail. The envelopes of oxalate binding can be described assuming a bidentate inner sphere complex (table 2.5 and figure 2.7; no.1). Both oxygens of one carboxylate group (mono nuclear) or two oxygens of different carboxyl groups (bi nuclear) form coordinative bonds with surface Fe ions. The reaction equation is:

$$2\ (\text{-FeOH}^{0.5\text{-}}) + 2\ H^{+} + Ox^{2\text{-}} \Leftrightarrow \text{Fe}_2\text{-Ox} + 2\ H_2O \qquad \log K_{\text{Fe2-Ox}} \qquad [2.5]$$

The surface hydroxyl groups are protonated to surface water groups, which are subsequently released upon adsorption of oxalate. The values of Δz_i of table 2.5 can be calculated using table 2.6 and $p = 2$, $q = 2$ and $s = 2$.

Parfitt *et al.* (1977a) suggested two species (see figure 2.2). Using IR spectroscopy, they found a monodentate and a bidentate species. Assumption of the additional presence of the monodentate species did not improve our description and is neglected.

Phthalate binding can also be described using only one surface species, again a bidentate inner sphere complex. The change in charge of 0.8 units in the zero plane arises due to a charge attribution of +2 vu via the adsorption of two ($q = 2$) protons that are required to release two water molecules, a contribution of -1 vu ($p = 2$) due to the coordinated adsorption of two carboxylate oxygens of the phthalate molecule. An attribution of -0.2 vu due to the change in the strength of the H bond between a surface hydroxyl group and an oxygen of the free carboxyl group ($r = 1$) (see figure 2.7 no.2). The species used to describe the data is in accordance with the surface species for phthalate suggested by Tejedor-Tejedor *et al.* (1980) (see figure 2.2). On the basis of IR data they suggested a bidentate inner sphere complex in which one of the carboxylate groups is involved in the coordination with the surface. Nilsson *et al.* (1996) argued that the IR spectroscopy data of phthalate binding should be interpreted with caution because of the complexity of the vibrational properties of phthalates. They explained their spectra by assuming an outer sphere complex with an intramolecular H bond (see figure 2.2).

For malonate adsorption, no IR spectroscopy data are available. In modeling, the obtained data and taking into account concentration, pH, and salt dependency, three surface species are used, all of them inner sphere complexes (see table 2.5 and figure 2.7; nrs. 3 - 5). As for lactate and citrate, the adsorption data of malonate could be described by using different sets of surface species. Here, we use the species which are considered chemically most realistic and give adequate descriptions. The most important species is the bidentate inner sphere species with an uncomplexed carboxylate group (species 3 of table 2.5 and figure 2.7). At low pH, one of the oxygens of the uncomplexed carboxylate group can form an H bond with an adjacent surface water group. This species becomes important at low pH. Note the resemblance of these two species and the species of respectively oxalate and phthalate. The third species used involves the formation of a Na^+ complex. This species becomes important at high Na^+ concentrations and pH values higher than 4. At lower pH and

also low Na^+ concentration, there will be strong competition between H^+ and Na^+ for the free carboxylate group and the formation of Na^+ complexes can be neglected.

Cornell and Schindler (1980) investigated the binding of lactate by goethite. From their spectra they inferred that lactate was bound as a monodentate inner sphere complex (see figure 2.2). Furthermore, they found that the alcoholic hydroxyl group of lactate can deprotonate upon adsorption to amorphous iron oxide surfaces. Here, we assume that the hydroxyl group of the lactate ion can act as the proton donor in an H bond between the organic hydroxyl group and the surface hydroxyl group. The formation of this type of H bond is thought to occur in addition to the formation of an inner sphere coordinative bond of lactate with the surface. The charge of the proton of the organic hydroxyl group is mainly located in the 1-plane ($\Delta s_{O\bullet\bullet\bullet H}$ = 0.8 vu)(see table 2.5 and figure 2.7; no. 8). The overall reaction equation for the formation of this species is:

$$2\,(\text{-FeOH}^{0.5-}) + H^+ + \text{HLact}^- \Leftrightarrow \text{Fe}_2\text{OH-HLact}^- + H_2O; \qquad \log K_{\text{Fe2OH-HLact}} \qquad [2.6]$$

This surface species is the most important species we found for lactate binding. However, it is in contrast with the inferred surface species of Cornell and Schindler (1980) because they did not interpreted their results in terms of an H bond. In the other two species, the bond between the surface and the lactate ion involves an outer sphere complex instead of an inner sphere complex as proposed by Cornell and Schindler (1980). Fitting the salt dependency, it became clear that the surface species with the complexed Na^+ plays an important role at higher $NaNO_3$ concentrations and high pH. This was not very surprising as the formation of Na^+ complexes occurs also in solution. However, the sodium affinity constant used for the lactate surface species is rather high.

Cornell and Schindler (1980) also investigated citrate binding by goethite. Using IR spectroscopy, they found that citrate was bound to the surface as a tridentate species at pH 3. From steric considerations, a surface structure is proposed in which only one oxygen atom of each carboxyl group is involved in the ligand exchange. The adsorption data of citrate could be described adequately using a set of surface species of which a tridentate surface species was the most important one at pH 3. However, the adsorption data were described better using the set of surface species as listed in table 2.5. The bidentate inner sphere complex with two H bonds to adjacent surface water groups is normally the most important species by far. At low pH, our model calculations show that the protonated bidentate inner sphere complex

with one H bond becomes more important (see table 2.5 and figure 2.7). All the surface species used for describing citrate adsorption closely resemble one another. The carboxyl groups not involved in inner sphere coordinative bonds can form H bonds with surface groups, react with H^+ or Na^+ ions, or stay uncomplexed. The protonation constant of the carboxyl group of citrate that does not form an inner sphere coordinative bond can be derived from the logK value of table 2.5. The constant is comparable in magnitude with the second highest proton affinity constant for the acid in solution. The Na^+ ions in solution compete with the surface water groups and the protons in solution for the formation of a complex with a free carboxylate group. As for malonate and lactate, the sodium-citrate surface species are very important in describing the salt dependency of the binding.

For species 12, we assume that when the pH rises the hydroxyl group of citrate can become deprotonated in the vicinity of the goethite surface. The oxygen of the deprotonated organic hydroxyl group can act as a proton acceptor in an H bond with a surface hydroxyl group. The proton of a surface water group can act as the proton donor. The $\Delta s_{O\cdots H}$ is 0.2 vu. The proton affinity of the surface hydroxyl group to form a surface water group should exceed the proton affinity of the organic ligand. This means that the proton affinity of the organic hydroxylate group should be smaller than 9.2, which is small based on the affinity constant of this reaction in solution. The reaction might occur due to presence of the goethite surface and the H bond formed. The spectra of Cornell and Schindler (1980) didn't indicate such a species but their spectra were made at pH 3. At higher pH, "deprotonation" of the alcoholic hydroxyl group is more likely to occur as can be shown by the model calculations. The calculations show an increase of this surface species with increasing pH. The solution orientated carboxylate group of this surface species can form an ion pair with a sodium ion as is depicted in figure 2.7.

Bowden *et al.* (1980) determined the binding of citrate by goethite in 0.01 M KCl. We tried to predict the binding using the same surface species as listed in table 2.5. The predictions indicate a larger adsorption than found in the experiments. We decreased the log K values for the K^+ complexes of the solution oriented reactive groups of citric acid with 0.4 units in order to get a very good description as can be seen from figure 2.8. Adjusting the complexation constant of K^+ for citric acid in solution seems to be justified by the fact that the complexation constant of K^+ is somewhat lower than the complexation constant of Na^+ for citric acid in solution.

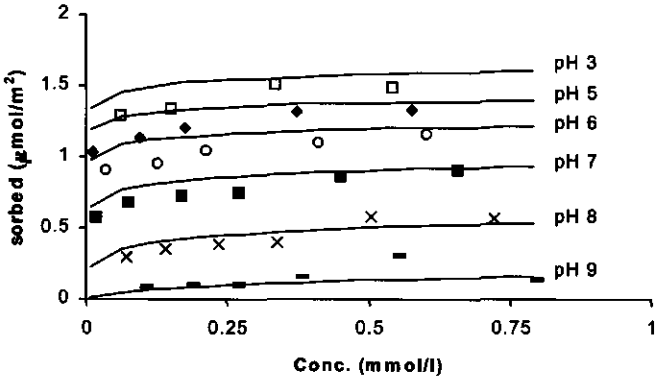

Fig. 2.8 The adsorption of citrate by goethite in 0.01 M KNO_3 at various pH values, with data of Bowden *et al.* (1980). The lines are calculated with the same parameters used for describing the citrate adsorption data obtained in this study. For details see text.

The steepness of the first part of the adsorption isotherms of three of the organic acids as shown in figure 2.6, increases with increasing number of reactive groups. This can be explained by the number of bonds of the organic acids with the surface and the increased electrostatic attraction between the surface and the organic molecule with increasing amount of reactive groups. The free energy that is involved in the formation of one Fe-OOC-R bond can be interpreted as an exchange of a surface water group with one oxygen of a carboxylate group. These exchange constants per bond can be calculated from the given logK of table 2.5 writing reaction [2.3b] as:

$$\text{-FeOH}_2^{0.5+} + {}^1/_n\, L^{m-} \Leftrightarrow {}^1/_n\, \text{-Fe}_n L^{(m+0.5n)-} + H_2O; \qquad \log K_{\text{exch per bond}} \qquad [2.7]$$

The $\log K_{\text{exch per bond}}$ values are all relatively small (around $\log K_{\text{exch per bond}} = 0$; see table 2.7). As a molecule can make three or four bonds with the surface (citrate), more energy is involved in the binding of this molecule than for a molecule that can only make two or one bond (malonate or lactate). Besides this effect the citrate molecule has the highest charge in solution and lactate the lowest. Therefore the electrostatic energy involved in the binding will decrease going from citrate to lactate. These phenomena result in the fact that citrate is stronger bound by the goethite surface and shows a higher initial slope of the adsorption isotherms than malonate or lactate.

When electrostatic effects are disregarded, the small or even negative $\log K_{exch\ per\ bond}$ values of table 2.7 indicate very little binding for all organic anions investigated. As there is a considerable amount of organic acid bound by goethite at low pH (see figure 2.3), one may conclude that the binding of organic anions by goethite is to a large extent electrostatic in nature with a relatively small chemical contribution.

2.6 Conclusions

The size and structure of adsorbed polyprotic weak organic acids indicate that the charge of the surface species is distributed over a surface region with a thickness of two to three water molecules. The charge of the surface complexes is moreover pH dependent. The adsorption of weak organic acids can be well described with the CD-MUSIC model. For small datasets (oxalate and phthalate), only one surface species is required to describe the data. For more extended datasets, more species are required to obtain good descriptions (lactate, malonate, and citrate). From the model, it is possible to distinguish between inner sphere and outer sphere complexation. Outer sphere complexation was found to be of importance for lactate adsorption. Other surface species used in modeling the obtained data are all inner sphere complexes.

At present, conclusive evidence of the exact structure of surface species from spectroscopic data is still somewhat speculative, as is the interpretation of surface species from adsorption modeling. A strict comparison between adsorption modeling and surface structures inferred from spectroscopy is therefore not warranted. Only for oxalate, the surface species used in the model agree fully with surface species inferred from IR spectroscopy. For the other acids, differences between IR-inferred and model-inferred surface species were found. For lactate, the surface species found from modeling suggest outer sphere adsorption while IR data of Cornel and Schindler (1980) suggest inner sphere coordination. However, the species of bound salicylate as inferred from FTIR data by Yost *et al.* (1990) resembles the most important lactate surface species used in the model. For phthalate, the model results agree with IR data of Tejedor-Tejedor *et al.* (1992) and Biber and Stumm (1994), but are in contradiction with the interpretation of the data by Nilsson *et al.* (1996). For citrate adsorption, Cornell and Schindler (1980) proposed a different surface species than we used in

3

Transport of malonate in a goethite - silica sand system

Abstract—The mobility of weak organic acids is of great importance for the transport of heavy metals and other contaminants. This work discusses the breakthrough behavior of malonic acid through a column packed with goethite coated sand. The transport of malonic acid is dominated by multicomponent chemical interactions of protons and the malonic acid on the goethite surface and in solution. The experimental results show a fast breakthrough and a slow desorption of malonate. The binding capacity of the goethite coated silica sand column for malonic acid and acidity are discussed and their impact on elution is illustrated. The data have been predicted with a combination of the CD-MUSIC model (Hiemstra and Van Riemsdijk, 1996) and a one dimensional convective-dispersive transport code. Reasonable agreement was obtained between data and model predictions.

Jeroen D. Filius, Johannes C.L. Meeussen and Willem H. van Riemsdijk
Colloids and Surfaces A **151**, (1999), 245-253

3.1 Introduction

The transport of simple weak organic acids in natural porous media is of importance for several topics of environmental science. Simple weak organic acids are well defined carboxylic acids that are commonly found in natural systems. The behavior of these well-defined weak organic acids is of importance for processes such as subsoil acidification, exudation of the acids from plant roots, and the enhanced transport of contaminants by colloids. As the type of reactive groups and the binding behavior of small, well defined organic acids are similar to those of larger less well defined organic acids, well defined weak organic acids can be used as model compounds for larger weak organic acid such as fulvic or humic acids.

This paper discusses the transport of malonic acid through a column packed with goethite coated sand. The goethite-coated sand has well defined characteristics. The silica sand has a small surface area and is hardly reactive for anions. Therefore, the binding of ions is mainly determined by goethite and can be used to predict the transport of those ions through goethite coated sand columns. Scheidegger *et al.* (1994) and Meeussen *et al.* (1996 and 1998) used the goethite-coated sand in their studies. Scheidegger *et al.* (1994) studied a pseudo-monocomponent situation with H^+ and OH^- as the only reactive components during transport and showed good agreement between theoretical predictions and experimental results. The transport of anions is a more complex problem. When the anion interacts with protons, either in solution or during surface complexation, the binding of the anion becomes pH dependent and the transport of the anion is influenced by the transport of protons. Meeussen *et al.* (1996) studied the multicomponent transport of fluoride. Fluoride in solution exists only of F^- for a large pH range. In this pH range, there is no interaction between fluoride and protons in solution. Fluoride and protons do interact, however, during surface complexation of the fluoride. Therefore, the transport of fluoride is a function of both fluoride concentration and pH. Meeussen *et al.* (1996) used a one pK approach with a Basic Stern double layer model (Hiemstra *et al.*, 1989a) combined with a convective-dispersive solute transport model to predict the transport of fluoride. The agreement between predicted and experimental curves was good. To predict the transport of well defined organic acids here, we will use a similar approach as applied by Meeussen *et al.* (1996). The CD-MUSIC adsorption

Table 3.1

Equations for the reactions in solution and on the goethite surface.

	Reaction	logK
	Solution	
1	$H^+ + OH^- \Leftrightarrow H_2O$	-14
2	$Mal^{2-} + H^+ \Leftrightarrow HMal^-$	5.70
3	$HMal^- + H^+ \Leftrightarrow H_2Mal$	2.85
4	$Mal^{2-} + Na^+ \Leftrightarrow Mal\text{-}Na^-$	0.74
	Proton complexation	
5	$FeOH^{0.5-} + H^+ \Leftrightarrow FeOH_2^{0.5+}$	9.2
6	$Fe_3O^{0.5-} + H^+ \Leftrightarrow Fe_3OH^{0.5+}$	9.2
7	$FeOH^{0.5-} + Na^+ \Leftrightarrow FeOH\text{-}Na^{0.5+}$	-1.0
8	$Fe_3O^{0.5-} + Na^+ \Leftrightarrow Fe_3O\text{-}Na^{0.5+}$	-1.0
9	$FeOH^{0.5-} + H^+ + NO_3^- \Leftrightarrow FeOH_2\text{-}NO_3^{0.5-}$	8.2
10	$Fe_3O^{0.5-} + H^+ + NO_3^- \Leftrightarrow Fe_3OH\text{-}NO_3^{0.5-}$	8.2
	Organic acid complexation	
11	$2\ FeOH^{0.5-} + 2\ H^+ + Mal^{2-} \Leftrightarrow Fe_2\text{-}Mal^-$	17.80
12	$2\ FeOH^{0.5-} + 2\ H^+ + Na^+ + Mal^{2-} \Leftrightarrow Fe_2\text{-}Mal\text{-}Na^0$	19.80
13	$3\ FeOH^{0.5-} + 3\ H^+ + Mal^{2-} \Leftrightarrow Fe_3\text{-}Mal^{0.5-}$	26.70

model (Hiemstra and Van Riemsdijk, 1996) for ion adsorption by oxides is combined with a convective-dispersive transport code.

In the column experiment of the present study, we used malonic acid (see table 3.1) as an example of a weak organic acid. Filius *et al.* (1997) studied the binding of malonic acid by goethite and interpreted the binding with the CD-MUSIC model. As for fluoride, they found that protons were involved in the surface complexation of malonate. However, malonic acid also interacts with protons in solution. Due to this interaction, the adsorption and transport of one component is influenced by the other component.

For comparison between the transport of malonate and protons, the breakthrough curve of pH is difficult to use. First of all, the pH is a logarithmic scale, whereas the malonate in solution is expressed on a linear scale. Secondly, only a minor part of all the protons in solution are present as H^+. Most of the protons in solution are bound to malonate. As the breakthrough of malonate is expressed as total concentration in solution, the proton

breakthrough should also be expressed as total H concentration minus total OH concentration in solution, or acidity. The acidity in this case can be calculated according to:

$$Ac = [H^+] - [OH^-] + [HMal^-] + 2 \times [H_2Mal] \quad [3.1]$$

The effects of the binding of weak acids and protons on the breakthrough of the solution acidity has not been studied before and is therefore one of the main aspects studied in this paper.

3.2 Model description and transport predictions

3.2.1 Chemistry

To model the transport of substances in multi component systems, a proper description is needed of all the interactions between the different chemical components present. The interactions occurring in these multi component systems are schematized in figure 3.1. In solution malonate can become protonated and can form complexes with Na^+. In table 3.1 these interactions are given by equations 1-4.

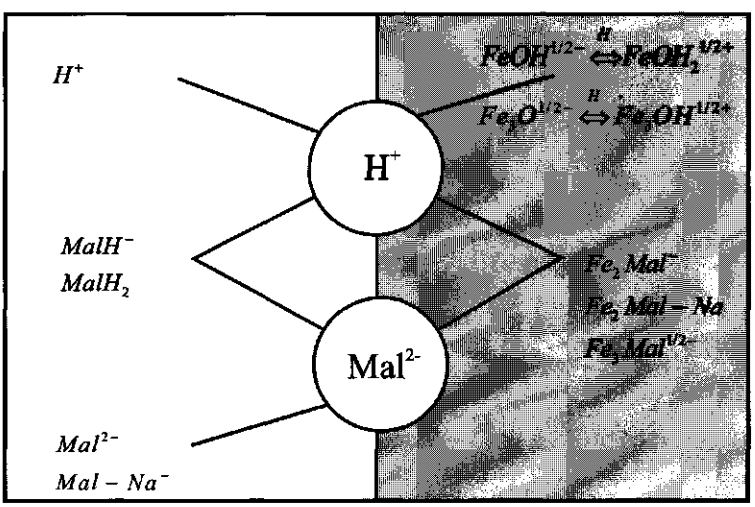

Fig. 3.1 Interactions and speciation occurring in a multicomponent system with goethite and sodium nitrate, protons, and malonate.

The adsorption of protons by the goethite surface is assumed to be due to interaction with different types of sites. A singly coordinated FeOH site with a site density of 3.45 sites/nm^2 and a triply coordinated Fe_3O site with a density of 2.7 sites/nm^2 can complex protons according to equations 5 and 6 of table 3.1. The logarithm of both affinity constants of the reactions are set equal to the Pristine Point of Zero Charge (PPZC) of the goethite. The surface charge of the goethite surface is compensated by electrolyte ions in a diffuse double layer (ddl). The ions present in the DDL are hydrated and have a finite size, thereby preventing the neutralization of charge to start directly from the close-packed goethite surface. The ions in the ddl have a distance of closest approach to the surface. This has led to the formulation of a charge-free layer, called the Stern layer. The primary charging behavior of the goethite can be described with a fitted Stern layer capacitance of 0.9 F/m^2 and assuming ion pair formation (reactions 7 - 10 of table 3.1) located at the head end of the ddl.

Figure 3.2 shows the adsorption curves of malonate by goethite in a 0.01 M $NaNO_3$ solution. For the description of the adsorption of malonate by goethite the surface speciation of malonate is important. Malonate is a large molecule compared to the size of a proton and has two reactive groups. If one is interested to model the adsorption with surface species that may have physical significance, the charge of the bound malonate molecule should not be regarded as being a point charge, but should be distributed in space. The interaction between

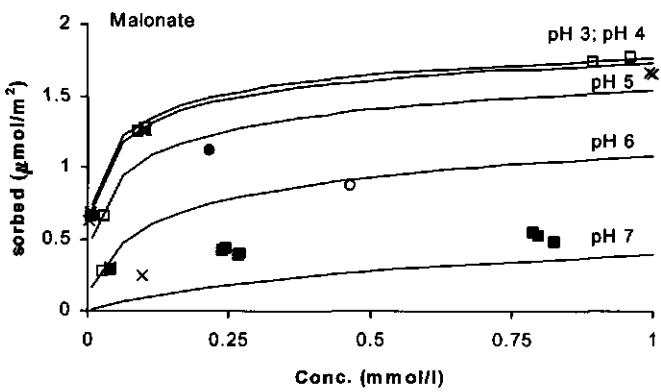

Fig. 3.2 The adsorption isotherms of malonate determined in 0.01 M $NaNO_3$. The lines indicate model calculations with the CD-MUSIC model (data from Filius *et al.*, 1997).

protons, salt ions, and malonate with the goethite surface has been studied by Filius *et al.* (1997). They used the CD-MUSIC model (Hiemstra and Van Riemsdijk, 1996) to describe the surface complexation of protons, salt ions and malonate taking the distribution of charge into account. In the CD-MUSIC approach, the charge of the organic anion is distributed over three electrostatic planes. The first two planes are located at either side of the Stern layer (0- and d-plane). The third plane (1-plane) is located between the other two planes and divides the Stern layer into two layers with a capacitance of respectively 1.1 and 5.0 F/m^2. The charge of the reactive groups of the malonate anion can be located in all three electrostatic planes depending on the type of complex formed. Filius *et al.* distinguished between the formation of inner sphere and outer sphere complexes. The carboxylate groups of the malonate are assumed to bind as both inner and/or outer sphere complexes. An equal distribution of the charge of the two carboxylate groups over both oxygens was assumed. Each oxygen of the carboxylate groups thus carries half a unit negative charge. For inner sphere complex formation, the charge of the carboxylate oxygen that exchanges for a protonated singly coordinated surface groups is located in the 0-plane and is fully neutralized by the charge of an Fe-O bond (+0.5 vu; Hiemstra and Van Riemsdijk, 1996). Outer sphere complexes can be formed as a result of H bond formation between carboxylate oxygens and singly and triply coordinated surface groups. In the CD-MUSIC approach, the charge of the surface proton is fully attributed to the surface oxygen, although H bonds may transfer charge between the oxygens of the surface and water molecules in solution (Hiemstra *et al.*, 1996). According to Brown (1978), the H bond involved in organic complexes can be stronger than the H bonds between water molecules. This implies that extra charge is transferred between the surface and the 1-plane due to a stronger H bond between the organic molecule and the surface water or hydroxyl. Filius *et al.* (1997) found that the extra charge that is transferred between the surface and the 1-plane is about 0.2 vu. This means that in case of H bonding, 0.8 vu of the charge of the proton is attributed to the surface plane and 0.2 vu to the 1-plane.

The formation of the malonate surface species which Filius *et al.* used are given by equations 11-13 of table 3.1. The protons on the left-hand side of the equations are used to protonate the surface hydroxyl groups to surface water groups. The surface water groups can exchange or make an H bond with a carboxylate oxygen (Parfitt *et al.*, 1977a,b,c).

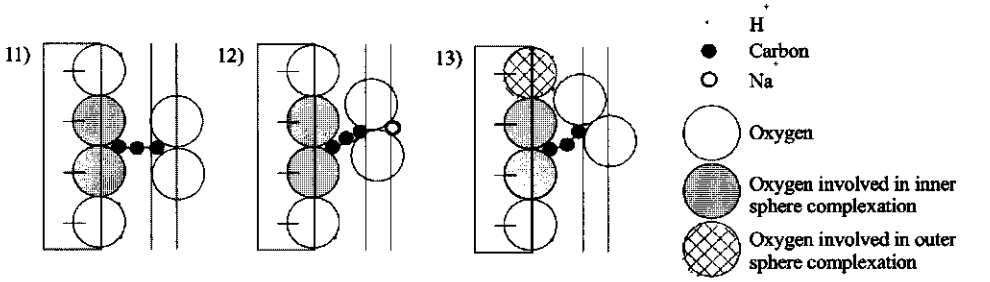

Fig. 3.3 Schematic representation of the surface species used in modeling of the adsorption of malonate as proposed by Filius *et al.* (1997).

The surface species are depicted in figure 3.3. In all surface species used, two carboxylate oxygens are exchanged for surface water groups. In the first surface species the charge of the two non-coordinated surface oxygens are situated in the d-plane. The second surface species is the same as the first one, but the charge of the two carboxylate oxygens in the d-plane is compensated by the complexation of a sodium ion. In the last surface species an additional H bond is formed and the charge of only one non-coordinated carboxylate oxygen is situated in the d-plane.

The stoichiometry coefficients of the reactions 11-13 of table 3.1 are given in table 3.2 together with the logarithm of the formation constants. Furthermore the overall changes of charge in the different electrostatic planes (Δz_i) are given. These changes of charge are calculated according to the equations given in table 3.3.

Table 3.2

Speciation table used in modeling the adsorption of malonate on goethite.

	Organic anion	Species	logK	FeOH	H	Org. anion	Na	Δz_0	Δz_1	Δz_2
11	Malonate	Fe_2-Mal	17.80	2	2	1	0	1.00	0	-1.00
12		Fe_2-Mal-Na	19.80	2	2	1	1	1.00	0	0
13		Fe_3-Mal	26.70	3	3	1	0	1.80	-0.30	-0.50

Note The coefficients Δz_i express the change of charge in electrostatic layer *i* due to ion adsorption. The values of these coefficients are calculated according to the scheme given in table 3.3.

Table 3.3

Calculation scheme of coefficients for the change in charge in table 3.2

$\Delta z_0 = p.z_O + q.z_H - r.\Delta s_{O\bullet\bullet\bullet H}$
$\Delta z_1 = s.z_O + r.\Delta s_{O\bullet\bullet\bullet H}$
$\Delta z_2 = t.z_O + u\,.\,z_{Na}$

Note. Δz_i: change of charge in plane i; $\Delta s_{O\bullet\bullet\bullet H}$ = change of charge due to change in strength of H bonds; z_O, z_H and z_{Na} = charge of respectively carboxylate or hydroxyl oxygens, protons and sodium ions; p, q, r, s, t, u = coefficients corresponding to the various quantities. Note further that z_O = -0.5 in case of a carboxylate oxygen and -1 in case of a hydroxyl oxygen.

3.2.2 Transport

As stated above, the system under study involves interactions between protons, malonate, sodium ions, and the goethite surface. The breakthrough curve of such a multi-component system consists of regions of constant composition separated by several fronts. The theoretical number of fronts is equal to the amount of components that have interaction with each other and that can be transported (Cernick *et al.*, 1994). Thus, theoretically, there will be three fronts in this system. As Na^+ and NO_3^- hardly adsorb, the changes in solution concentration of these species can be neglected. The column experiment presented in this paper involves a step change of the malonate concentration in the feed solution at $t = 0$. The conditions were taken such that, according to model predictions, two fronts are expected to be visible in the experimental breakthrough of both components.

The mathematical solution of the convection dispersion equation used to model the transport of malonate is achieved by a two step method (Cederberg *et al.*, 1985; Engesgaard and Christensen, 1988; Herzer and Kinzelbach, 1989). The set of chemical equations is solved for each node and time step using the approximation of equilibrium. The chemical model is combined with a simple one-dimensional transport code that accounts for convexity and diffusion/dispersion. All the parameters used have been determined before the experiment. The transport calculations are therefore pure predictions.

3.3 Materials and Methods

3.3.1 Goethite

The goethite used to coat the silica sand is the same material as used for the determination of the adsorption of small organic acid by goethite (goethite I of Filius *et al.*, 1997). The material was prepared according to the method of Atkinson *et al.* (1967) with the adjustments described by Hiemstra *et al.* (1989b). The goethite has a BET-N_2 surface area of 96.8 m^2/g. The point of zero charge of the material was 9.2.

3.3.2 Goethite coated silica sand

The goethite coated quartz sand is composed of quartz and goethite. The quartz sand is purified in 2 steps. 1) 1 kg sand is washed with 1 L 0.1 M HF/0.1 M HCl solution and washed twice with bidest. 2) The sand is extracted twice with NaOH and washed three times with bidest. After the purification, the sand is dried at 60 ^{0}C for 24 h.

The quartz sand was then coated with goethite using the method described by Scheidegger *et al.* (1993). We added 5 kg purified quartz sand to 7 L of a 0.01 M $NaNO_3$ solution with a goethite concentration of 1.425 g/L. This suspension was brought to pH 5 with HNO_3. The goethite was coated irreversibly to the quartz sand at a ratio of 0.44 mg goethite per gram sand.

3.3.3 Column experiments

Column experiments were performed using columns with a diameter of 43.8 mm and a length of 18.3 cm. The feeding solutions were pumped with a peristaltic pump at flow rates of 0.6 mL/ min. The column was packed with 443.9 g goethite coated sand. The porosity of the column (θ) was 0.39. One pore volume of the column therefore equals 108 mL. In addition to this volume, the tubes and pH flow cel connected to the column had a volume of approximately 3.5 mL. The column dispersivity was determined with conservative tracers (NaCl) in the same column set up used in the breakthrough experiment. Observed dispersivity was 0.282 ± 0.005 mm and was independent of the flow rate and comparable to the particle

size. The column Peclet number (Pe, defined as $Pe = L/D_L$ where L is the column length, and D_L is the dispersivity) was >500. The pH of the effluent was measured on line with a flow-through cell. For the determination of the concentration of organic acid, the effluent was collected in discrete fractions of approximately 5 mL by a fraction collector. The concentration of the organic acid was measured using a Skalar SK12 Organic Carbon analyzer.

Before the column was used, it was pretreated with $NaNO_3$ solutions containing 10^{-3} M NaN_3, in order to prevent microbiological degradation. The column was then equilibrated with a 0.01 M $NaNO_3$ solution at pH 5.38. The acidity in solution is 4.17×10^{-6} M. Subsequently, at 0 pore volumes (pv; volume of effluent / volume of pores), a solution of 0.5 mM malonate with the same pH and ionic strength was percolated through the column. The acidity of this solution equals 3.06×10^{-4} M. Therefore, there is a step change in both malonate concentration and acidity.

The effluent of the column was checked on its iron content. No evidence for the dissolution of the goethite could be found. All chemicals used were of the p.a. grade.

The simulations of the transport experiment were carried out with ECOSAT (Keizer and Van Riemsdijk, 1995).

3.4 Results and Discussion

The set-up of the first experiment was chosen in such a way that all fronts are expected to be visible. The experimental breakthrough curve shows 2 fronts in both malonate concentration and the breakthrough curves can be explained as follows: As a result of the binding of malonate and protons by the goethite, the pH in the column will rise. The pH increases from 5.38 to 6.79 due to the release of OH^- upon binding of the malonate by goethite. As the rate of the binding of malonate by the goethite decreases due to the elevated pH, less OH^- is released. When this elevated pH value breaks through, the column is saturated with malonate at this pH. The breakthrough curve of malonate shows a front at the same time as the first pH breakthrough. The amount of OH^- released upon further adsorption of malonate together with the complexation of protons to malonate in solution causes a sort of steady state situation with a constant pH and malonate concentration in the effluent. After about 1.9 pore volumes, the second front appears in both the pH and malonate breakthrough.

The column now becomes completely in equilibrium with the feed solution. There will be no more adsorption of malonate and subsequently no release of OH^-. The pH drops back to its initial value and the malonate concentration in solution increases to the influent concentration.

The arrows in figure 3.4 indicate the switch in the feed solution back to the initial composition (0.01 M $NaNO_3$; pH 5.38; no malonate). Shortly after one pore volume, there is a steep decrease in malonate concentration. After this steep decrease in concentration, a "slow" desorption process takes place until all the malonate has been desorbed. The very gradual desorption which takes more than 10 pore volumes is caused by the highly non-linear character of the adsorption curve as can be seen in figure 3.2. A low equilibrium concentration still corresponds with a relatively large amount of malonate bound in the column, and it therefore takes a long time to elute the column completely. This is better illustrated with the use of the pH elution curve. In this curve the pH decreases due to proton release upon malonate desorption. After this decrease, the pH slowly increases to the pH of the feed solution. As can be seen from figure 3.4b, at the end of the experiment, the pH of the effluent is still below the pH of the feed which indicates that the desorption process is still continuing.

As stated before, the transport of malonate and protons should have similarities due to the interaction of malonate and protons. In figure 3.4c, the breakthrough curve of the acidity is given. The shape of this curve is similar to that of the malonate. In both curves, two fronts are visible in the adsorption part. The fronts occur at the same time for acidity and malonate. The main difference between the breakthrough curves is the level of the first plateau. This difference is caused by the difference in binding capacity for malonate and acidity in the column.

The binding capacity of the column is the amount of malonate or acidity which can be bound by the solid phase of the column. It can be expressed as the surface between the line $y = C_{feed}$ or $y = ac_{feed}$ and the breakthrough curve of malonate or the acidity respectively before the switch to the elution solution. This area should be corrected for the tracer breakthrough. The binding capacity for malonate at pH 5.38 is approximately 22.5 µmol {[0.20 pv × 0.5 mM + 0.9 pv × (0.5 - 0.38 mM)] × 108.27 mL/pv }. This can also be calculated with the CD MUSIC model with the use of the description for malonate binding. The equilibrium concentration of malonate is 0.5 mM and the total surface area in the column

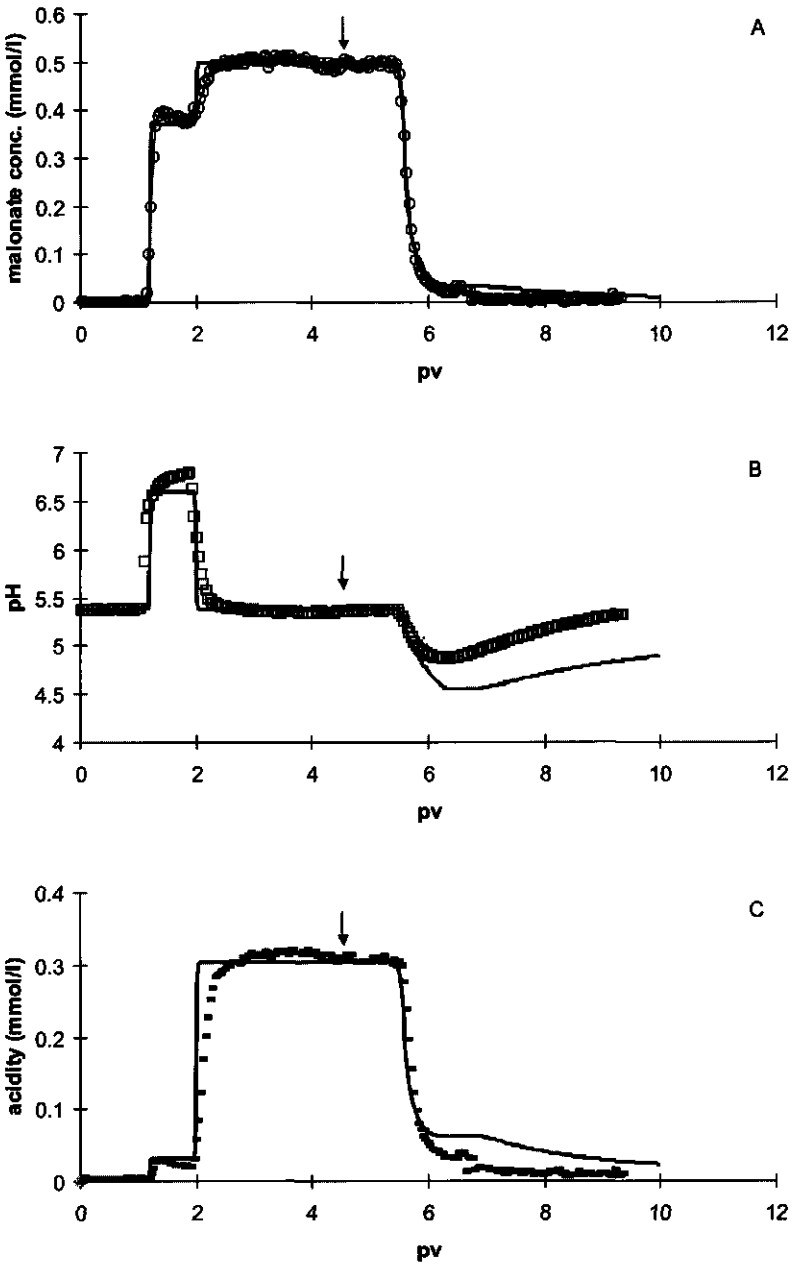

Fig. 3.4 The breakthrough curves of a) malonate concentration, b) pH and c) acidity. Note the similar shape of the curve for malonate concentration and acidity and the fact that the fronts occur at the same time.

is 18.9 m^2. For malonate, the binding capacity of the column calculated with the CD-MUSIC model is 23.9 μmol. The binding capacity of the acidity is increased with 33.1 μmol due to the presence of malonate in the column. Assuming no interaction between protons and malonate and sharp fronts, complete breakthrough for malonate and acidity will be reached at 1.4 and 2.0 pv respectively. These two fronts can also be distinguished in the experimental data. The first front is the "malonate front" which starts at 1.2 pv. The shift of this front to an earlier breakthrough is caused by the increased pH due to hydroxyl release upon malonate adsorption. The lower binding capacity at high pH causes the earlier breakthrough. As the malonate concentration increases, the acidity in solution also increases due to the protonation reactions of dissolved malonate (reaction 2 of table 3.1). The second front is the "acidity front". This front is hardly shifted because only a small part of the acidity has broken through in the malonate front. In between the two fronts, there is a steady state between the malonate and protons adsorbed by the column. When the column becomes saturated for the acidity complete breakthrough for both malonate and acidity is the result.

From the binding capacity of the column, the number of pore volumes for complete recovery of the column can be estimated roughly. For complete recovery, the same amount of malonate or acidity that is flushed in should be flushed out. For malonate, this means that the area between the elution curve and the line $y = C_{feed;ini}$ corrected for a tracer should be equal to the area indicating the binding capacity. This means that 23.9 μmol has to be flushed out. From figure 3.4a, one can estimate an average concentration in the effluent. If we take 0.01 mM it takes about 22 pv to flush out all the malonate.

The model predictions with the CD-MUSIC model are represented in figure 3.4 by the solid lines. The start of the breakthrough curves is predicted within 0.1 pv of the experimental curves. The appearance of a second front and complete breakthrough is also predicted reasonably well. However, the fronts in the experimental breakthrough are more diffuse than predicted and the position of the second front differs from the predictions. The elution curve of malonate is predicted well, although one should be careful with the interpretation of the tailing of the curve. The values of the malonate concentration in the tail are within the experimental error. In this range, it is hard to distinguish between errors in modeling and experiment. As the pH can be measured more precise, the comparison between predicted and observed pH is more accurate. As can be seen from figure 3.4b, the model

prediction is somewhat off, as the model predicts a lower pH during elution than observed in the experiment.

The fact that the fronts in the experimental breakthrough are more diffuse might be caused by the "dead volume" in the column, tubes and the pH flow through cell. In this volume the column effluent will mix. As a result, the fronts will be less sharp. An explanation for the higher pH during elution than predicted are non-equilibrium sorption effects. Generally, adsorption kinetics are faster than desorption kinetics. Therefore, it may be expected that non-equilibrium effects are more obvious during the desorption process than during the adsorption process. However, because the adsorption isotherms of weak organic acids have often the shape of a convex type isotherm the breakthrough fronts of these organic acids are generally sharp and faster than their diffuse elution front (Scheidegger *et al.*, 1994). The combinations of fast adsorption kinetics/fast breakthrough and slow desorption kinetics/slow elution might cause non-equilibrium effects in both the breakthrough and elution curves. For desorption of malonate, non-equilibrium interaction would result in less proton release and therefore in a higher pH than predicted assuming local equilibrium.

3.5 Conclusions

In the present study, we investigate the breakthrough of malonate and pH through a column packed with goethite coated sand. The increase in pH during the breakthrough of malonate indicates the release of OH^- upon malonate adsorption. The fronts and plateaus in the breakthrough curves of malonate and protons occur at the same time. This indicates the interaction chemistry of both components on the goethite surface and in solution. The figures of malonate concentration and pH breakthrough show a fast initial breakthrough of the first front and a complete breakthrough within three pore volumes. A better insight into the distribution of protons over solution and surface is given by the breakthrough of the acidity. This breakthrough shows the same shape as the malonate breakthrough. However, the level of the first plateau is different. The second part of the breakthrough is important for the change in acidity, whereas there is only a small change in malonate concentration. The occurrence of the fronts is related to the binding capacities of the column for both malonate and acidity. The first front is the "malonate front" while the column becomes almost saturated with malonate. The second front is the "acidity front" while the column becomes saturated with protons.

During elution of a column initially in complete equilibrium with malonate, the concentration of malonate in the effluent decreases sharply after 1 pore volume. This decrease is caused by the flushing out of the equilibrium malonate concentration in a saturated column. After the sharp decrease, there is a slow desorption of malonate from the column as a result of the strongly non-linear sorption behavior of malonate. This desorption process will last for a large number of pore volumes although this cannot be illustrated from the malonate desorption data.

The fact that the pH in the effluent is lower than the pH of the feed solution indicates that protons are released upon desorption of malonate. The fact that this lasts for a large number of pore volumes illustrates the slow desorption process more obvious than the malonate desorption data.

The experimental data were predicted with a combination of the CD-MUSIC model and a transport equation. The model gave a reasonable prediction. The discrepancy between model predictions and experiment can either be caused by the "dead volume" of the column set up or can be due to non-equilibrium interaction chemistry.

Acknowledgments

The authors thank Mr. J. Dijkstra and Mr. E. Heij for their efforts in carrying out the experimental analyses.

4

Adsorption of fulvic acid on goethite

Abstract – The adsorption of fulvic acid by goethite was determined experimentally as a function of concentration, pH, and ionic strength. The data were described with the CD-MUSIC model of Hiemstra and Van Riemsdijk (1996), which allows the distribution of charge of the bound fulvate molecule over a surface region. Simultaneously, the concentration, pH, and salt dependency of the binding of fulvic acid can be described. Using the same parameters, the basic charging behavior of the goethite in the absence of fulvic acid could be described well. The surface species used in the model indicate that inner sphere coordination of carboxylic groups of the fulvate molecule is important at low pH, whereas at high pH the outer sphere coordination with reactive groups of the fulvate molecule with high proton affinity is important.

Jeroen D. Filius, David G. Lumsdon, Johannes C. L. Meeussen, Tjisse Hiemstra, and Willem H. Van Riemsdijk

Geochmimica et Cosmochimica Acta (2000), **64**, 51-60

4.1 Introduction

Metal (hydr)oxides play an important role in the adsorption and transport of organic substances in many natural aquatic systems. Retention of organic acids by geo colloids influences the mobility of organic matter and also the physical/chemical behavior of the geo colloids. In the last two decades, a considerable amount of work has been published on the binding of weak organic acids (Balistrieri and Murray, 1986; Ali and Dzombak, 1996; Filius *et al.*, 1997) and organic matter by minerals (Parfitt *et al.*, 1977c; Tipping, 1981; Davis, 1982; Jardine *et al.*, 1989; Gu *et al.*, 1994 and 1995; Wershaw *et al.*, 1995;). The results show that the adsorption of organic acids by mineral surfaces is dependent on pH and electrolyte concentration. The organic acids are bound over a large pH range, even at pH values well above the point of zero charge (PZC) of the adsorbing surface.

Gu *et al.* (1995) investigated the binding of natural organic matter (NOM) by hematite using FTIR spectroscopy. They found that both carboxylic and hydroxyl groups are involved in the binding of NOM by hematite. Kaiser *et al.* (1997) showed similar results for organic matter binding by goethite. In order to provide further insight into the mechanisms and functional groups that are involved in the interactions, Gu *et al.* (1995) and Evanko and Dzombak (1998) studied the pH-dependent adsorption of organic acids containing carboxylic or phenolic groups. Compounds with carboxylic groups show an adsorption maximum at low pH, whereas compounds containing phenolic groups show a maximum at high pH. This suggests that carboxylic groups are relatively important for the binding of NOM at low pH, whereas hydroxyl groups are relatively important at high pH. Similar conclusions follow from the work of Kummert and Stumm (1980) on the adsorption of catechol and benzoic acid on Al_2O_3.

Only a few attempts were made to model the adsorption of NOM. To date, most studies modeling NOM sorption by mineral surfaces employ sorption isotherms (Tipping, 1981; Gu *et al.*, 1994; Van der Weerd *et al.*, 1999). This approach is quite limiting in the sense that the model is only applicable under limited conditions (*e.g.*, constant pH, ionic strength, and competing ion concentration). A first attempt to include the charging and binding of NOM in speciation calculations is made by Karltun (1998). However, his study discusses the binding of fulvic acid (FA) for a rather small set of data (1 adsorption edge with or without SO_4^{2-} present at constant ionic strength). Vermeer *et al.* (1998) simulated the

binding of humic acid by hematite by using polyelectrolyte adsorption theory. Their model calculations suggest internal induction of charge, resulting in a more positively charged oxide surface and more negatively charged humic acid. This suggests the proton reactive groups of the humics and the hematite internally titrate each other.

In this paper, the adsorption of fulvic acid (FA) by goethite is studied. FA was chosen as a model compound for NOM because FA molecules are highly soluble and relatively small. This enables distinction between the different functional groups of the acid. The aim of the present study is to include the pH- and salt-dependent binding of FA by goethite in speciation calculations. For this purpose, the binding of FA by goethite is measured in batch equilibration experiments as a function of pH, FA concentration, and ionic strength. The approach we use here is built upon the insights gained from the description of the binding of relatively small, well-defined weak organic acids by goethite (Filius *et al.*, 1997).

4.2 Model description

4.2.1 The CD-MUSIC model

In this study, we will use the CD-MUSIC (Charge Distributed MUlti SIte Complexation) approach in order to describe the binding of FA by goethite. For more details about this approach, refer to Hiemstra and Van Riemsdijk (1996).

Following Hiemstra and Van Riemsdijk (1996), the charging behavior of the goethite in absence of FA can be described assuming the protonation of singly and triply coordinated surface groups according to:

$$\text{-FeOH}^{0.5-} + \text{H}^{+} \Leftrightarrow \text{-FeOH}_2^{0.5+}; \qquad \log K_{H1} \qquad [4.1]$$

$$\text{-Fe}_3\text{O}^{0.5-} + \text{H}^{+} \Leftrightarrow \text{-Fe}_3\text{OH}^{0.5+}; \qquad \log K_{H2} \qquad [4.2]$$

The proton affinity constants (K_{H1} and K_{H2}) are set equal to the pristine point of zero charge (ppzc) of the goethite. In addition to the protonation of surface groups, the formation of ion pairs influences the charging behavior of the surface.

The charging behavior of goethite can be described using the Basic Stern model. Protons are located in the surface plane (0-plane), whereas the ion pair formers are present at the head end of the diffuse double layer (1-plane) (Hiemstra and Van Riemsdijk, 1996.). The

Stern layer has a capacitance, C, which is for goethite approximately 0.9 F/m^2. This capacitance is found by fitting the model to the charging curves of the goethite. It is possible to interpret the capacitance value in terms of a distance, d, if the dielectric constant is known. Both are related according to:

$$C = \frac{\varepsilon_0 \varepsilon_r}{d} \qquad [4.3]$$

At the interface, the dielectric properties change from a high value at the solution side (ε_r water = 80) to a low value in the solid (ε_r goethite = 11). Assuming an average relative dielectric constant between the 0- and 1-plane of 45, the separation between the 0- and 1-plane is 0.44 nm; approximately 1½ water molecule.

Table 4.1 lists the parameters used for the description of the charging behavior of the goethite used.

Table 4.1

Basic physical chemical parameters used for the description of the charging behavior of goethite.

A:	94 m^2/g
C:	0.9 F/m^2
N_s (FeOH):	3.45 s/nm^2
N_s (Fe_3O):	2.7 s/nm^2
PPZC:	9.2
Log K_{Na+}	-1
Log K_{NO3-}	-1

4.3 The binding of organic anions

Filius *et al.* (1997) were able to describe the binding of several well-defined weak organic acids with the CD-MUSIC model. Based on the size and structure of the adsorbed polyprotic weak organic acids, a distribution of charge of the complexed organic molecule over three electrostatic planes was assumed. Filius *et al.* (1997) distinguished between the formation of inner sphere complexes and outer sphere complexes. The carboxylic groups are assumed to bind as inner sphere complexes with singly coordinated surface groups (Parfitt *et al.*, 1977a;

Table 4.2

Reaction equations for the reactions possible to occur on the surface with the corresponding change of charge (Δz_i) in plane i.

	Reactions	Δz_0	Δz_1
1	$-FeOH^{0.5-} + H^+ + RCOO^- \Leftrightarrow -FeOOCR]^{0.5-} + H_2O$	+0.5	-0.5
2	$-FeOH^{0.5-} + H^+ + RCOO^- \Leftrightarrow -FeOH_2\cdots OOCR]^{0.5-}$	+0.8	-0.8
3	$-Fe_3O^{0.5-} + H^+ + RCOO^- \Leftrightarrow -Fe_3OH\cdots OOCR]^{0.5-}$	+0.8	-0.8
4	$-FeOH^{0.5-} + H^+ + RCO^- \Leftrightarrow -FeOH_2\cdots OCR]^{0.5-}$	+0.8	-0.8
5	$-Fe_3O^{0.5-} + H^+ + RCO^- \Leftrightarrow -Fe_3OH\cdots OCR]^{0.5-}$	+0.8	-0.8

Note: In the change of charge in the 0-plane (Δz_0) the charge of the proton is also included.

reaction 1 of table 4.2) or outer sphere complexes with both singly and triply coordinated surface groups (reactions 2 and 3 of table 4.2). Hydroxyl groups bind only as outer sphere complexes (reactions 4 and 5 of table 4.2). An equal distribution of the charge from a carboxylate group ($R\text{-}COO^{-1}$) over both oxygens was assumed. Each oxygen atom of a carboxylate thus carries half a unit negative charge (-0.5 vu). Inner sphere complex formation of the carboxylate oxygen with a Fe ion in the surface leads to a full neutralization of the bridged oxygen since the Pauling charge (Pauling, 1929) of a Fe-O bond equals +0.5 vu. Filius *et al.* (1997) did not assume inner sphere interaction with organic hydroxyl groups (R-COH) since this leads to undersaturation of the common ligand charge (-0.5 vu) if Fe-O-C-R is formed or overcompensation if Fe-OH-C-R is formed (+0.5 vu). For cases where inner sphere formation occurs, an oxygen of the carboxylate group exchanges for a singly coordinated surface group (Parfitt *et al.* 1977a). In the ligand exchange process, -0.5 vu of the coordinating carboxylate oxygen is located in the 0-plane. The -0.5 vu of the second carboxylate oxygen is located in the 1-plane (see table 4.2).

Outer sphere complexes can be formed as a result of H bond formation between carboxylate and hydroxyl groups of the organic molecule and singly and triply coordinated surface groups. In the present MUSIC model, the charge of the surface proton is fully attributed to the surface oxygen, although H bonds may transfer charge between, for instance, the oxygens of the surface and water molecules in solution (Hiemstra *et al.*, 1996). This simplification can be accepted as long as the strength of the H bonds are not changed in the adsorption process. According to Brown (1978), the H bond involved in organic complexes

can be stronger than the H bond between water molecules. This implies that extra charge will be transferred between the surface and the 1-plane due to the stronger H bond. This extra charge transfer agrees with the infrared spectra of adsorbed catechol (Gu *et al.*, 1995), salicylate, and NOM bound by goethite (Yost *et al.*, 1980; Gu *et al.*, 1995; Kaiser *et al.*, 1997). In these spectra, a strong single band appears around 1270/cm. Novack (1974) showed empirically that low infrared frequencies are correlated with smaller O-O distances, which leads to more symmetrical H bonds. If the band around 1270/cm is attributed to H bonds, we estimate that the H bond transfers between 0.2 (H bond with H_2O) and 0.5 vu. (symmetrical H bond). According to Filius *et al.* (1997), this extra charge transfer equals about 0.2 vu. It means that in case of H bonding, the charge contribution of the proton to the surface plane will be 0.2 vu smaller. A value of 0.2 vu flows to the 1-plane (see table 4.2).

Gu *et al.* (1995) and Evanko and Dzombak (1998) studied the binding of anions containing carboxylic and/or phenolic groups. Both studies show that compounds containing carboxylic groups have their adsorption maximum at low pH whereas compounds containing phenolic groups have their adsorption maximum at high pH. This adsorption behavior is similar to adsorption behavior of anions and cations, respectively. The pH dependence of ion adsorption is directly related to the macroscopic "exchange" with protons. Co-adsorption of protons leads to a decrease of the adsorption with increasing pH, whereas release of protons leads to an increase of adsorption with increasing pH.

At low pH, the goethite surface is positively charged. In solution carboxylic groups can be deprotonated even at low pH. Therefore carboxylic groups can bind as anions according to:

$$FeOH_2^{0.5+} + RC(-O^{0.5-})(=O^{0.5-}) \Leftrightarrow Fe-{}^{0}O-C(=O^{-0.5})R + H_2O \qquad [4.4]$$

This reaction will cause a co-adsorption of protons (or release of OH^-) due to the near-Nernstian behavior of the surface.

The opposite holds for the binding of phenolic groups to the goethite surface. At high pH, the surface is negatively charged and the phenolic group in solution is uncharged. The adsorption behavior of a phenolic group can be explained assuming that the proton from the hydroxyl group of the catechol molecule protonates (or "titrates") a surface hydroxyl groups forming an H bond:

$$FeOH^{0.5-} + RC\text{-}OH \Leftrightarrow \begin{matrix} FeO^{0} \cdots H \cdots^{-0.5} O-CR \\ \backslash \\ H \end{matrix} \quad [4.5a]$$

or

$$FeOH^{0.5-} + RC\text{-}OH \Leftrightarrow Fe-OH_2^{+0.3} \cdots^{-0.8} O-CR \quad [4.5b]$$

In equation [4.5a], the depicted H bond is symmetrical. In this study, the charge distribution of the H bond is based on the extra transfer of charge due to differences in the strength of the H bonds between the surface and organic complexes or H_2O (see equation [4.5b]).

Part of the positive charge of the proton is now attributed to the surface plane. Due to the near-Nernstian behavior of the surface charge, this will result in a net release of protons.

4.4 Materials and Methods

4.4.1 Goethite

Goethite preparation was based on the procedure of Atkinson *et al.* (1967) and is described in more detail by Hiemstra *et al.* (1989b). The BET-N_2 surface area of the sample was 94 m^2/g.

4.4.2 Fulvic acid extraction

Soil humic and fulvic acids were extracted from a soil using methods based on those recommended by the International Humic Substances Society (Aiken *et al.*, 1979; Swift, 1996). The soil used was a Bs horizon from a peaty podzol (Strichen association). Soil, 1 kg, was extracted in 10 dm^3 of redistilled 1 M hydrochloric acid for 24 h and then centrifuged at 10,000 *g* using a Alpha Laval centrifugal separator. The supernatant was retained and pumped onto a column of XAD-8 resin [poly(methyl methacrylate)]. The column was then water-washed and the FA fraction 1 was removed from the column using 0.1 M NaOH. The recovered material (FA fraction 1) was acidified and retained for further treatment.

The soil residue was rolled in 10 dm^3 of 0.1 M NaOH for 4 h and then left to stand overnight. The suspension containing the extracted humic material was removed from the remaining sediment and centrifuged to remove additional mineral material. The suspension

was then acidified to pH 1.3 using 6 M hydrochloric acid and left to stand for up to 48 h to allow the precipitated humic acid fraction to settle. The supernatant remaining after precipitation of the humic acid (FA fraction 2) was removed from the humic acid and pumped onto the XAD-8 column. The column was water-washed and FA fraction 2 was back eluted from the column with 0.1 M NaOH then acidified with 6 M HCl. At this stage, both FA fractions were combined and pumped onto the XAD-8 column. Following removal from the XAD-8, the Strichen fulvic acid (SFA) was treated with Amberilite resin 120 in the H^+ form (1 h), pH 2.3, then freeze dried and stored for further use.

4.4.3 Potentiometric titrations

Potentiometric titrations were carried out at two electrolyte concentrations (0.01 and 0.1 M NaCl) by using the automated Wallingford titrator (Kinniburgh *et al.*, 1995). Fifty-five milligrams of SFA was dissolved in 50 ml Milli-Q water giving a concentration of 1.1 g/L. Carbon dioxide was excluded using a thermostated reaction vessel under a nitrogen atmosphere. The pH was read using a pH electrode calibrated with pH 4.005 and 6.857 buffers before and after each titration. A single calomel reference electrode was connected to the vessel via an electrolyte bridge (0.1 M KNO_3). The electrode readings were stable within drifts of 0.2 mV/min. The titration of the FA included 2 up and down cycles carried out at increasing ionic strength. Before the start of the first titration cycle, the solution was titrated with 0.1 M NaOH to approximately pH 10.5. NaCl was added to obtain the initial ionic strength. Data points were collected at approximately 5 mV intervals in the range of -200 mV to 200 mV (pH range 3.8-10.6). After finishing the first acid and base titration, NaCl was added to obtain the ionic strength for the second cycle.

4.4.4 Data analyses

The ionic strengths were calculated for each data point explicitly taking into account both the background electrolyte ions and free H^+ and OH^-. From the calculated ionic strength (I), the activity coefficients (f) were determined using an adapted Davies equation:

$$-\log f = 0.51 * z^2 * \{\frac{\sqrt{I}}{1+\sqrt{I}} - 0.2 * I\} \quad [4.6]$$

Blank correction was carried out by calculating, for each data point, the amount of titrant required to increase the pH of an equivalent volume of background electrolyte solution. This was subtracted form the volume of titrant used for the sample.

4.4.5 Adsorption experiments

The FA adsorption by goethite was measured in background electrolytes of 0.01 M and 0.1 M $NaNO_3$, using a batch equilibration procedure. Samples for equilibration were prepared by adding 1 mL of $NaNO_3$ (0.2 or 2 M) to a series of polyethylene vessels, followed by 1.5, 3, or 6 mL of a FA stock solution containing 1 g FA L^{-1}. The pH was adjusted by adding various amounts of 0.1 M HNO_3 to give pH values in the range from 3 to 11. Then, ultrapure water (UV-oxidized) was added to bring the volume in the vessels to 10 mL. Finally, 10 ml of a goethite suspension (10 g/L) was added to each vessel to bring the total volume to 20 mL. During each addition, the vessels were N_2-sparged to avoid CO_2 contamination. The suspensions were equilibrated for 72 h in an end-over-end shaker in the dark. To avoid possible artefacts introduced from filtering, the equilibrium supernatant was separated from the solid phase by centrifugation (26,500 *g* for 30 min). Samples of the supernatant were taken for total organic carbon (TOC) analysis (samples were acidified and immediately analyzed with a Skalar SK12 Organic Carbon Analyzer). The pH of the solutions was measured in the remaining supernatant using an electrode that was calibrated (EMF-pH relationship) with standard pH 4.00 and 7.01 buffers (Merck Darmstadt, Germany, accurate to ± 0.01). The amount of FA adsorbed was determined from the difference between the initial and final FA concentrations in the equilibrating solution. The initial FA solution concentration was calculated from experimental blanks treated as above, but in the absence of goethite.

The model calculations were carried out with the computer program Orchestra (Meeussen et al, 1997).

4.5 Results

4.5.1 Fulvic acid in solution

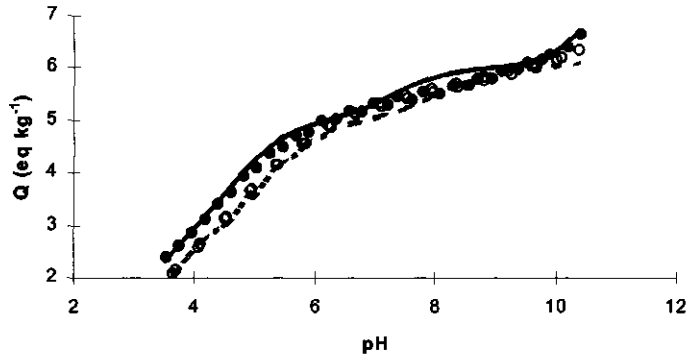

Fig. 4.1 Charging behavior of SFA in 0.1 (solid line and symbols) and 0.01M NaCl (dotted line and open symbols). The lines are fitted using 8 discrete $\log K_H$ values for the different sites.

The charging behavior of the SFA is given in figure 4.1. Similar charging behavior of fulvic acids was found in several studies (Ephraim *et al.*, 1986; Christensen *et al.*, 1998). The data show an increase in negative charge of the FA with increasing pH. Furthermore, the data show very little salt dependency.

Often, the charging behavior of FA in solution is described using a site-binding model with a continuous distribution of affinity constants. The site-binding model is combined with a double layer model that accounts for electrostatic effects (De Wit *et al.*, 1993b; Milne *et al.*, 1995; Benedetti *et al.*, 1996). According to De Wit *et al.* (1993a) fulvic acids are relatively small molecules, which can easily be seen as small rigid particles. Based on their small size and small ionic strength-dependent charging behavior we will treat the FA in this study as small molecules (like citrate or EDTA). Although FA is a mixture of molecules with a range of molecular sizes and number of reactive groups, we assume a constant molecular weight and a constant, discrete number of reactive groups of the FA molecules. The molecular weight is set to 1000 Dalton (Hansen and Schnitzer, 1969; Aiken *et al.*, 1985; Xu *et al.* 1989). The total number of reactive groups of the FA is estimated using the NICA-Donnan model

Table 4.3

Number of carboxylic and phenolic groups of the SFA

	[a]NICA-Donnan (meq g^{-1})	%	[b]this study (mol eq mol^{-1})
Total	8.38	100	8
Carboxylic	5.56	66	5
Phenolic	2.82	33	3

[a] fitted with the NICA-Donnan model, [b] used in the present study. Note that 1 meq/g equals 1 eq/mol because the molar mass of FA is taken as 1000 g/mol. Therefore1 meq/g is equal to 1 group per FA molecule.

(Benedetti *et al.*, 1995). Table 4.3 shows the number of reactive groups used in the NICA-Donnan model required to fit the charging behavior of the SFA. The numbers used in the present study are presented in the last column of table 4.3. The numbers found agree with the numbers obtained by Christensen *et al.* (1998).

Table 4.4

Protonation reactions of reactive FA groups in solution and corresponding affinity constants.

$FA^{8-} + H^+ \Leftrightarrow FAH^{7-}$	$\log K_{H1} = 12.45$
$FAH^{7-} + H^+ \Leftrightarrow FAH_2^{6-}$	$\log K_{H2} = 11.97$
$FAH_2^{6-} + H^+ \Leftrightarrow FAH_3^{5-}$	$\log K_{H3} = 8.54$
$FAH_3^{5-} + H^+ \Leftrightarrow FAH_4^{4-}$	$\log K_{H4} = 6.07$
$FAH_4^{4-} + H^+ \Leftrightarrow FAH_5^{3-}$	$\log K_{H5} = 5.30$
$FAH_5^{3-} + H^+ \Leftrightarrow FAH_6^{2-}$	$\log K_{H6} = 4.12$
$FAH_6^{2-} + H^+ \Leftrightarrow FAH_7^{1-}$	$\log K_{H7} = 3.40$
$FAH_7^{1-} + H^+ \Leftrightarrow FAH_8$	$\log K_{H8} = 1.67$

The reactive groups above the dashed line are believed to be hydroxyl groups. The reactive groups below the dashed line are believed to be carboxylic groups.

The proton affinity constants (Table 4.4) are fitted to the FA charge data using the speciation program ECOSAT (Keizer and Van Riemsdijk, 1995) coupled with Kinniburgh's FIT software (Kinniburgh, 1993). In this approach, the proton affinity constants depend on the type of activity correction used for the FA. For simplicity, the activity coefficients of salt ions, protons and FA in solution are calculated using the Davies equation (equation [4.6]). The Davies equation is often used to calculate the activity coefficient of small ions. With this simplified approach, it is possible to get a reasonable agreement between data and model description using the Davies equation. The lines in figure 4.1 represent the model description. In this approach, the FA contributes to the ionic strength. The presence of the FA (1.1 g/L ≈ 1.1 mmol/L) affects the ionic strength up to a factor 4 at low salt levels. However, model calculations using low FA concentrations (not affecting the ionic strength) show that the change in ionic strength due to FA only affects the charging behavior of FA significantly at pH > 10.

4.5.2 The adsorption of FA by goethite

Figure 4.2 shows the binding of SFA by goethite. The data set covers a broad range of conditions. Over the whole pH range investigated, sorption of FA by goethite was found. At pH values below the PZC (PZC = 9.2), the goethite surface and the FA have an opposite charge. This results in a high adsorption of FA. At pH values above the PZC, the goethite surface and the FA are both negatively charged. Despite the electrostatic repulsion, a considerable amount of FA is adsorbed by the goethite.

The salt dependency of the FA binding by goethite is negligible within the experimental error of the data over the entire pH range.

4.5.3 Modeling the sorption data

Mechanistic modeling requires the introduction of the basic physical chemical surface characteristics. The description of the FA adsorption by goethite is built upon the framework that describes both the charging behavior of the goethite surface and the charging behavior of the FA in solution. The same parameter values as given in table 4.1 and 4.4 are used in the description of SFA adsorption. Furthermore, it is assumed that the charging behavior of the

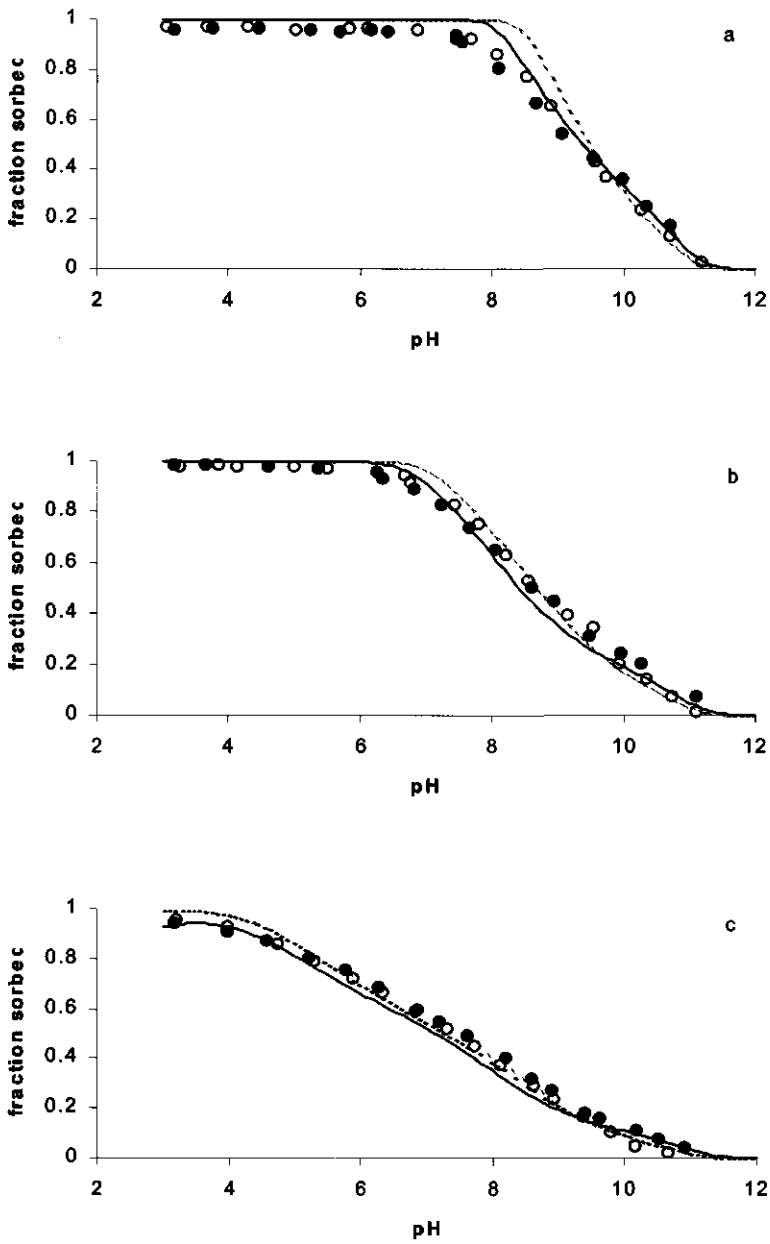

Fig. 4.2 Adsorption envelopes of SFA binding by goethite in 0.01 M (open symbols and dotted lines) and 0.1 M $NaNO_3$ (solid symbols and full lines). The suspension density of goethite is 5 g/L and three total concentration of FA are used: a) 75 mg/L; b) 150 mg/L; and c) 300 mg/L. The lines indicate model calculations.

reactive groups of adsorbed FA can be described using the same proton affinity constants as in solution (table 4.4).

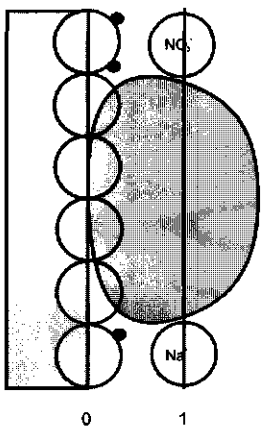

Fig. 4.3. Schematic representation of adsorbed fulvic acid on the goethite surface. The lines (0- and 1-plane) indicate the boundaries of the Stern layer.

Compared to the size of a proton, the FA is a large molecule with a considerable number of reactive groups. If one is interested to model the adsorption with surface species that may have physical significance it is obvious that the charge of the bound FA should not be regarded as being a point charge. The charge of the bound molecule is distributed to some extent into solution (figure 4.3). There are no experimental data available that quantify this distance. De Wit *et al.* (1993a,b) estimated an average spherical radius for fulvic acids in solution of 0.75 nm. This value is in agreement with the radii deduced from viscometry by Avena *et al.* (1999). The extent to which the adsorbed fulvate molecule will protrude into the solution is at the most similar in magnitude to the diameter of the molecule in solution. However, the configuration of the FA molecule is likely to be flattened as a result of the coordination with the surface. Vermeer *et al.* (1998) suggested that humic acid molecules adsorb relatively flat on the mineral surface at high pH and have a reduced contact with the surface at low pH. Due to this reduced contact it is expected that the bound FA molecules will protrude further into solution at low pH. However, the charge of these non-coordinated groups is low due to the protonation of the reactive groups at low pH. Therefore, we assume that only a limited amount of charge protrudes into solution. In the present study the negative

charge of groups on the fulvate molecule that are not directly involved in the inner and outer sphere coordination to the surface is located in the 1-plane.

Table 4.5

Affinity constants for ligand exchange and H bonding.

$LogK_{exch}$:	-0.45
$LogK_{h\text{-}b,carb}$:	1.24
$LogK_{h\text{-}b,phen}$:	5.21

4.5.4 Affinity constants

Following Filius *et al.* (1997), we assume that the FA molecules can become bound by the surface due to ligand exchange or H bond formation. The overall logK of the surface complexation reaction of FA consists of the summation of the affinities of the protonation of the coordinating surface groups, the formation of inner and outer sphere complexes, and the protonation of non-coordinated fulvate groups. An example of the calculation of the overall logK is given in Appendix A.

- The affinity constants for the ligand exchange reaction and H bond formation (reactions 1-5 of table 4.2, respectively) are assumed to be constant. The constants are found by curve fitting and listed in table 4.5.
- The intrinsic proton affinities for the reactive groups of the fulvate molecule are the same on the surface as they are in solution (see table 4.4).
- The FA groups with the highest proton affinity may become protonated.
- H bonds are formed between surface groups and FA groups. It is assumed that the FA group with the highest proton affinity will be preferred in H bond formation with the surface except the groups orientated towards the solution that are protonated (see previous point).

4.5.5 Degrees of freedom and constraints

There are several degrees of freedom left in the modeling:

- the affinity constants for ligand exchange and the formation of an H bond,

- the number of groups involved in ligand exchange (k),
- the number of groups forming an H bond (l),
- the number of non-coordinated groups that may become protonated (n),

where k, l, and n refer to the coefficients used in table 4.6 in order to calculate the change in charge in the electrostatic planes.

However, there is a constraint to the degrees of freedom mentioned:

- the total number of reactive groups per fulvate molecule equals 8,

This gives a total of four degrees of freedom in the model.

Table 4.6

Calculation scheme for the change of charge in the electrostatic planes of the CD-MUSIC model.

$\Delta z_0 = k.z_O + (k+l).z_H - l.\Delta s_{O\bullet\bullet\bullet H}$
$\Delta z_1 = m.z_O + n.z_H + l.\Delta s_{O\bullet\bullet\bullet H}$

Note: Δz_i, change of charge in plane i; z_0, z_H, charge of, respectively, carboxylate or hydroxyl oxygens and protons; $\Delta s_{O\ldots H}$, change of charge due to change in strength of H bonds; k - n, coefficients corresponding to the various quantities. Note that z_0 is -0.5 for a carboxylate oxygen and -1 for a hydroxyl oxygen.

4.5.6 Number of surface species

FA molecules can bind in many different configurations to the surface. The total number of possible surface species is approximately 10,000. However, in case of inner or outer sphere complexation the model cannot differentiate between the reactive groups that are deprotonated. Still, the model can distinguish between more than a thousand different surface species. To limit this number, we assume that the reactive FA groups will form complexes in the order of: protons > outer sphere > inner sphere. This means that in the surface complexation of a FA molecule with 1 inner sphere complex, 1 outer sphere complex, and 1 protonated group, the reactive group with the highest proton affinity is protonated, the second highest proton affinity group forms an outer sphere complex and one of the rest of the groups

forms an inner sphere complex. This assumption limits the number of possible surface species to approximately 100.

The number of possible species is further limited by the chemical characteristics of the FA binding. The protonation of the non-coordinated FA groups will be influenced by the electric field near the surface. At low pH, protons are repelled from the positively charged surface. The pH near the surface (pH_s) is higher than in solution. At high pH, pH_s is lower than in solution due to the attraction of protons. This electrostatic effect results in a smaller pH window near the surface than in solution. At low pH, fewer reactive groups of the bound FA will be protonated than in solution. At high pH, the opposite holds. This reduces the number of possible surface species.

For model purposes it is not convenient to use a large number of surface species. Therefore, we try to model the data with a minimum number of species. In this study, we will try to determine the most important surface species that can account for the effect of concentration, pH, and salt on the binding of fulvate molecules. Apart from simplicity, the chosen approach will also give more insight in the main factors that dominate the binding behavior of FA on variable charge minerals.

4.5.7 Model results

The lines in figure 4.2 represent the model description of the data. Four surface species are required to obtain a satisfactory description. The assumed surface species, charge distribution, and affinity constants for the model description are given in table 4.7. Using this set of surface species, the adsorption of FA as function of pH, FA concentration, and ionic strength is described well. Figure 4.4 shows the relative contribution of the different surface species to the total binding of the fulvate by goethite.

At pH>5, the binding is described using a surface species with 4 H bonds. Note that is has been assumed that the groups with the highest proton affinity are considered to participate in the H bond formation. At high pH, the rest of the reactive groups are deprotonated. At lower pH, the two phenolic groups with highest proton affinities are not involved in H bonding with the surface, but are assumed to be orientated towards the solution and to be protonated.

Table 4.7

Surface species assumed for describing the adsorption of Strichen fulvic acid by goethite

Species	Surf.site	H	FA	logK	Δz_0	Δz_1
$Fe_{(4)}(OH_2)_3FAH_3]^{-3}$	1+3	7	1	73.0	2.9	-3.9
$Fe_{(4)}(OH_2)_4FAH_2]^{-4}$	0+4	6	1	70.2	3.2	-5.2
$Fe_{(4)}(OH_2)_4FAH]^{-5}$	0+4	5	1	62.2	3.2	-6.2
$Fe_{(4)}(OH_2)_4FA]^{-6}$	0+4	4	1	53.7	3.2	-7.2

Note: The subscripts between brackets indicate the number of goethite surface groups involved in the goethite-fulvate complex. The subscript after (OH_2) indicates the number of outer sphere complexes. The difference between both subscripts is the number of inner sphere complexes. $Fe_{(4)}(OH_2)_3FAH_3$, 4 outer and 1 inner sphere bond, the hydroxyl groups remain protonated; $Fe_{(4)}(OH_2)_4FAH_2$, 4 outer sphere bonds, two hydroxyl groups with highest $logK_H$ remain protonated; $Fe_{(4)}(OH_2)_4FAH$, 4 outer sphere bonds, hydroxyl group with highest $logK_H$ remains protonated (see also Appendix A).

At pH<5, the data give little information because the two lowest FA additions are almost fully adsorbed by the goethite. The adsorption of the highest FA addition can be modeled assuming one inner and three outer sphere complexes and all phenolic groups protonated.

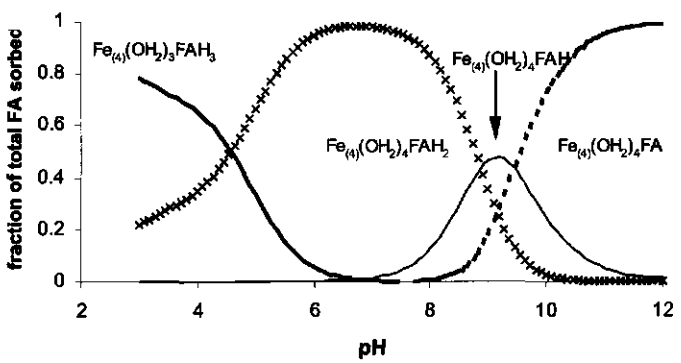

Fig. 4.4 The contribution to the total adsorption of the four surface species used to describe the FA binding by goethite for a FA_{tot} concentration of 300 mg/L and a background electrolyte concentration of 0.01 M.

4.6 Discussion

The surface species used to describe the SFA binding data are based on three macroscopic binding characteristics: 1) pH dependency; 2) concentration dependency; and 3) salt dependency. These three characteristics are strongly related to the structure of the adsorbed species and the electrostatic potential profile near the surface.

Figure 4.4 shows that at low pH the surface species with inner and outer sphere complexation are important whereas at high pH outer sphere complexation is important. The pH dependence of the formation of inner and outer sphere complexes might be explained by the differences in the change of the standard Gibbs fee energy (ΔG^{0}_{r}) and the electrical energy (ΔG_{el}) of the reactions.

The change in standard Gibbs fee energy can be related to the intrinsic affinity constant of the reaction ($\log K^{int} \equiv -\Delta G^{0}_{r} / 2.3RT$) and the change in electrical energy is determined by the electrostatic potential (ΔG_{el}). The intrinsic affinity constants for the formation of inner and outer sphere complexes are constants (table 4.5), whereas the electrostatic potential is a variable that depends on pH, ionic strength, and surface coverage.

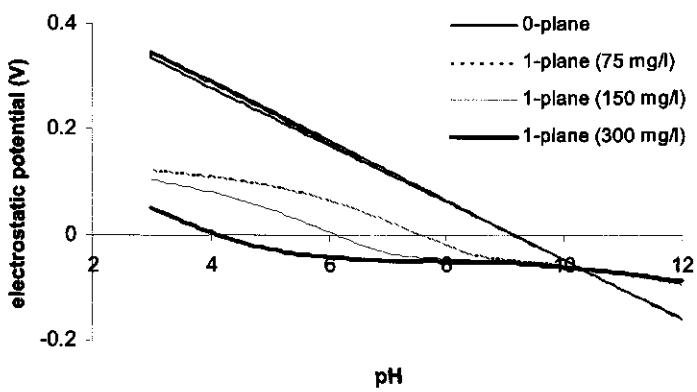

Fig. 4.5 Electrostatic potential of the 0- and 1-plane as function of pH for the three FA additions and a background electrolyte concentration of 0.1 M. Legend is in the same order as the model lines. The calculation of the 0-plane shows the three lines for the different FA additions.

Figure 4.5 shows the electrostatic potential in the 0- and 1-plane. The potential in the 0-plane shows near-Nernstian behavior. At low pH, there is a high positive potential that decreases with increasing pH. The potential in the 1-plane depends on pH, ionic strength, and surface coverage.

The intrinsic affinity for the formation of outer sphere FA-surface complexes is much higher than for inner sphere complexes. Nevertheless, at low pH, inner sphere complexes are found to be important for the binding of organic material (Gu *et al.*, 1995; Kaiser *et al.*, 1997; Nordin *et al.*, 1998). This can be explained by the changes in electrical energy. In both inner and outer sphere complexation, negative charge of the anion is distributed over the 0- and 1-plane. At low pH, the positive potential of the 0-plane is much higher than in the 1-plane. In case of inner sphere complexation, more negative charge is located in the 0-plane. Therefore, the electrical energy gained during inner sphere complexation is much larger than for outer sphere complexation. At low pH, the sum of the change in standard Gibbs free energy and the electric energy ($\Delta G^0_r + \Delta G_{el}$) is higher for inner sphere complexation than for outer sphere complexation. With increasing pH, the difference between the electrostatic potential in the 0- and 1-plane decreases strongly. This means that less electric energy is gained by the location of negative charge in the 0-plane instead of the 1-plane. Therefore, its larger intrinsic affinity favors the formation of outer sphere complexes.

At pH values above the PZC, the electrostatic potential in both planes is negative. For adsorption, the electrostatic repulsion between surface and FA molecule has to be overcome. The intrinsic affinity of phenolic FA groups for outer sphere complexation is large (see table 4.5). Furthermore, the electrical energy gained by the location of the proton of the phenolic group in the negative 0-plane is larger than the loss of energy due to the corresponding negative charge of the phenolate group in the 1-plane. This results in a reduced electrostatic repulsion.

4.6.1 pH dependency

The binding of FA by goethite is strongly dependent on pH. In systems with FA and goethite present there are three types of reactions involving protons: 1) protonation of FA in solution; 2) protonation of reactive goethite surface groups; and 3) proton co-adsorption/desorption upon FA adsorption. The description of the first two types of reactions

is determined by the charging behavior of the FA in solution and the goethite in absence of FA. The co-adsorption/desorption of protons upon the adsorption of FA is the only unknown type of reaction and is directly related to the pH dependency of the adsorption.

Several authors (Fokkink *et al.*, 1987; Venema *et al.*, 1996; Rietra *et al.*, 1999) discussed the proton (or hydroxyl) exchange ratio of ion adsorption. They showed that the exchange ratio depends on the charge of the ion and the location of the charge at a finite distance from the surface. The charge and charge distribution of adsorbed FA molecules are determined by the number of inner and outer sphere complexes formed and the protonation of non-coordinated reactive groups of the sorbed FA. It is assumed that the proton affinity of the non-coordinated reactive groups of the sorbed FA is the same as in solution. Therefore, the number of inner and outer sphere complexes of each surface species and the relative contribution of each surface species to the total adsorption (determined by the affinity constants of inner and outer sphere complexes) determines the proton exchange ratio and the pH dependence of FA adsorption.

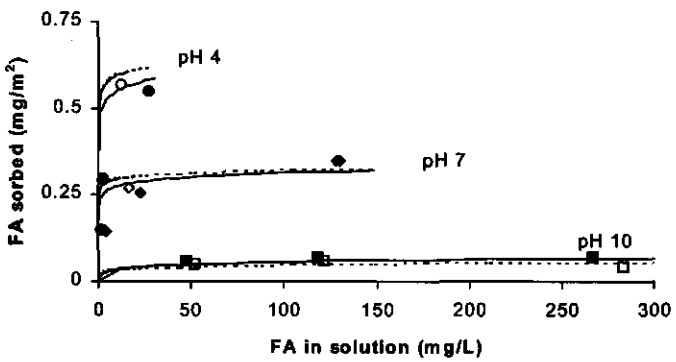

Fig. 4.6 Model predicted adsorption isotherms for FA adsorption by goethite at different pH values. Open symbols show experimental data at 0.01 M (model calculated, dashed line) and closed symbols data at 0.1 M (model, solid line).

4.6.2 Concentration dependency

In figure 4.6, adsorption isotherms of FA by goethite are given at three pH values and two ionic strengths. The data in figure 4.6 are obtained from using smooth interpolation of the adsorption envelopes. The lines are model descriptions based on the parameters obtained in this study. Figure 4.6 illustrates the high-affinity character of the binding at low FA concentrations. For weak organic acids, Filius *et al.* (1997) showed that the increase in the slope of the adsorption isotherms at low concentrations is related to the number of reactive acid functional groups involved in the binding of the organic anion by the surface. The FA adsorption data reveal a steeper adsorption isotherm than for the citrate data of Filius *et al.*, which is consistent with the proposed number of coordinating groups assumed for the FA.

After the high affinity part, the adsorption isotherms in figure 4.6 show a plateau. The effects of elevated surface loading and/or electrostatics might explain the observed adsorption plateau. With increasing adsorption, more of the goethite surface becomes covered by FA. Therefore, each additional FA molecule has less surface to which it can bind. Statistically, this means that the chance an additional FA molecule can bind becomes smaller. This effect results in a reduced slope of the adsorption isotherm with increasing surface loading. At high surface loading an adsorption plateau can occur long before the surface is physically saturated with FA molecules. In our model, this effect is accounted for by multiplying the overall affinity constant by the term $(1-\theta)^n$, in which θ is the surface coverage (number of sites involved in inner or outer sphere formation as fraction of the total number of sites) and n is the number of inner and outer sphere complexes formed per bound molecule. At pH 4 and highest FA concentration, the surface coverage is approximately 0.25 times the theoretical maximum. Note that the adsorbed molecule covers most probably a larger area than the n sites due to the physical size of the molecule. This affects the binding statistics. In the present approach this is not taken into account.

A second cause of the adsorption plateau is the behavior of the surface charge. Due to the sorption of FA, the surface becomes less positive (or more negative). Therefore, each additional molecule is less attracted (or more repelled) by the goethite surface. With increasing adsorption, this means a reduced slope of the adsorption isotherm. This effect can cause an adsorption plateau in case of charge reversal. In our model calculations, we don't observe charge reversal at low pH (see figure 4.5). Therefore, the observed plateau cannot

solely be explained by electrostatics. Most likely, a combination of increased surface loading and electrostatics cause the observed adsorption plateau.

4.6.3 Salt dependency

In case of FA adsorption by goethite, we can distinguish between two situations: 1) the FA and goethite are both charged negatively (high pH); and 2) the FA and goethite are charged oppositely (low pH). When both components are charged equally, the adsorption is favored by a higher background electrolyte concentration. The charge of both components is screened more effectively. This will result in less electrostatic repulsion between the two components. In case FA and goethite are oppositely charged, the goethite surface charge can either be neutralized by bound FA or by NO_3^- pair formation.

The experimental data don't show any salt dependency. Due to the strong adsorption at low pH, all FA is adsorbed at the two lowest FA additions. This gives little information about the salt dependency. For the highest FA addition, the electrostatic potential in the 1-plane is very low. This might explain the lack of salt dependency observed in the data at low pH. Model calculations (data not shown) show that at high pH the protonation of the solution-orientated reactive groups increases at decreasing ionic strength. When the charge reduction near the surface due to protonation of the solution-orientated groups is in the same order of magnitude as the reduction of charge due to the difference in ion pair formation, this might explain the absence of the salt dependency at high pH.

The model describes the salt dependency adequately at both low and high pH as illustrated in figures 2 and 6.

4.7 Conclusions

FA is bound over a wide range of pH values reaching well above the PZC of the goethite. The adsorption of FA by goethite can be described well with the CD-MUSIC model. The data set of FA binding is relatively large although little information can be gained from the data at low pH. Regardful of the assumptions made, the data can be described with only four surface species. Interpretation of the charge distribution of the assumed surface species is consistent with the assumption of inner sphere coordination at low pH and outer sphere

coordination at high pH. The same types of mechanisms are proposed for the binding of compounds containing carboxylic and phenolic groups respectively.

The affinity constant for the ligand exchange of a carboxylate oxygen of the fulvate molecule and a surface water group is very low, indicating a low chemical affinity and a strong electrostatic interaction at low pH. The intrinsic affinity constant for the formation of H bonds is higher and the electrostatic interaction is less than for the inner sphere complexes. At high pH (weak electrostatic attraction or repulsion), outer sphere formation in the FA-surface complex out-competes the inner sphere formation due to the high chemical energy involved in outer sphere complexation. At low pH, the reverse is the case because the electrostatic contribution of inner sphere complexes is stronger dependent on pH. Therefore, at low pH, the combination of a low intrinsic affinity and a high electrostatic contribution of inner sphere complexes out-competes the formation of outer sphere complexes.

The fulvate adsorption isotherms show a steep slope at low FA concentrations followed by a pseudo plateau at higher concentrations. The effects of increased surface loading and electrostatics most probably cause the plateau.

The FA adsorption data show little salt dependency. The model describes the salt dependency accurately.

Acknowledgments— The authors like to thank Pat Cooper and Stefan Jansen for their assistance with the experiments and preliminary interpretation of the results. This research was partly funded by the Scottish Office Agriculture, Environment and Fisheries Department (SOAEFD) as part of its Soils and the Environment program. The reviewers of Geochimica et Cosmochimica Acta are gratefully acknowledged for their helpful comments on the manuscript.

Appendix A

For the first surface species of table 4.7, we show how we calculated the overall affinity constant.

$FeOH^{1/2-} + H^+ \Leftrightarrow FeOH_2^{1/2+}$	$\log K_{H,FeOH}$	(= 9.20)
$3\ Fe_3O^{1/2-} + 3\ H^+ \Leftrightarrow 3\ Fe_3OH^{1/2+}$	$3 \times \log K_{H,Fe3O}$	(= 27.60)
$FA^{8-} + 3\ H^+ \Leftrightarrow FAH_3^{5-}$	$\Sigma_{i=3} \log K_{H,FA}$	(= 32.96)
$FeOH_2^{1/2+} + FAH_3^{5-} \Leftrightarrow Fe_{(1)}FAH_3^{4½-} + H_2O$	$\log K_{exch.}$	(= -0.45)
$3\ Fe_3OH^{1/2+} + Fe_{(1)}FAH_3^{4½-} \Leftrightarrow Fe_{(4)}(OH)_3FAH_3^{3-}$	$3 \times \log K_{h\text{-}b,carb}$	(= 3.72)
$FeOH^{1/2-} + 3\ Fe_3O^{1/2-} + FA^{8-} + 7\ H^+ \Leftrightarrow Fe_{(4)}(OH)_3FAH_3^{3-}$	$\log K_{overall}$	(= 73.03)

The subscripts between brackets indicate the number of goethite surface groups involved in the goethite-fulvate complex, not the number of Fe atoms involved. Note that the formation of H bonds is represented here by bonds with triply coordinated sites while it is assumed also to take place with singly coordinated sites. In our equilibrium calculation scheme, we accounted for the formation of H bonds with two different surface groups by defining a surface species with H bonds with singly coordinated groups and an additional surface species with H bonds with triply coordinated groups. Defining surface species with mixed H bonds did not change the results. Therefore, these species are disregarded.

5

Modeling the binding of benzenecarboxylates by goethite. The ligand and charge distribution (LCD) model

Abstract-A heterogeneous complexation model approach has been developed in order to describe the adsorption of large organic molecules by goethite taking the full speciation of the adsorbed molecules into account. The essence of the ligand and charge distribution (LCD) model is the calculation of the mean mode of an adsorbed organic molecule, defined by an overall affinity, charge distribution, and reaction stoichiometry. The calculation of the mean mode of the adsorbed organic molecule is based on the pH dependent interaction of a functional group for binding a proton or forming an inner or outer sphere complex with specific surface sites. The distribution of the organic molecules over the solid and solution phase is calculated using the CD-MUSIC model (Hiemstra and Van Riemsdijk, 1996) with parameters obtained from the mean mode of the adsorbed molecule. The mean mode of the adsorbed molecule is calculated using the competitive Langmuir-Freundlich or NICCA equation (Kinniburgh et al., 1999) in combination with an electrostatic model comprising charge distribution, taking the competitive binding of functional groups with protons or surface sites into account.

The LCD model is applied to the adsorption data of a series of benzenecarboxylic acids (Boily et al., 2000b). The model approach can describe simultaneously the concentration, pH and salt dependency of the benzenecarboxylate adsorption. Furthermore, the model is applied to describe data obtained from IR spectroscopy. The new approach predicts the data reasonably. In future work the new model will be applied to the adsorption of larger organic acids, *e.g.* fulvic acid.

Jeroen D. Filius, Johannes C.L. Meeussen, Tjisse Hiemstra and Willem H. van Riemsdijk

Accepted by Journal of Colloid and Interface Science

5.1 Introduction

The adsorption of weak organic acids has been subject of many studies (Balistrieri and Murray, 1986; Biber and Stumm, 1994; Ali and Dzombak, 1996; Filius *et al.*, 1997; Evanko and Dzombak, 1998, 1999). Various types of surface complexation models have been used to describe the adsorption successfully. All models are to a certain extent based on the physical and chemical aspects of adsorption. However, realistic surface complexation modeling should meet some chemical and physical constraints. First of all, surface complexation models should be thermodynamically consistent. Furthermore, they should account for the structure of the surface (number and types of surface sites and corresponding proton affinities), the structure of the adsorbate (inner sphere vs. outer sphere, monodentate or bidentate, *etcetera*), the electrostatic profile near the surface, and the position of ions located in this profile.

In situ spectroscopic techniques provide important information about the structure of the adsorbed ions. This information can help to discriminate among the wide variety of models. In order to establish the coordination modes of weak organic acids by oxide surfaces *in situ* infra red (IR) spectroscopy is recently used. However, IR spectroscopy yields information about the local environment of the individual reactive groups of the organic acid rather than about the adsorption mode of the complete organic molecule. Therefore, it is difficult to establish the complete structure of the adsorbed molecule decisively when the adsorbed organic molecule has multiple reactive groups.

For carboxylic acids, Boily *et al.* (2000a) found three states of adsorbed carboxylic groups. They identified the different states or modes as an outer sphere complex, an inner sphere complex, and a protonated carboxylic group. The different adsorption modes compete with each other for the total number of carboxylic groups present at the surface. For organic acids with multiple reactive groups, this competition results in a wide spectrum of speciation possibilities of the adsorbed organic acid molecule. Each of the many surface species has its individual affinity constant and charge distribution (CD). In the surface complexation modeling, the number of adjustable parameters is commonly reduced by taking only the most prominent surface species into account. However, this may lead to an incomplete speciation of the adsorbed molecule and a less realistic model.

In this contribution, we will present a new adsorption modeling approach. The essence of the model is the calculation of the mean mode of an adsorbed organic molecule, defined by an overall affinity, charge distribution, and reaction stoichiometry. The mean mode can be

used in combination with a surface complexation model. The calculation of the mean mode of the adsorbed organic molecule is based on the pH dependent interaction of a functional group for binding a proton or forming an inner or outer sphere complex with specific surface sites. The competitive binding of functional groups with protons or surface sites is calculated using a competitive Langmuir-Freundlich or NICCA equation (Kinniburgh *et al.*, 1999) in combination with an electrostatic model comprising charge distribution.

The model developed in this study is applied to the adsorption of a series of organic molecules with varying number of reactive groups attached to a benzene ring (Boily *et al.*, 2000b). Phthalate has the fewest number of reactive groups (two carboxylic groups). Trimellitate and pyromellitate contain respectively three and four carboxylic groups.

5.2 CD-MUSIC model

Hiemstra and Van Riemsdijk (1989a,b; 1996) describe the ion adsorption behavior of goethite with the Charge Distribution MUlti SIte Complexation (CD-MUSIC) model and discuss the most important characteristics of goethite in detail. Surface groups are distinguished based on metal coordination and bond distances. Singly, doubly and triply coordinated surface oxygens are found on the two main crystal faces of goethite, the 110 and 021 face. The proton reactive oxygens in the pH range between 2 and 12 are supposed to be the singly and triply coordinated surface oxygens. Charge is attributed to the surface oxygens using the Pauling bond valence principle. For the charge of the singly coordinated surface oxygens, the charge is –1.5 vu. ($FeO^{1.5-}$) and for the charge of the triply coordinated surface oxygens one finds –0.5 vu. ($Fe_3O^{0.5-}$). Due to the high undersaturation of the oxygen charge $FeO^{1.5-}$, this group will always bind a proton in the normal pH range, yielding $FeOH^{0.5-}$. Both types of surface groups ($FeOH^{0.5-}$ and $Fe_3O^{0.5-}$) can become positive by binding a proton according to:

$$-FeOH^{0.5-} + H^{+} \Leftrightarrow -FeOH_2^{0.5+} \qquad \log K_{H1} \qquad [5.1]$$

$$-Fe_3O^{0.5-} + H^{+} \Leftrightarrow -Fe_3OH^{0.5+} \qquad \log K_{H2} \qquad [5.2]$$

Following Hiemstra and Van Riemsdijk (1996), the proton affinity constants (K_{H1} and K_{H2}) are set equal to the pristine point of zero charge (PPZC) of the goethite. The site densities of

proton reactive groups are calculated on the basis of the relative presence of the groups on the 110 and 021 face of the goethite surface known from electron spectroscopy.

In the CD-MUSIC approach, the charging curves of the goethite can be described using the basic Stern (BS) double layer model. In the BS model, two electrostatic planes (0- and d-plane) enclose the Stern layer, which is free of charge. The Stern layer has a capacitance, which is found by fitting the model to the experimental charging curves of goethite. Ion pairs are assumed to be formed and located at the solution side of the stern layer, which coincides with the head end of the diffuse double layer (ddl).

Filius *et al.* (1997) showed that the electrostatic energy is very important for the binding of small, well-defined weak organic acids by goethite. The electrostatic potential gradient near the surface is extremely large, and a correct location of charge is essential. If one is interested in chemically and physically realistic modeling of the adsorption, the charge of the bound organic molecules should not be regarded as a point charge. Compared to the size of a proton, organic molecules are large and therefore charge is not located at one position but distributed. The most important factor in the distribution of charge is the distribution of the charged ligands of the organic molecule. The charge of the reactive groups of the organic molecules is distributed over the surface plane (0-plane) and the Stern plane (1-plane). In the present approach, the charge of the bound organic molecule is located in the 1-plane except for the charge of the groups that co-ordinate specifically with the surface. The charge of these groups is located closer to the surface and is therefore partly placed in the 0-plane. Due to the strong gradient in electrostatic potential near the oxide surface, even the distribution of the charge of the individual coordinating ligand is very important. The precise location of the charge of the coordinating ligands in the solid-water interface is not known explicitly. Although other charge distributions may be possible, we apply the charge distribution for inner and outer sphere complexes as we found in previous studies modeling the binding of weak organic acids by goethite (Filius *et al.*, 1997, 2000). The charge distributions applied are discussed into more detail in the next section.

5.3 Specific interactions

Recently, a lot of work has been done on the organic acid-mineral interactions on a molecular level using IR spectroscopy (Parfitt *et al.*, 1977a,c; Yost *et al.*, 1990; Biber and Stumm, 1994; Gu *et al.*, 1994; Kaiser *et al.*, 1997; Nordin *et al.*, 1998; Persson *et al.*, 1998;

Boily *et al.*, 2000a,b). The results are interpreted in terms of ligand exchange or H bond formation. In this study we assume that the carboxylic groups of the organic molecules can form inner sphere complexes with the singly coordinated surface groups and outer sphere complexes with singly and triply coordinated surface groups.

In case of inner sphere complexation, an oxygen atom of the carboxylate group exchanges for a surface water group (only singly coordinated surface groups) according to reaction 1 in table 5.1. The overall charge of the carboxylate groups (-1 vu.) is equally divided over both carboxylate oxygens (2 * -0.5 vu.). In case of inner sphere complexation, one carboxylate oxygen and corresponding charge (-0.5 vu.) is located in the surface (0-plane). This leads to a change of charge of Δz_0 = -0.5 (Table 5.1). The charge of the second carboxylate oxygen (-0.5 vu.) is located in the 1-plane (Δz_1 = -0.5). It is interesting to note that the CD values used leads to a full neutralization of the charge of the carboxylate oxygen that forms a bond with the surface due to the attribution of +0.5 vu. of the iron charge in the solid.

Outer sphere complexes are linked to the protonated surface site by an H bond (reaction 2 and 3 in table 5.1). Both singly and triply coordinated groups can form outer sphere complexes. This contrasts with inner sphere complexation, which is only possible for singly coordinated groups. The charge of the organic group (-1 vu.) is located in the 1-plane. The charge of the proton in the H bond is distributed over the 0- and 1-plane. About 0.2 vu of the proton charge is transferred from the surface to the 1-plane, leading to CD coefficients of Δz_0 = -0.2 and Δz_1 = +0.2–1 = -0.8. In the following text, outer sphere complexation will only be exemplified for singly coordinated surface groups. In the modeling both complexes with singly and triply coordinated groups (reactions 2 and 3) will be used assuming the same affinity constant and CD.

Reactions 4 and 5 in table 5.1 express the adsorption and protonation of the solution-orientated reactive groups of the bound organic molecule. The solution-orientated groups do not have a direct interaction with specific surface groups, but are bound by the surface due to the complex formation of surface sites with other functional groups of the same adsorbed organic molecule. This structural feature is indicated by # in reactions 4 and 5 in table 5.1.

5.3.1 Surface speciation

The speciation of an individual functional group is characterized by 4 modes, *i.e.* deprotonated, protonated, and complexed (inner or outer sphere) with a surface group (*e.g.* see table 5.1). In a multiple organic acid, the reactions can occur for each functional group.

Table 5.1

Reactions determining the speciation of the adsorbed organic groups

	Reaction	K	Δz_0	Δz_d
1	$FeOH_2^{1/2+} + RCOO^- \Leftrightarrow Fe-^0\ O^{-1/2}OCR_{ads} + H_2O$	K_{in}	-0.5	-0.5
2	$FeOH_2^{1/2+} + RCOO^- \Leftrightarrow FeOH_2^0O^{-1/2}OCR_{ads} + H_2O$	K_{out}	-0.2	-0.8
3	$Fe_3OH^{1/2+} + RCOO^- \Leftrightarrow Fe_3OH^0O^{-1/2}OCR_{ads} + H_2O$	K_{out}	-0.2	-0.8
4	$\#+RCOO^- \Leftrightarrow \#-R_{ads}COO^-$	K_H	0	0
5	$\#+RCOO^- + H^+ \Leftrightarrow \#-R_{ads}COOH$	K_H	0	0

in which R represents the rest of the molecule (*e.g.* a benzene ring). Note that it is assumed here that the charge of the electrostatically bound $RCOO^-$ (-1) and of the RCOOH (0) is located in the 1-plane.

Therefore, the total number of possible surface species for an organic molecule (Y) is given by $Y = 4^N$, in which N represents the number of functional groups present in the organic molecule. In principal, each surface species has its individual affinity constant and its individual charge distribution near the surface.

The above analysis shows that for modeling purposes the degrees of freedom increase dramatically with the number of reactive groups. In order to reduce the number of adjustable parameters, two main strategies can be followed. One strategy can be the use of a minimum of surface species needed for a thermodynamically correct description of the adsorption. However, this strategy does not represent the full range of surface species that may form. We will follow another strategy, which can be identified as a statistical type of approach.

5.4 Ligand and charge distribution (LCD)

The model we developed comprises several elements. The structure of the LCD model is shown in figure 5.1. To calculate the organic acid adsorption with the CD-MUSIC model (I), first a reaction should be formulated (1a,b). The affinity constant ($\log K_{overall}$), charge distribution (Δz_0, Δz_1), and the reaction stoichiometry coefficients (a, b, and c) of this reaction are calculated with the ligand distribution (LD) model (II). The LD model uses the

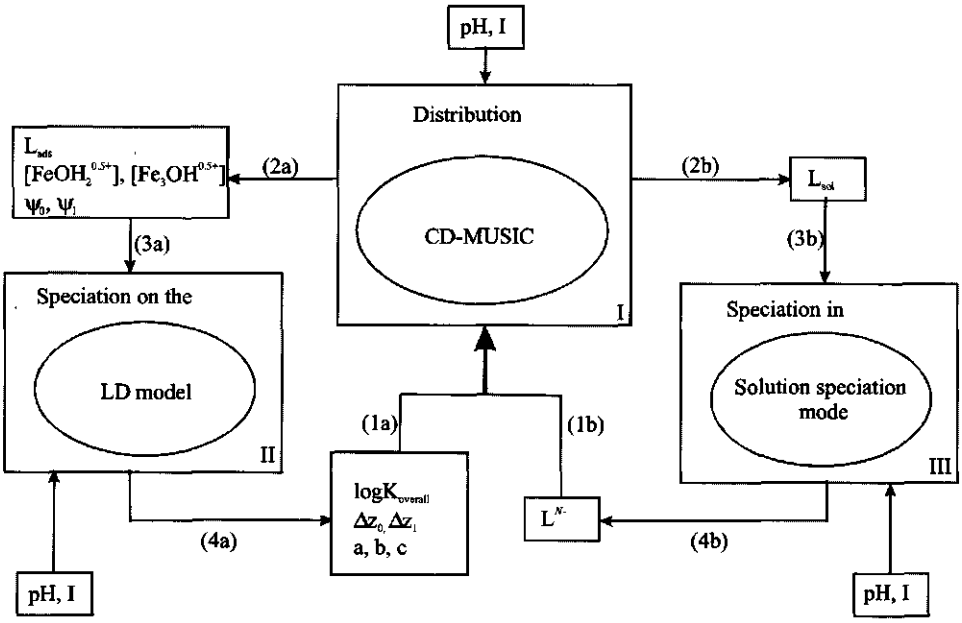

Fig. 5.1 Calculation scheme for the new model approach. I) CD-MUSIC model calculates the distribution of the organic molecules over the solid and solution phase. II) The LD model calculates the mean adsorption mode of the adsorbed organic molecules, which determines the input parameters for the CD-MUSIC model. III) Converts the dissolved amount of organic molecules into a reference species L^{N-}, which is used as input for the CD-MUSIC model. For details refer to the text.

activity of the singly and triply coordinated surface species, the amount of adsorbed organic acid (L_{ads}), the electrostatic potentials (ψ_0 and ψ_1), pH, and ionic strength as input parameters. The speciation in the equilibrium solution (III) is calculated separately transforming the total concentration of the dissolved organic acid (L_{sol}) into the activity L^{N-}. Note that the solution speciation depends on pH, and ionic strength.

The solution speciation and the LD model results are used as input for the CD-MUSIC model (I), which calculates the distribution of the organic acid over the solution (L_{sol}) and the interface (L_{ads}) (2a and 2b), the surface speciation, and the electrostatic potentials (2a). These variables are again the input for both other modules (II and III). The different aspects of figure 5.1 will be explained in detail below.

5.4.1 The adsorption reaction

We start our analysis by formulating the overall adsorption reaction of a molecule L^{N-} with N functional groups:

$$L^{N-} + a\mathrm{FeOH}_2^{1/2+} + b\mathrm{FeOH}_2^{1/2+} + c\mathrm{H}^+ \Leftrightarrow \mathrm{Fe}_{(a+b)}(\mathrm{OH}_2)_b - \mathrm{L}_{\mathrm{ads}}\mathrm{H}_c + a\mathrm{H}_2\mathrm{O}\,;\quad \mathrm{K}_{\mathrm{overall}} \qquad [5.3]$$

in which the coefficients a represents the number of inner sphere complexes, releasing a water molecule, b the number of outer sphere complexes interacting with $FeOH_2$ via a H bond, and c the number of protons bound by ligands that do not interact with surface groups.

In order to use this reaction in the CD-MUSIC model, the coefficients a, b, and c, as well as the H^+ and L^{N-} activity should be known. We will treat the stoichiometry of the organic acid adsorption as a statistical average. The statistical mean configuration of the adsorbed molecule (given by the coefficients a, b, and, c in the right hand side of eq. [5.3]) will change with pH, ionic strength, and surface loading. For instance, outer sphere complexation is relatively important at high pH. It implies a relatively high number for the stoichiometry coefficient b at this condition. At low pH, inner sphere complexation and protonation are relatively important. This means that at low pH, a and c are relatively high. In the LD model the coefficients a, b, and c are calculated based on the solution conditions and the electrostatic interactions at the surface, as will be discussed below.

5.4.2 Ligand distribution (LD)

In the LD model, the overall speciation of the adsorbed molecule results from the average speciation of all individual reactive ligands of the organic molecule. The speciation of each individual group (R_jCOO^-) is given by the following reaction equation:

$$a_j\mathrm{FeOH}_2^{1/2+} + b_j\mathrm{FeOH}_2^{1/2+} + c_j\mathrm{H}^+ + \mathrm{R}_j\mathrm{COO}^- \Leftrightarrow \mathrm{Fe}_{(a_j+b_j)}(\mathrm{OH}_2)_{b_j} - \mathrm{OOCR}_{\mathrm{j,ads}} + a_j\mathrm{H}_2\mathrm{O} \quad ;\mathrm{K} \qquad [5.4]$$

in which subscript j indicates the individual reactive group. Reaction [5.4] can be considered as a binding reaction of ligands to surface sites and protons. However, it can also be considered from the opposite perspective, *i.e.* the binding of surface sites and protons by a ligand j. In the latter case the stoichiometric coefficients ($\nu_{i,j}$) can be interpreted as the relative amount of surface sites ($\nu_{i,j} = a_j$ and b_j) or protons ($\nu_{i,j} = c_j$) bound at a particulate site j

(R_jCOO^-), *i.e.* the coefficients represent a relative occupation of site *j* with protons or surface sites, yielding:

$$v_{i,j} = \theta_{i,j} \qquad [5.5]$$

in which subscripts *i* and *j* indicate the type of complexes (inner sphere, outer sphere, proton) and individual group *j* respectively. Equation [5.5] is the central equation of the LD model. The relative occupation of site *j* is the result of competition of surface sites and protons for the ligand.

Reaction [5.3] describes the overall adsorption reaction of the whole molecule (L^{N-}), which is the sum of the speciation of the *N* ligands. The mean speciation of an individual ligand (R_jCOO^-) is given by reaction [5.4]. The summation of the speciation of the ligands implies that the stoichiometry coefficients of reaction [5.3] are linked to those of eq. [5.4]. The stoichiometry coefficients in equation [5.3] (v_i) are expressed as the number of complexes *i* per bound organic molecule. The coefficients v_i (*a*, *b*, and *c*) can be calculated taking the formation of complex *i* per functional group *j* and multiplying with the number of groups *j* per mol of molecule L^{N-}, called S_j, followed by summation over all groups:

$$v_i = \sum_{j=1}^{N} S_j v_{i,j} = \sum_{j=1}^{N} S_j \theta_{i,j} = Q_i \qquad [5.6]$$

This summation results in the amount of complex *i* per mol L^{N-}, which is the adsorbed amount of *i*, called Q_i (mol *i*/mol L^{N-}). Note that in a discrete approach, each group is treated individually. Therefore we always have one group *j* per molecule L^{N-}, *i.e.* $S_j = 1$.

The overall binding of surface sites or protons by a ligand can be considered as a combination of the formation of inner and outer sphere complexes and protonation, each with its individual affinity constants, being respectively $\log K_{in,j}$, $\log K_{out,j}$, and $\log K_{H,j}$. These logK values are defined here per mol of surface sites and protons. The affinity per mol R_jCOO^- can be found by summation of the $\log K_{in,j}$, $\log K_{out,j}$, and $\log K_{H,j}$, weighed by the contribution of each reaction as expressed in the stoichiometry coefficients, leading to:

$$\log K_{overall,j} = a_j \log K_{in,j} + b_j \log K_{out,j} + c_j \log K_{H,j} \qquad [5.7a]$$

or

$$K_{overall,j} = K_{in,j}^{a_j} K_{out,j}^{b_j} K_{H,j}^{c_j} \quad [5.7b]$$

The overall reaction constant of eq. [5.3] is composed of the constants of the individual states formed according to:

$$\log K_{overall} = \sum_{j=1}^{N} \log K_{overall,j} = \sum_{j=1}^{N} a_j . \log K_{in,j} + \sum_{j=1}^{N} b_j . \log K_{out,j} + \sum_{j=1}^{N} c_j . \log K_{H,j} \quad [5.8]$$

The charge distribution of the individual complexes formed with site *j* as used in eq. [5.4] is given in table 5.1. The mean charge distribution of site *j* is given by the weighed contribution of the reactions in table 5.1:

$$\Delta z_{0,j} = a_j(-0.5) + b_j(-0.2) \quad [5.9a]$$

$$\Delta z_{1,j} = a_j(-0.5) + b_j(-0.8) + (S_j - a_j - b_j - c_j)(-1) \quad [5.9b]$$

The latter term in eq. [5.9b] represents the charge of the adsorbed molecule minus the charge that is involved in the complex formation. The overall charge distribution as used in eq. [5.3] can be found as the summation of the charge distributions of the individual groups:

$$\Delta z_0 = \sum_{j=1}^{N} \Delta z_{0,j} = a(-0.5) + b(-0.2) \quad [5.10a]$$

$$\Delta z_1 = \sum_{j=1}^{N} \Delta z_{1,j} = a(-0.5) + b(-0.8) + (S_T - a - b - c)(-1) \quad [5.10b]$$

in which S_T represents the total number of functional groups of molecule L^{N-}.

The competition in reaction [5.4] can be calculated with a competitive adsorption model. For simple systems, the competition can be calculated with a competitive Langmuir equation. For larger heterogeneous organic molecules, the competition can be assessed using the recently developed NICCA model. In both models an electrostatic component should be added since the binding of the ligand occurs in the charged interface. This electrostatic contribution is calculated with our charge distribution concept (*e.g.* table 5.1).

5.4.2.1 Discrete statistical approach

The coefficients for, or the occupation of, group *j* ($v_{i,j}$) can be calculated using a competitive Langmuir equation:

$$\nu_{i,j} = \theta_{i,j} = \frac{Q_{i,j}}{S_j} = \frac{K_{i,j} c_i X_{0,i} X_{1,i}}{1 + \sum_i (K_{i,j} c_i X_{0,i} X_{1,i})} \qquad [5.11]$$

and the coefficients for the whole molecule L^{N-} (ν_i), according to

$$\nu_i = \sum_{j=1}^{N} S_j \nu_{i,j} = \sum_{j=1}^{N} S_j \frac{Q_{i,j}}{S_j} = \sum_{j=1}^{N} Q_{i,j} = \sum_{j=1}^{N} \frac{K_{i,j} c_i X_0 X_1}{1 + \sum_i (K_{i,j} c_i X_0 X_1)} = Q_i \qquad [5.12]$$

in which c_i is the concentration of protons or protonated reactive surface groups ($FeOH_2^{1/2}$; in mol/l). Note that in equation [5.11], $X_{0,i}$ and $X_{1,i}$ represent $e^{-\Delta z_{0,i} F \Psi_0 / RT}$ and $e^{-\Delta z_{1,i} F \Psi_1 / RT}$ respectively, in which $\Delta z_{0,i}$ and $\Delta z_{1,i}$ are the charge distribution coefficients of complex type i (see table 5.1). In equation [5.12], X_0 and X_1 represent the Bolzmann factors for the whole organic molecule, in which Δz_0 and Δz_1 are calculated according to eq. [5.10a] and [5.10b]. The $K_{i,j}$ values in eq. [5.11] and [5.12] are $K_{in,j}$, $K_{out,j}$ and $K_{H,j}$ for the inner sphere, outer sphere, and proton complexes respectively.

5.4.2.2 Continuous heterogeneity equation

In the modeling approach presented in the previous section, the number of possible surface species and degrees of freedom (*e.g.* the number of affinity constants) increase significantly with increasing number of functional groups present in the molecule. A surface complexation model can in practice only be applied sensibly when the number of adjustable parameters is limited. In stead of neglecting most of the possible surface species, the number of adjustable parameters can be reduced by realizing that a series of reactions, each with its own affinity, can be characterized by a continuous affinity distribution function. This affinity distribution can be characterized by parameters like the mean $\log \tilde{K}$ and a distribution width, *i.e.* a very large reduction of parameters.

The overall binding of a component i can be described by integrating over the affinity distribution (Jaroniec, 1983). In case of a distribution, the overall adsorption of a component i is found by integrating the fractional adsorption on a particular site j ($\theta_j f_j S_T$) over all sites, by expressing the θ_j and the fraction f_j as function of logK yielding:

$$S = \int \theta_j f_j S_T = S_T \int \theta(K) f(\log K) d\log K = S_T \frac{\tilde{K} c_i^{\,m}}{1 + \tilde{K} c_i^{\,m}} \qquad [5.13]$$

in which $f(\log K)$ is a particular distribution function. The solution given in equation [5.13] applies to the Sipps distribution (Sips, 1948). This distribution function is defined by a mean $\log \tilde{K}$, and a distribution width *m*.

The outcome of equation [5.13] is known as the Langmuir-Freundlich (LF) equation and is valid for a monocomponent adsorption reaction. If two or more components are in competition, one has to make assumptions with respect to the degree of correlation between the individual distribution functions. Assuming full correlation, the following competitive LF equation can be derived (Van Riemsdijk *et al.*, 1986, 1987):

$$Q_i = S_T \cdot \frac{(\tilde{K}_i c_i)}{\sum_i (\tilde{K}_i c_i)} \frac{\sum_i (\tilde{K}_i c_i)^p}{1 + \sum_i (\tilde{K}_i c_i)^p} \qquad [5.14]$$

The integration, necessary for the derivation of the LF equation, can only be done assuming that the affinity distributions are equal, and that the $\log \tilde{K}_i$ values are fully correlated. In practice, the distributions are often non-ideally and only partially correlated.

Van Riemsdijk and co-workers later developed another analytical binding equation for competitive ion binding on chemically heterogeneous substances. For a heterogeneous system with one type of functional groups, the NICCA equation is given by (Koopal *et al.*, 1994; Benedetti *et al.*, 1995; Kinniburgh *et al.*, 1996, 1999):

$$Q_i = \frac{n_i}{n_H} \cdot S_T \cdot \frac{(\tilde{K}_i c_i)^{n_i}}{\sum_i (\tilde{K}_i c_i)^{n_i}} \frac{\{\sum_i (\tilde{K}_i c_i)^{n_i}\}^p}{1 + \{\sum_i (\tilde{K}_i c_i)^{n_i}\}^p} \qquad [5.15]$$

in which Q_i is the total amount of component *i* bound by the heterogeneous substance. The distribution of affinity constants for component *i* is characterized by a median affinity constant ($\tilde{K}_i$), the width of the distribution (*p*) and by a parameter *n*, which may account for stoichiometry and non-ideality effects. Note that if all n_i are 1, eq. [5.15] simplifies to eq. [5.14].

In our case, the basic reaction stoichiometry is for all three types of reactions (inner sphere complex, outer sphere complex, and protonation) the same and equal to one. This would suggest a value of n_i of one, if n_i is interpreted solely as an average stoichiometry coefficient. The work of Rusch *et al.* (1997) has shown that the NICCA model with one and the same n parameter for all $\tilde{K}_i$ values can be interpreted as being the result of the degree of correlation between the individual distributions. It can be shown that p=1 and n<1 is the result of an approximation of the result that would be obtained for the integration assuming fully uncorrelated distributions with a certain width of distribution which is wider the smaller the value of n. The other extreme has already been discussed above (eq. [5.14]), which results from the assumption of a full correlation between the individual distributions. The combination of one n and one p value in the NICCA equation can be interpreted to be the result of a partial correlation between distribution functions (Rusch *et al.*, 1997). We will use here the NICCA model using one and the same n value for the three different binding modes.

The NICCA equation can be used to calculate the speciation of the adsorbed organic ligands (parameters a, b, and c in equation 5). Combining the electrostatics near the surface, calculated with the BS approach, and the NICCA equation in this case results in:

$$\nu_i = Q_i = S_T \cdot \frac{(\tilde{K}_i c_i X_{0,i} X_{1,i})^n}{\sum_i (\tilde{K}_i c_i X_{0,i} X_{1,i})^n} \cdot \frac{\{\sum_i (\tilde{K}_i c_i X_{0,i} X_{1,i})^n\}^p}{1+\{\sum_i (\tilde{K}_i c_i X_{0,i} X_{1,i})^n\}^p} \qquad [5.16]$$

Q_i expresses the number of complexes formed per bound organic molecule in case S_T is expressed as the number of carboxylic groups per molecule. In this case the coefficients a, b, and c in equation [5.3] are equal to Q_i of the complex concerned. Note that in equation [5.11], c_i represents the concentration (mol/l) of the protonated surface groups ($FeOH_2^{½}$) in case of inner or outer sphere complexes, or the concentration of protons (H^+) in case of the protonation of solution orientated reactive groups of the bound organic molecule.

The overall reaction constant which is used for the description of the adsorption of the whole organic molecule in the CD-MUSIC model can be calculated analogous to equation [5.8]:

$$\log K_{overall} = a.\log\tilde{K}_{in} + b.\log\tilde{K}_{out} + c.\log\tilde{K}_H \qquad [5.17]$$

The overall charge distribution can be calculated according to equations [5.7a] and [5.7b].

5.4.3 Solution speciation

The calculation of the adsorption of an organic molecule (eq.[5.3]) requires, beside log K and stoichiometry coefficients, the calculation of the solution speciation transforming the overall concentration (L_{sol}) into the activity L^{N-} (figure 5.1). With the *LD* model, the log K value and stoichiometry coefficients of the overall reaction are formulated. For a consistent thermodynamic treatment, the solution speciation is calculated in the same way as is done for the adsorbed organic molecules. For simple, well-defined molecules, the reactivity of the dissolved organic molecules is treated as the summation of the reactions of the individual functional groups, similar as is done above for the surface speciation. The overall reaction for the molecules in solution can be formulated as:

$$L^{N-} + nH^{+} \Leftrightarrow H_nL \qquad [5.18]$$

and the individual protonation reactions as

$$R_jOO^{-} + H^{+} \Leftrightarrow R_jOOH \qquad [5.19]$$

Summation of eq. [19] leads to the following equilibrium condition:

$$\prod_{j=1}^{N} K_j = \frac{\prod R_jOOH}{\prod R_jOO^{-}.H^{n}} \equiv \frac{H_nL}{L^{N-}.H^{n}} \qquad [5.20]$$

By definition, the activity of the molecule with n deprotonated reactive groups is equal to the product of the activity of the different deprotonated groups:

$$[L^{N-}] = \prod_{j=1}^{N} [R_jCOO^{-}] \qquad [5.21]$$

For heterogeneous systems, the activity of the fully deprotonated organic molecule in solution ($[L^{N-}]$) is defined as the fraction of empty sites of the total number of sites (θ^{-}) multiplied by the total amount of the organic acid in solution (L_{sol}). The fraction θ^{-} can be calculated with the mono-component NICCA equation, which is equivalent to the mono-component LF equation (eq. [5.14]) since the non ideality factor *n* and the distribution width parameter *p*, are combined in the value *m* of the LF equation. It can be shown that for

monocomponent situations the activity of the fully deprotonated organic molecule in solution is given by:

$$[L^{N-}] = L_{sol}\theta^{-} = L_{sol}(1-\theta_H) = L_{sol}\left(\frac{1}{1+(\tilde{K}H)^m}\right) \qquad [5.22]$$

5.5 Model calculations

The model calculations were carried out with the computer program ORCHESTRA (Objects Representing CHEmical Speciation and TRAnsport; Meeussen *et al*, 1997) that is developed specifically to facilitate the implementation of advanced adsorption models. Most chemical speciation programs like MINEQL, MINTEQ, PHREEQ, FITEQL, GEOCHEM, ECOSAT, define the equilibrium reactions in terms of components and species, and a matrix that contains the stoichiometric coefficients for the chemical mass-action and mass-balanced interactions between components and species. The algorithms that are based on this matrix approach generally allow chemical reactions to be defined in an input file, but model types (adsorption, ion activity correction) have to be predefined in the program source code. This makes it impossible for users to change or add model types without access to the source code.

The most contrasting difference with any of the standard speciation algorithms is that in ORCHESTRA the model type definitions are completely separated from the calculation kernel, and even from the source code. Model types are defined in the form of objects in a separate database. This allows users to freely change or add new model definitions without changing the source code. The object-oriented structure of the model type definitions makes it possible to design a small set of fundamental object classes that can be used as building blocks for specific model implementations. This greatly simplifies the implementation of new chemical models and combination of existing models as done in this study.

5.6 Results

In principle, the use of a distribution of affinity constants in the LCD model is restricted to the adsorption of organic molecules with a large number of functional groups. In order to test the new model, we describe the binding of phthalate, trimellitate, and pyromellitate, which contain two, three or four reactive groups respectively. Although the

number of functional groups per organic molecule is rather limited for the application of an affinity distribution, the use of Boily's data set has several great advantages for testing of the model. The data set contains detailed information about the proton titration behavior of the goethite and the organic acids in solution. Furthermore, the interactions between goethite and the organic acid are studied by IR spectroscopy. Therefore, the parameters for proton binding and the relative presence of the different surface complexes are constrained by separate experiments.

For the adsorption of trimellitic and pyromellitic acid, the configuration of the adsorbed molecule is calculated using the NICCA equation. Note that the organic molecule should contain at least three reactive groups in order to use an affinity distribution. In case of the description of phthalic acid adsorption, the number of reactive groups (S_T=2) is too limited to use an affinity distribution. Therefore, the data of phthalic acid adsorption are described using a bimodal competitive Langmuir equation in the LD part of the model.

5.6.1 Speciation in solution

In the LCD model, the calculation of the speciation in solution and on the surface is essential for an accurate description of the organic acid adsorption. The charging behavior of the goethite used by Boily *et al.* (Boily *et al.*, 2001) is very similar to the data we reported in previous studies (Venema *et al.*, 1996; Rietra *et al.*, 2000). The CD-MUSIC proton parameters used to describe the charging behavior of goethite in absence of organic molecules are given in table 5.2.

Table 5.2

Basic physical chemical parameters used for the description of the charging behavior of the goethite.

A:	94 m^2/g
C:	0.9 F/m^2
N_s (FeOH):	3.45 sites/nm^2
N_s (Fe_3O):	2.7 sites/nm^2
PPZC:	9.2
Log K_{Na+}	-1
Log K_{NO3-}	-1

The solution speciation for phthalate, tri- and pyromellitate is normally calculated using discrete protonation reactions. The affinity constants for this classical discrete approach are given in table 5.3. However, for consistent thermodynamic treatment, the solution speciation in the LCD model is calculated in the same way as is done for the adsorbed organic molecules. For tri- and pyromellitate, the monocomponent NICCA equation is used, whereas for phthalate the bimodeal Langmuir model is used. In figure 5.2, the charge of the carboxylic acids ($\bar{n}$) is calculated with the classical discrete approach (data points). The lines are model calculations with the NICCA or bimodal Langmuir model. The proton parameters for both models are given in table 5.4 and found by fitting the calculated "data points". Note that in the bimodal Langmuir and LF models, no correction for the activity is taken into account for the organic molecules. Therefore, the fitted $\log K_H$ or $\log \tilde{K}_H$ values are conditional constants. Note that this explains the differences between the $\log K_H$ (table 5.3) and $\log \tilde{K}_H$ values (table 5.4).

Table 5.3

Thermodynamic proton affinities of three benzenecarboxylic acids at zero ionic strength (Martell and Smith, 1977)

	No. groups	$\log K_{H,1}$	$\log K_{H,2}$	$\log K_{H,3}$	$\log K_{H,4}$
Phthalate	2	5.41	2.95		
Trimellitate	3	5.54	4.04	2.48	
Pyromellitate	4	6.23	4.92	3.12	1.70

5.6.2 The adsorption data

Boily *et al.* (2000a) determined three types of data on the adsorption of the benzenecarboxylic acids on goethite. First of all, they determined the distribution of the organic acid over the solution and the oxide surface (figures 5.3a, 5.4a and 5.5a). During the same experiment they also determined the proton balance (Z_B) (figures 5.3b, 5.4b and 5.5b), which is defined as:

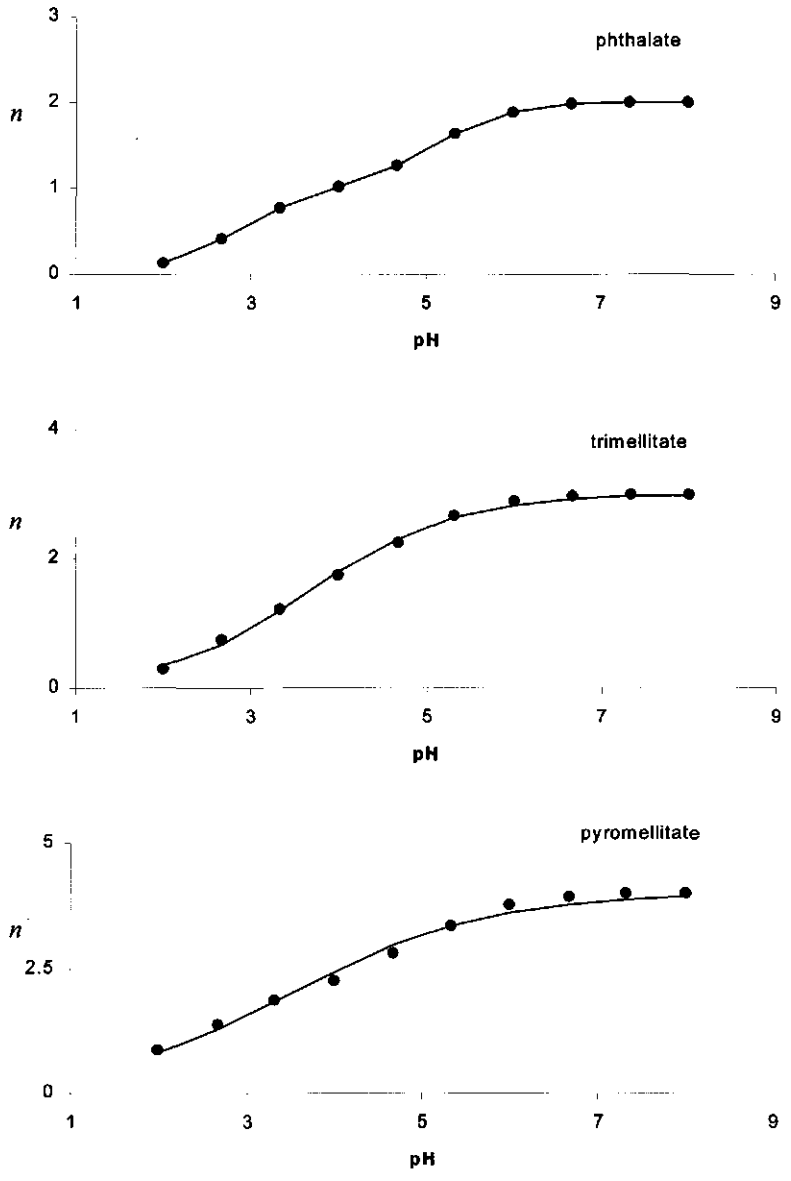

Fig. 5.2 Charging behavior of the phthalate, trimellitate, and pyromellitate in solution. The data points are calculated using the classical discrete approach. The model lines are fitted with the bimodal Langmuir or LF equations for phthalate and tri- and pyromellitate respectively.

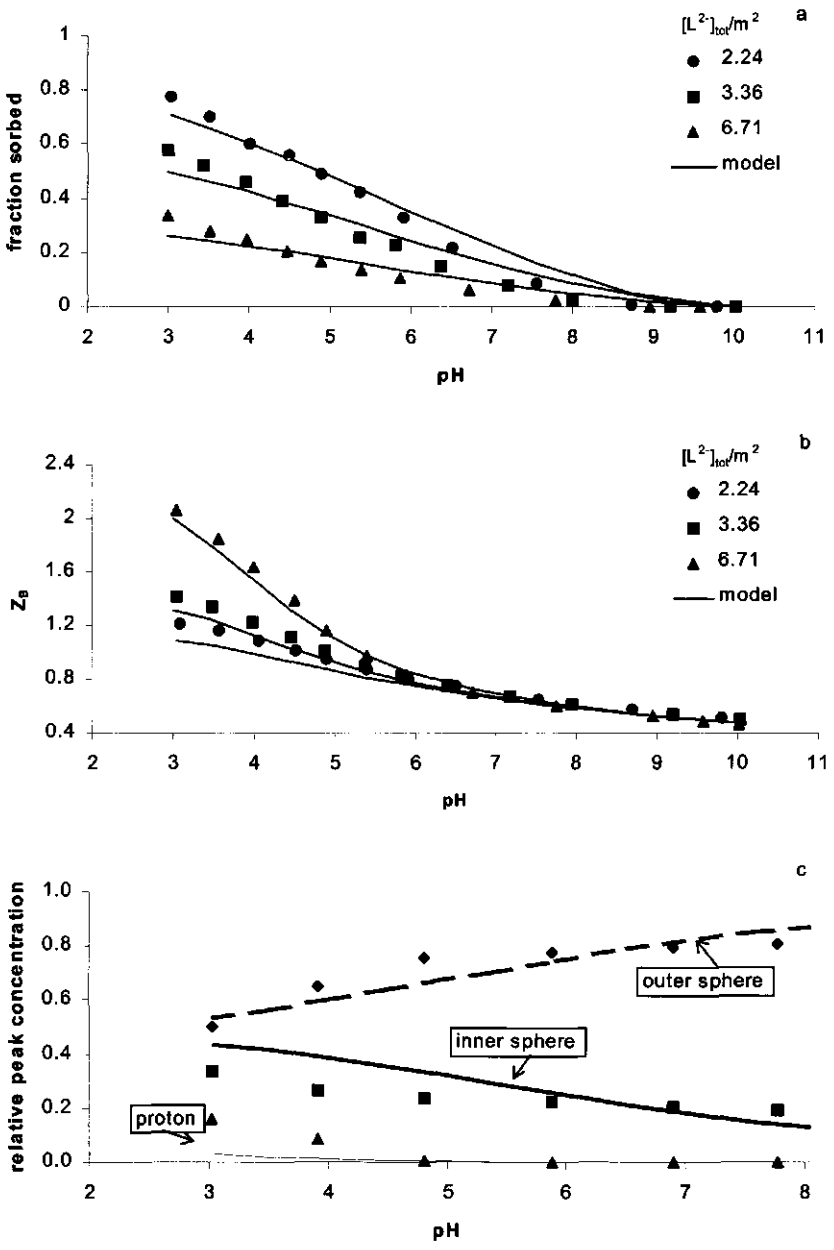

Fig. 5.4 Adsorption of trimellitate for 5 g/L (initial) of 90 m^2/g goethite suspensions in 0.1 mol/L $NaNO_3$. a) adsorption, b) proton balance, c) surface concentrations at a total surface coverage of 2.24 $\mu mol/m^2$. The total surface coverages studied are expressed in terms of μmol trimellitate/m^2 of goethite surface. (Data: Boily *et al.*, 2000b)

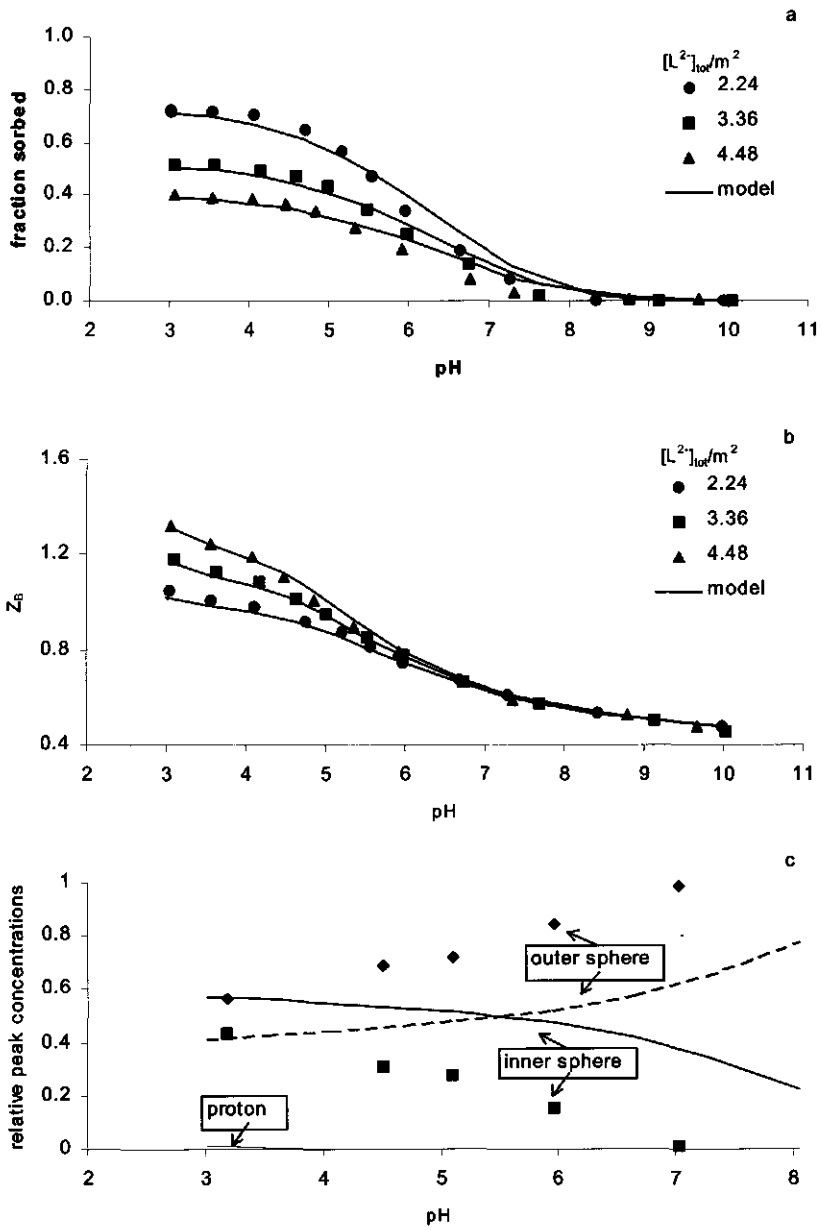

Fig. 5.5 Adsorption of phthalate for 5 g/L (initial) of 90 m^2/g goethite suspensions in 0.1 mol/L $NaNO_3$. a) adsorption, b) proton balance, c) surface concentrations at a total surface coverage of 2.24 µmol/m^2. The total surface coverages studied are expressed in terms of µmol phthalate/m^2 of goethite surface. (Data: Boily *et al.*, 2000b)

In the NICCA part of the surface complexation, the separation of the *n*- and *p*-parameters is based on trial and error under the restriction that the *n*-value of trimellitate and pyromellitate are equal. Note that determining *n* fixes *p* because of their relation to *m*. As $\log\tilde{K}_{in}$ and $\log\tilde{K}_{out}$ are the only additional adjustable parameters, the adsorption of tri- and pyromellitate can be described with only 3 degrees of freedom. The parameters used are given in table 5.4.

Table 5.4

Model parameters

	S_T	$\log\tilde{K}_H$	*m*	$\log\tilde{K}_{in}$	$\log\tilde{K}_{out}$	*n*	*p*
Pyromellitate	4	3.52	0.39	-0.65	1.55	0.6	0.67
Trimellitate	3	3.68	0.53	0	1.70	0.6	0.88
	S_j	$\log K_{H,j}$	m_j	$\log K_{in,j}$	$\log K_{out,j}$	n_j	p_j
Phthalate j_1	1	5.07	1	0	2.25	1	1
j_2	1	2.84	1	0.5	1.25	1	1

In solution, the NICCA model reduces to the LF model (or bimodal Langmuir for phthalate), and is calculated with the $\log\tilde{K}_H$ and *m* parameters. The surface speciation is calculated with the NICCA model (or bimodal competitive Langmuir for phthalate) using the $\log\tilde{K}_{in}$, $\log\tilde{K}_{out}$, *n*, and *p* parameters. For phthalate, *j* indicates the functional groups j_1 and j_2.

As stated before, it is not realistic to use an affinity distribution for molecules with only two functional groups. Therefore, the stoichiometry coefficients ($\nu_{i,j}$) are calculated separately for both functional groups of the phthalate using a bimodal competitive Langmuir equation. In table 5.4 the $\log K_{H,j}$, $\log K_{in,j}$, and $\log K_{out,j}$ are given for both groups. Note that in the competitive Langmuir model *n* and *p* are fixed to 1. The number of adjustable parameters is 4 ($2*S_T$). A reasonable model description of the phthalate adsorption data can be obtained with different sets of $\log K_{in}$ and $\log K_{out}$ values. However, describing the features of the normalized IR peak areas is only possible when it is assumed that the affinity for outer sphere formation of the weak acid carboxylic group was larger than of the strong acid group while the reverse holds for inner sphere formation. Note that although the model describes the trends of the complex speciation reasonably, on an absolute level the prediction is not accurate for phthalate.

5.7 Interpretation

Comparison of the affinity constants for the inner sphere, outer sphere, and proton complex formation of the adsorbed benzenecarboxylic acids (table 5.4) shows that the affinity constants for outer sphere complexation are significantly larger than for inner sphere complexation. This is in agreement with the model results of Boily *et al.*, who used an inner sphere, an outer sphere, and a protonated outer sphere surface species.

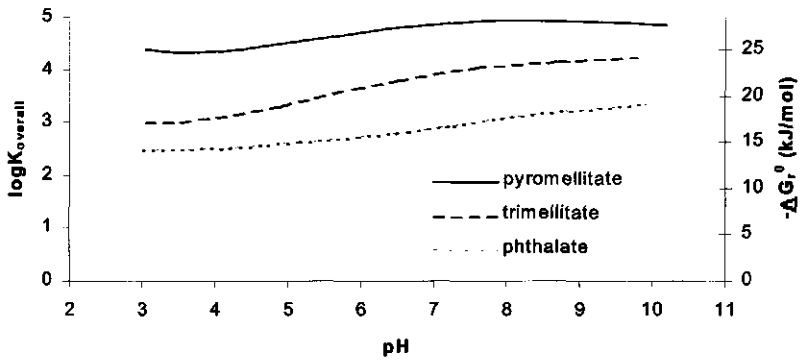

Fig. 5.6 $\log K_{overall}$ as function of pH at a total surface coverage of 2.24 μmol/m^2. The second y-axis expresses the chemical energy (ΔG_r^0) involved in the binding.

Figure 5.6 shows that the calculated overall chemical affinity of the mean surface configuration does not change significantly with increasing pH. The second y-axis in figure 5.6 expresses the chemical energy (ΔG_r^0) involved in the organic acid complexation. Although there is a shift from proton and inner sphere complexation at low pH towards the formation of outer sphere complexes at high pH (see figures 5.3c, 5.4c and 5.5c), the chemical energy involved remains rather constant.

Furthermore, figure 5.6 shows that the calculated values of the overall affinity constants of the adsorption of the benzenecarboxylates increases in the order of phthalate < trimellitate < pyromellitate. Boily *et al.* used similar surface species for the descriptions of tri- and pyromellitate. They found, in line with Filius *et al.* (1997) and Evanko and Dzombak (1999), that the affinity constants for the same type of surface species increased with increasing number of reactive groups present in the organic molecule. In the model approach

presented here, no distinct increase in the individual affinity constants ($\log\tilde{K}_{in}$, $\log\tilde{K}_{out}$) of the different type of complexes is found for the three carboxylic acids. However, as shown in eq. [5.17], the overall affinity is a product of ν_i and $\log\tilde{K}_i$. Model calculations show that $\Sigma\nu_i$ increases for the organic molecules with increasing number of reactive groups. Therefore, the overall affinity of the mean adsorption mode of the bound organic molecule increases as a result of the increased number of bonds formed between surface and organic molecule. These observations might suggest that pyromellitate ($S_T = 4$) will have higher adsorption levels than trimellitate ($S_T = 3$). However, the adsorption data indicate that at low pH the adsorption of trimellitic acid is higher than of pyromellitate adsorption. In order to explain the higher adsorption of trimellitate compared to pyromellitate, additional adsorption characteristics should be taken into account. Figure 5.7 shows the product of the boltzmann coefficients of both electrostatic planes, which is a measure of the electrostatic energy involved in the complexation.

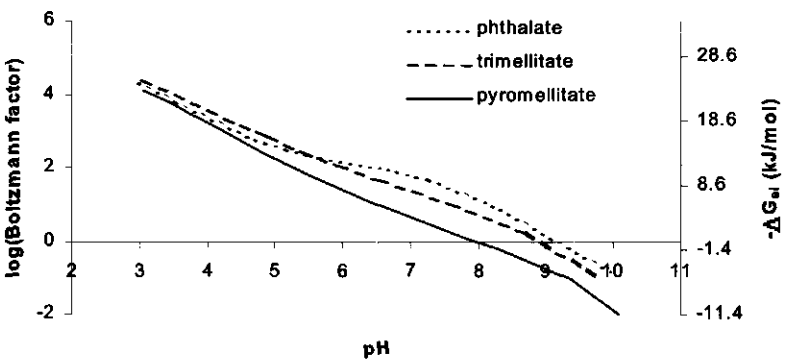

Fig. 5.7 Combined Boltzmann factors X_0 and X_1 (see eq. [5.12]) involved in the binding of organic acid by goethite as function of pH at a total surface coverage of 2.24 μmol/m^2. The second y-axis expresses the electrostatic energy (ΔG_{el}) involved in the binding.

Figure 5.7 shows that in case of trimellitate adsorption the electrostatic energy involved is higher than for pyromellitate adsorption at low pH. Despite the lower chemical affinity the adsorption of trimellitate can be higher due to the favorable electrostatic interactions. This effect becomes less pronounced and even reverses at high pH. At high pH,

the electrostatic repulsion between organic acid and goethite surface can become overcome by a large chemical affinity. In case of pyromellitate adsorption, more outer sphere complexes are formed between the organic molecule and the goethite surface. As a result, the chemical affinity is higher, making it easier to overcome the electrostatic repulsion, and the adsorption is higher. The observed decrease in the adsorption of the organic acids with increasing pH is most probably caused by the decrease in electrostatic energy (ΔG_{el}) involved.

Additionally to the electrostatic effects, the effects of surface statistics can account for the lower adsorption of pyromellitate than trimellitate. The number of goethite surface groups involved in the binding of an organic molecule is equal to the number of inner and outer sphere bonds formed by one molecule ($a + b$). With increasing adsorption, more of the goethite surface becomes covered by the organic molecules. Therefore each additional molecule has less surface to which it can bind. Statistically, this means that the chance to bind an additional molecule becomes smaller.

5.8 Discussion

In order to gain more insight in the adsorption of well defined organic molecules with a known number of reactive groups, Evanko and Dzombak (1999) and Boily *et al.* (2000b) studied the adsorption of a series of benzenecarboxylic acids. The classical discrete modeling approach is used in both studies. A minimum of hypothetical surface species was used in order to describe the adsorption data. Comparison of the two studies showed that Boily *et al.* (2000b) are able to describe the adsorption data of trimellitate and pyromellitate with fewer surface species (and fewer degrees of freedom) assuming a distribution of the charge of the organic molecule over the solid-water interface than Evanko and Dzombak who used only point charges.

For the benzenecaboxylic acids, it is feasible to use this discrete adsorption modeling approach since a relatively small number of reactive groups is involved. However, if one is interested in modeling the adsorption of these acids with the complete speciation of the adsorbed organic molecules, the discrete modeling approach becomes unattractive as the number of possible surface species already becomes very large with a limited number of reactive groups (4^{S_T} = 16, 64, and 256 for phthalate, tri-, and pyromellitate respectively). This problem becomes even more evident for organic molecules with many more reactive groups (fulvic and humic acid). In order to account for the wide range of possible surface

configurations of larger adsorbed organic molecules, the number of surface species in the modeling strongly increases. The discrete modeling approach with a full speciation of the large adsorbed organic molecule is definitely unmanageable. The importance of the full statistical speciation of the adsorbed molecule becomes important in case a wide range of environmental conditions is under investigation. For example, the description of the adsorption of an ion in a multi-component system (*e.g.* competitive or cooperative adsorption) is very sensitive to an accurate description of the mono-component situation. The use of hypothetical surface species may be a too limited approach for the proper description of the adsorption under these conditions.

We have developed a more statistical approach to account for the many possible surface species, the LCD model. The distribution of the organic molecules over solid and solution phase is calculated with the CD-MUSIC model using parameters obtained from the mean configuration of the adsorbed molecule for specific experimental conditions. The mean configuration of the adsorbed organic molecule is calculated with the LD model. When the molecule contains a large number of functional groups, the number of complexes formed with the surface, and the number of protons bound, can be calculated using a distribution of affinity constants. In this case, the NICCA equation can be used for the LD model. In this work we have shown that this approach can be used for molecules with a number of reactive groups per molecule down to three or four. For smaller molecules (*e.g.* phthalate), the number of reactive groups per organic molecule is too small to apply a distribution of affinity constants for the formation of the different complexes. For the description of the binding of phthalate, we use a bimodal competitive Langmuir equation for the LD model in order to calculate the full statistical configuration of the individual groups. The overall stoichiometric coefficients and charge distribution that are used in the CD-MUSIC model are calculated by the addition of the parameters of the individual groups.

Due to the self-consistent nature of the LCD approach, all adjustable parameters are in the LD part of the model. For the description of the phthalate adsorption, the adjustable parameters in the bimodal competitive Langmuir equation are the affinity constants for inner sphere ($\log K_{in,j}$) and outer sphere ($\log K_{out,j}$) for both groups (4 adjustable parameters). Note that for each additional group, the number of adjustable parameters in this approach increases with 2. In case the NICCA equation is used for the LD model (tri- and pyromellitate), the calculation of the full statistical configuration of the adsorbed organic acid only requires 3

adjustable parameters, *i.e.* the mean affinity of the two types of surface complexes and the value for *n*.

The model calculations indicate that it is possible to use the same *n* for the various types of interactions in the NICCA approach (inner sphere, outer sphere, protons). It is possible to use the same *n* for tri- and pyromellitate. An advantage is that the *n* and *p* parameters can be interpreted in a chemical sense. A single *n* value in the NICCA approach can in this case be interpreted to be the result of a partial correlation between the distributions of the inner sphere, outer sphere, and proton binding reactions. The relatively low value of *n* combined with a value of *p* close to one is indicative of a rather wide distribution with little correlation (Rusch *et al.*, 1997). The rather wide distribution is to be expected due to the large variation in $\log K_H$ for these two acids (see table 5.1). The fact that the wide distribution is due to the reactivity of basically the same reactive carboxylic units may explain why there is little correlation between the distributions for the various reactions in the heterogeneous reaction model. Recently, Milne *et al.* (2001) determined the NICCA parameters for a large set of humic and fulvic acids. The *n* value for the complexes used in our study (0.60) is comparable to the generic value Milne *et al.* obtained for the large range of fulvic acids (0.66).

Another advantage of the calculation of the complex speciation of adsorbed organic molecules using a heterogeneous binding equation is the close connection to the information obtained form IR spectroscopy. For adsorbed organic molecules, IR spectroscopy yields information about the speciation of the individual groups rather than about the structure of the complete organic molecule. The competitive Langmuir equation used for modeling the adsorption data of phthalate gives rather poor results for the prediction of the relative importance of inner sphere, outer sphere and proton complexes, whereas the NICCA model used for modeling the larger molecules predicts the IR data rather well. The better result of the NICCA approach is probably due to the fact that it can handle partial correlation between the distribution functions.

In a coming paper, the LCD model will also be used to describe the binding of larger, more complex molecules with multiple organic acid groups (fulvic acid) by goethite.

6

Modeling the binding of fulvic acid by goethite. The speciation of adsorbed fulvic acid molecules.

Abstract- Under natural conditions, the adsorption of ions at the solid-water interface may be strongly influenced by the speciation of adsorbed organic matter. In this paper, we describe the adsorption of fulvic acid (FA) by (hydr)oxide surfaces with a heterogeneous surface complexation model, the Ligand and Charge Distribution (LCD) model. The model is a self-consistent combination of the NICCA equation and the CD-MUSIC model. The NICCA model calculates the speciation of the adsorbed FA molecules for a large range of conditions. The CD-MUSIC model calculates the overall distribution of FA over the solution and the (hydr)oxide surface using the overall affinity constant, charge distribution, and stoichiometry coefficients obtained from the surface speciation. Both models are combined within one electrostatic framework (*e.g.* the Basic Stern (BS) model). The model can describe simultaneously the concentration, pH, and salt dependency of the adsorption. Furthermore, the model predicts the co-adsorption of protons accurately for an extended range of conditions.

Jeroen D. Filius, Johannes C.L. Meeussen, David G. Lumsdon, Tjisse Hiemstra and Willem H. van Riemsdijk

Submitted to *Geochimica et Cosmochimica Acta*

6.1 Introduction

Natural organic matter (NOM) and metal(hydr)oxide surfaces can both be regarded as geo-colloids. Considerable attention has been and is still given to the understanding of the (surface) chemistry of these geo-colloids per se. In natural systems, both type of geo-colloids are simultaneously present and they will interact. The mutual interaction may influence their role as reactive surfaces in the natural environment. NOM and metal(hydr)oxides are for instance very important for the chemical speciation and transport of nutrients and pollutants in the sediment and subsoil. The interaction between organic matter and oxide surfaces can significantly alter the characteristics of both the organic matter and the oxide surface. For example, the facilitated transport of heavy metals in aquifers is influenced due to the adsorption of dissolved organic matter by the oxide surface of the soil matrix (McCarthy and Zachara, 1989; Dunnivant *et al.*, 1992; Van de Weerd *et al.*, 2000). Also, organic matter competes with oxyanions like phosphate and sulfate for the same sites on the oxide surface and therefore reduces the adsorption of these oxyanions by the oxide (Sibanda and Young, 1986; Hawke *et al.*, 1989; Geelhoed *et al.*, 1998; Karltun, 1998). Large differences have been found for the adsorption of phosphate and sulfate for pure minerals and for natural systems. The presence of NOM may explain some of the observed differences.

Davis (1982) stated that a realistic representation of the surfaces of natural particulate matter might require a heterogeneous multi-site model. To date, only a few attempts have been made to include NOM in speciation calculations (Vermeer *et al.*, 1998; Karltun, 1998; Evanko and Dzombak, 1999; Filius *et al.*, 2000). For such an important challenge, a fundamental understanding of the adsorption behavior of NOM by oxide surfaces is required in order to make progress.

Well-defined weak organic acids have often been used as model compounds to study the adsorption of larger ill-defined weak organic acids. (Balistrieri and Murray, 1986; Ali and Dzombak, 1996; Filius *et al.*, 1997; Boily *et al.*, 2000b). The description of the adsorption of these well-defined organic molecules has shown that three factors are essential 1) the stoichiometry of the reaction, 2) the chemical affinity of the organic molecules for the oxide surface, and 3) electrostatic interactions between the charged organic molecules and the oxide surface. However, the description of the adsorption of large, ill-defined organic molecules (humic and fulvic acid; HA and FA) is more difficult for several reasons: 1) HA and FA are mixtures of molecules with different size, number of reactive groups, etc., 2) FA and especially HA have many more reactive groups per molecule that can form bonds with the

oxide surface, 3) the organic molecules and the goethite surface have both a variable charge, and 4) HA and FA have a relatively large size.

In the studies of Karltun (1998), Evanko and Dzombak (1999), and Filius *et al.* (2000), the adsorption of FA by goethite is described assuming a discrete number of surface species. We refer to this type of modeling as "discrete modeling". In these studies, as well as in the present approach, FA is treated as a mixture of the same molecules with averaged properties.

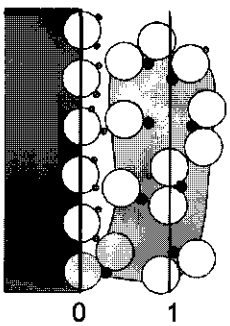

Fig. 6.1 A schematic representation of an adsorbed FA molecule

Figure 6.1 shows a bound FA molecule. The reactive groups of the FA molecule (carboxylate and phenolate groups) can react with mineral surface groups, with protons, or remain deprotonated. This speciation of the bound FA molecule varies widely with pH, salt level, surface loading, *etc.* In the discrete modeling, the speciation is reflected in the differences in surface species used. Filius *et al.* (2000) calculated that in their model a FA molecule with 8 reactive groups can form potentially easily over a thousand different surface species. However, the number of surface complexes used is minimized in order to reduce the number of adjustable parameters. Filius *et al.* (2000) only used four surface species in order to describe the data. By reducing the number of surface species, the speciation of the bound organic molecule becomes very limited and the model is therefore physically and chemically less realistic. For larger molecules, *e.g.* HA, the number of reactive groups is even larger than for FA and the number of possible surface species is almost infinite. Therefore, the discrete model approach is not suitable for modeling the binding of molecules larger and more complex than FA molecules.

Recently, we developed the ligand and charge distribution (LCD) model (Filius *et al.*, 2001) to describe the adsorption of large organic molecules by goethite. The model calculates the distribution of organic molecules over the solid and solution phase and the speciation of

the adsorbed and dissolved molecules simultaneously and in a self-consistent way. The Charge Distributed MUltiSIte Complexation (CD-MUSIC) model (Hiemstra and Van Riemsdijk, 1996) calculates the distribution of organic molecules over the solid and solution phase. In this study, the speciation of the organic molecule in solution and adsorbed by the oxide surface is calculated with the Non-Ideal Consistent Competitive Adsorption (NICCA) equation (Koopal *et al.*, 1994; Kinniburgh *et al.*, 1999). Electrostatic effects on the speciation of the goethite and the adsorbed FA are taken into account with a united electrostatic model.

The aim of this study is to extend the model approach presented by Filius *et al.* (2001) in order to describe the adsorption of FA by goethite for a wide range of conditions (pH, ionic strength, and surface loading). As FA contains both carboxylic and phenolic groups, the original LCD model is extended taking the full speciation of the phenolate groups of the adsorbed FA molecules into account. The model is calibrated for the adsorption data of Strichen Fulvic Acid (SFA) by goethite. Furthermore, the model is used to predict the co-adsorption of protons as a function of SFA adsorption by goethite at constant pH for conditions where almost 100% of the SFA molecules are adsorbed.

6.2 Model description

6.2.1 NICCA model

In general, organic material contains functional groups with a wide range of affinities for protons and competing metal ions. The NICCA model is a site-binding model that takes heterogeneity and competition into account explicitly. A simple Donnan model can account for the non-specific binding (Benedetti *et al.*, 1996; Kinniburgh *et al.*, 1999). Several studies (Perdue *et al.*, 1984; Ephraim *et al.*, 1986; De Wit *et al.*, 1993a; Milne *et al.*, 1995) show that the affinity distributions of humic substances for proton and metal ion binding are the result of two major types of sites, *e.g.* carboxylic type groups and phenolic type groups. The NICCA model can take this feature into account by introducing a bimodal intrinsic affinity distribution. This bimodal NICCA equation is given by:

$$Q_{i,1} = Q_{max1}\frac{n_{i,1}}{n_{H,1}}\frac{(\tilde{K}_{i,1}c_{i,D})^{n_{i,1}}}{\sum_i(\tilde{K}_{i,1}c_{i,D})^{n_{i,1}}}\frac{\{\sum_i(\tilde{K}_{i,1}c_{i,D})^{n_{i,1}}\}^{p_1}}{1+\{\sum_i(\tilde{K}_{i,1}c_{i,D})^{n_{i,1}}\}^{p_1}} + Q_{max2}\frac{n_{i,2}}{n_{H,2}}\frac{(\tilde{K}_{i,2}c_{i,D})^{n_{i,2}}}{\sum_i(\tilde{K}_{i,2}c_{i,D})^{n_{i,2}}}\frac{\{\sum_i(\tilde{K}_{i,2}c_{i,D})^{n_{i,2}}\}^{p_2}}{1+\{\sum_i(\tilde{K}_{i,2}c_{i,D})^{n_{i,2}}\}^{p_2}} \qquad [6.1]$$

where $Q_{i,t}$ is the total amount of component i bound to the humic substance, Q_{max} is the total site density (mol/kg), subscript 1 and 2 refer to the first and second type of sites in the affinity distribution, $\tilde{K}_i$ is a median affinity constant, and $c_{i,D}$ is the concentration of i in the Donnan phase. The value of p ($0 < p \leq 1$) accounts for the intrinsic chemical heterogeneity of the sorbent, which is the same for all components i. The parameter n_i accounts for the ion specific heterogeneity or non-ideality of component i that is not accounted for by intrinsic heterogeneity and/or the electrostatic model ($n \neq 1$ non-ideal, $n = 1$ ideal).

6.2.2 Donnan model

The Donnan approach assumes that at each charge the overall electroneutrality is entirely preserved by the accumulation or depletion of salt ions in the gel phase.

$$q/v_D - \Sigma(z_j.c_{Dj} - c_j) = 0 \qquad [6.2]$$

where q is the charge of the fulvic acid in mol kg^{-1}, v_D is the specific volume of the gel phase in l/kg, c_{Dj} is the concentration of component j with charge z_j (including the sign) in mol/l in the Donnan volume. c_j is the concentration of ion j in the external solution in mol/l. c_{Dj} and c_j are related by a Boltzmann factor (X):

$$c_{Dj} = c_j X_D = c_j e^{-z_j F \psi_D / RT} \qquad [6.3]$$

in which subscript D indicates the potential in the Donnan phase. Combination of equations [6.2] and [6.3] gives:

$$q/v_D = \Sigma z_j c_j (X_D - 1) \qquad [6.4]$$

For a given charge density and salt level, v_D is the only unknown parameter in order to solve equation [6.4] for ψ_D. Kinniburgh *et al.* (1999) introduced an empirical relation between v_D and the ionic strength:

$$\log v_D = k.(1 - \log I) - 1 \qquad [6.5]$$

Although this relation shows a variation in v_D with ionic strength which is much larger than can be expected based on structural models of fulvic acid (Langford *et al.*; 1983; Avena *et al.*,

1999; Lead *et al.*, 2000), the Donnan model can mimic the salt effects on the charging very well.

6.2.3 CD-MUSIC model

Hiemstra and Van Riemsdijk (1989a,b; 1996) describe the ion adsorption behavior of goethite with the Charge Distribution MUlti SIte Complexation (CD-MUSIC) model and discuss the most important characteristics of goethite in detail. Surface groups are distinguished based on metal coordination and bond distances. Singly, doubly and triply coordinated surface oxygens are found on the two main crystal faces of goethite, the 110 and 021 face. The proton reactive oxygens in the pH range between 2 and 12 are supposed to be the singly and triply coordinated surface oxygens. Charge is attributed to the surface oxygens using the Pauling bond valence principle. For the charge of the singly coordinated surface oxygens, the charge is –1.5 vu. ($FeO^{1.5-}$) and for the charge of the triply coordinated surface oxygens, one finds –0.5 vu. ($Fe_3O^{0.5-}$). Due to the high undersaturation of the oxygen charge $FeO^{1.5-}$, this group will always bind a proton in the normal pH range, yielding $FeOH^{0.5-}$. Both types of surface groups ($FeOH^{0.5-}$ and $Fe_3O^{0.5-}$) can become positive by binding a proton according to:

$$\text{-FeOH}^{0.5-} + \text{H}^{+} \Leftrightarrow \text{-FeOH}_2^{0.5+} \qquad \log K_{H1} \qquad [6.6]$$

$$\text{-Fe}_3\text{O}^{0.5-} + \text{H}^{+} \Leftrightarrow \text{-Fe}_3\text{OH}^{0.5+} \qquad \log K_{H2} \qquad [6.7]$$

Following Hiemstra and Van Riemsdijk (1996), the proton affinity constants (K_{H1} and K_{H2}) are set equal to the (PPZC) of the goethite. The site densities of proton reactive groups are calculated on the basis of the relative presence of the groups on the 110 and 021 face of the goethite surface known from electron spectroscopy.

In the CD-MUSIC approach, the charging curves of the goethite can be described using the basic Stern (BS) double layer model. In the BS model, two electrostatic planes (0- and d-plane) enclose the Stern layer, which is free of charge. The Stern layer has a capacitance, which is found by fitting the model to the experimental charging curves of goethite. Ion pairs are assumed to be formed and located at the solution side of the stern layer, which coincides with the head end of the diffuse double layer (ddl).

6.3 Organic acid adsorption

In this study the adsorption of FA by goethite is represented by the following overall reaction:

$$(a+b_1+b_2)\mathrm{Fe_1OH^{1/2-}} + (a+b+c_1+c_2)\mathrm{H^+} + \mathrm{FA}^z \overset{K_{overall}, X_0, X_1}{\Leftrightarrow} (\mathrm{Fe_1})_a(\mathrm{Fe_1OH_2})_b\mathrm{FAH}_c^{z+½(a+b)+c} + a\mathrm{H_2O} \quad [6.8]$$

The macroscopic adsorption reaction (eq. [6.8]) is characterized by the stoichiometry coefficients *a, b,* and *c,* the overall affinity constant, and the overall electrostatic interactions (X_0, X_1) between the oxide surface and the organic molecule. The calculation of these parameters will be discussed later. Note that both singly and triply coordinated goethite surface groups are supposed to interact with the reactive groups of the FA molecule. However, in the text the reactions are written only for singly coordinated sites for reasons of simplicity.

At a more detailed level (the microscopic level), the reactive groups of the FA molecule interact with protons and the reactive groups of the surface. In this study, we assume that the reaction at the macroscopic level is the result of all interactions at the microscopic level. The interactions between the carboxylate and phenolate groups and the surface groups are discussed next.

6.3.1 Speciation of carboxylate groups

Recently, a lot of work has been done on the OM-mineral interactions on a molecular level using infrared (IR) spectroscopy (Parfitt *et al.*, 1977a,c; Yost *et al.*, 1990; Biber and Stumm, 1994; Gu *et al.*, 1994; Kaiser *et al.*, 1997; Nordin *et al.*, 1998; Persson *et al.*, 1998; Boily *et al.*, 2000b). They interpreted their results in terms of ligand exchange, H bond formation, or protonation. In this study, we assume that the carboxylic groups of FA can form inner sphere complexes with the singly coordinated surface groups and outer sphere complexes with singly and triply coordinated surface groups. Furthermore, the carboxylate groups can protonate and deprotonate.

Reactions 1 and 2 of table 6.1 represent the adsorption and protonation of a solution-orientated carboxyl group of the bound FA molecule. The solution-orientated group does not have a direct interaction with the goethite surface groups, but is bound by the surface due to

Table 6.1

Reaction equations for the reactions possible to occur on the surface with the corresponding affinity constants, change of charge (Δz_i) in plane i, and stoichiometry coefficients.

	Reactions	logK	Δz_0	Δz_d	St. coeff.
1	$\# + RCOO^- + H^+ \Leftrightarrow \#\text{-}RCOOH^0$	$\log\tilde{K}_{H,1}$	0	0	c_1
2	$\# + RCO^- \Leftrightarrow \#\text{-}RCO^-$	1	0	-1	$z_1\text{-}a_1\text{-}b_1\text{-}c_1$
3	$\# + RCO^- + H^+ \Leftrightarrow \#\text{-}RCOOH^0$	$\log\tilde{K}_{H,2}$	0	0	c_2
4	$\# + RCO^- \Leftrightarrow \#\text{-}RCO^-$	1	0	0	$z_2\text{-}a_2\text{-}b_2\text{-}c_2$
5	$\text{-}Fe_1OH_2^{0.5+} + RCOO^- \Leftrightarrow \text{-}Fe_1 - OOCR]^{0.5-}$	$\log\tilde{K}_{in}$	-0.5	-0.5	a
6	$\text{-}Fe_1OH_2^{0.5+} + RCOO^- \Leftrightarrow \text{-}Fe_1OH_2\cdots OOCR]^{0.5-}$	$\log\tilde{K}_{out,1}$	-0.2	-0.8	$b_{1,1,1}$
7	$\text{-}Fe_3OH^{0.5+} + RCOO^- \Leftrightarrow \text{-}Fe_3OH\cdots OOCR]^{0.5-}$	$\log\tilde{K}_{out,1}$	-0.2	-0.8	$b_{1,1,2}$
8	$\text{-}Fe_1OH_2^{0.5+} + RCO^- \Leftrightarrow \text{-}Fe_1OH_2\cdots OCR]^{0.5-}$	$\log\tilde{K}_{out,2}$	-0.2	-0.8	$b_{2,1,1}$
9	$\text{-}Fe_3OH^{0.5+} + RCO^- \Leftrightarrow \text{-}Fe_3OH\cdots OCR]^{0.5-}$	$\log\tilde{K}_{out,2}$	-0.2	-0.8	$b_{2,1,2}$
10	$\text{-}Fe_1OH^{0.5-} + H^+ + RCO^- \Leftrightarrow \text{-}Fe_1OH\cdots HOCR]^{0.5-}$	$\log\tilde{K}_{out,2} + \log\tilde{K}_{H,2}$	+0.2	-0.2	$b_{2,2,1}$
11	$\text{-}Fe_3O^{0.5-} + H^+ + RCO^- \Leftrightarrow \text{-}Fe_3O\cdots HOCR]^{0.5-}$	$\log\tilde{K}_{out,2} + \log\tilde{K}_{H,2}$	+0.2	-0.2	$b_{2,2,2}$

Note: R represents the rest of the molecule. # indicates the adsorbed FA molecule of which the solution orientated reactive groups can be protonated (reactions 1 and 3) or remain deprotonated (reactions 2 and 4). Note that the charge of the bound $RCOO^-$ and of the $RCOOH^0$ is located in the 1-plane.

the complex formation of surface sites with other functional groups of the same adsorbed organic molecule. This structural feature is indicated by # in the reactions.

Inner sphere complexation (reaction 5 of table 6.1) is characterized by the exchange of an oxygen atom of the carboxylate group for a surface water group of a singly co-ordinated surface group. We assume that the charge of the carboxylate groups (-1 vu.) is equally distributed over both oxygens (2 * -0.5 vu.). In case of the exchange reaction, the charge of the iron in the solid (+0.5 vu) is fully neutralized by the charge of the carboxylate oxygen (-0.5 vu). Inner sphere co-ordination therefore results in an uncharged bonding oxygen. The charge of the second carboxylate oxygen is located in the 1-plane.

In case of H bond formation, the –1 vu of the organic group is located in the 1-plane (reactions 6 and 7 of table 6.1). The proton involved attributes 0.8 vu of its charge to the

surface plane. The remaining 0.2 vu is located in the 1-plane together with the –1 vu of the carboxylate group. In the rest of the text, H bonding is described only for singly coordinated surface groups. In the modeling, the H bonding with triply coordinated groups is taken into account identically to the H bonding with singly coordinated groups.

6.3.2 The speciation of phenolic groups

The phenolic groups of the FA molecule are supposed to protonate and deprotonate and to form outer sphere complexes with singly and triply coordinated surface groups. The adsorption and protonation reactions of solution orientated reactive phenolic groups is given by reactions 3 and 4 of table 6.1. The outer sphere complexes are formed due to H bonding (reactions 8 to 11 in table 6.1).

In case of H bonding, both the protonated reactive surface group and the phenolic group of the FA can, in principle, act as the proton donor. Figure 6.2 shows both options and indicates the different charge distribution of both types of outer sphere complexes over the interface. When the goethite surface site is the proton donor, 0.8 vu of the charge of the proton is located in the surface plane. The remaining 0.2 vu is located in the 1-plane together with the –1 vu of the carboxylate or phenolate group (figure 6.2A). In case the reactive organic group is the proton donor, the 0.2 vu and 0.8 vu of the proton are located in the 0- and 1- plane respectively (figure 6.2B).

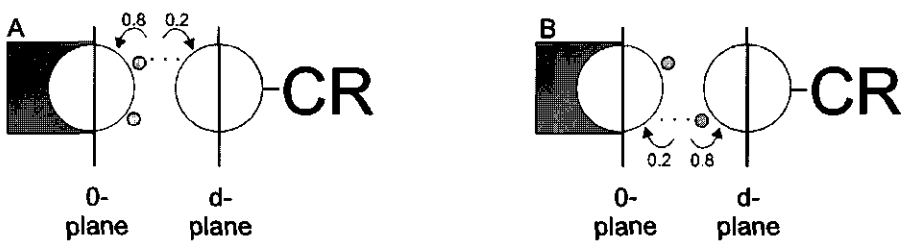

Fig. 6.2. Schematic representation of the formation of an H bond between a phenolic group of a FA molecule and a singly coordinated reactive surface group of the goethite surface. a) the reactive surface group act as the H bond donor, b) the phenolic group acts as the H bond donor.

To determine which group is the actual proton donor, the proton affinity of both groups as well as the electrostatic potential at the location of the reactive group should be taken into account. The overall affinity for the formation of the H bond in which the surface site is the donor is given a combination of the protonation of the surface group (K_H), the formation of the H bond ($\tilde{K}_{out,2}$), and the electrostatic interactions ($e^{-0.8F\psi_0/RT}.e^{+0.8F\psi_1/RT}$). The overall affinity for the formation of the H bond in which the phenolic group is the donor is a combination of the protonation of the reactive FA group ($\tilde{K}_{H,2}$), the formation of the H bond ($\tilde{K}_{out,2}$), and the electrostatic interactions ($e^{-0.2F\psi_0/RT}.e^{+0.2F\psi_1/RT}$). The surface site will therefore dominate as the H bond donor in case $K_H.e^{-0.8F\psi_0/RT}.e^{+0.8F\psi_1/RT} > \tilde{K}_{H,2}.e^{-0.2F\psi_0/RT}.e^{+0.2F\psi_1/RT}$ (reactions 8 and 9 of table 6.1; figure 6.2A). The phenolic group will dominate as the H bond donor in case $\tilde{K}_{H,2}.e^{-0.2F\psi_0/RT}.e^{-0.8F\psi_1/RT} > K_H.e^{-0.8F\psi_0/RT}.e^{-0.2F\psi_1/RT}$ (reactions 10 and 11 of table 6.1; figure 6.2B).

When the reactive surface group and the phenolate group have similar proton affinities, the relative presence of both types of H bond donors depends on the electrostatic potential in the 0- and 1-plane.

Note that in principle the carboxylic groups can also form both types of H bonds. However, because $\log\tilde{K}_{H,1} << \log K_H$, the overall affinity for the formation of the H bond in which the carboxylate oxygen is the donor is much smaller than in case the surface oxygen is the donor. Model calculations show that the carboxylic FA group will not act as the H bond donor for pH>3.

6.4 The LCD model

The adsorption of FA by goethite is calculated with the Ligand and Charge Distribution (LCD) model (Filius *et al.*, 2001). Figure 6.3 shows the basic structure of the new model approach. Starting point for the modeling is the reaction as given in eq. [6.8]. The distribution of the FA over the solution and the interface is calculated with the CD-MUSIC model (I in figure 6.3). The affinity constant ($\log K_{overall}$), charge distribution (Δz_0, Δz_1), stoichiometry coefficients (*a*, *b*, and *c*) of the reaction, and the activity of the FA in solution (FA^{z-}) are the model input parameters. $\log K_{overall}$, Δz_0, Δz_1, and *a*, *b*, and *c* are calculated with the LD model (II in figure 6.3). The activity of the FA in solution (FA^{z-}) is calculated by

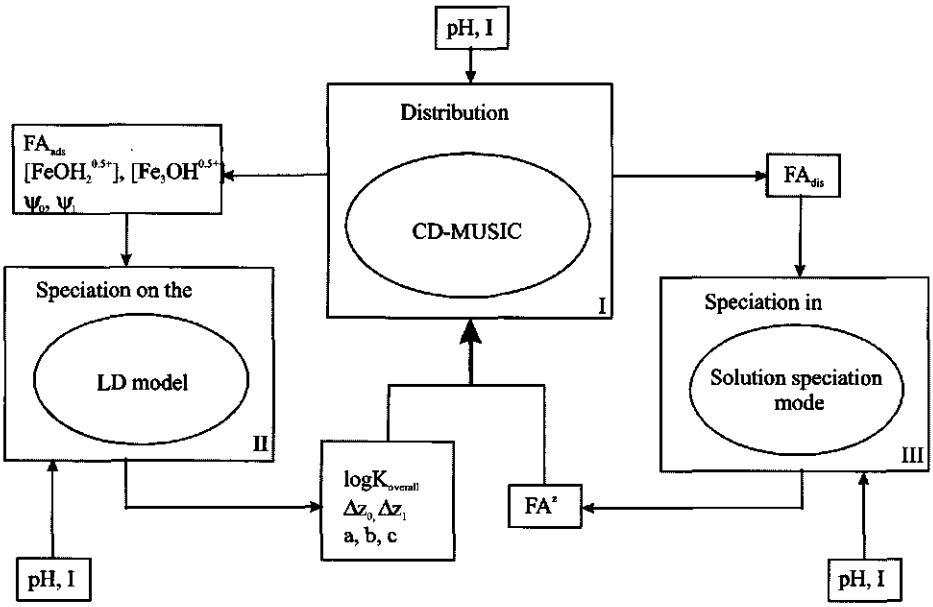

Fig. 6.3 Calculation scheme for the new model approach. I) CD-MUSIC model calculates the distribution of the organic molecules over the solid and solution phase. II) The LD model calculates the mean adsorption mode of the adsorbed organic molecules, which determines the input parameters for the CD-MUSIC model. III) Converts the dissolved amount of FA into a reference species FA^{z-}, which is used as input for the CD-MUSIC model.

transformation of the total amount of dissolved FA using solution speciation calculations (III in figure 6.3).The solution speciation and the LD model results are used as input for the CD-MUSIC model (I) which calculates the distribution of the organic acid over the solution (FA_{diss}) and the interface (FA_{ads}), the surface speciation, and the electrostatic potentials. These variables are again the input for both other modules (II and III).

6.4.1 Stoichiometry coefficients

In the LD model (III in figure 6.3), the mean speciation of the adsorbed FA molecule is calculated. The stoichiometry coefficients *a*, *b*, and *c* in equations [6.8] for the reactions with the reactive groups (table 6.1) of the adsorbed FA molecules are calculated with the NICCA model. So far, the NICCA model has been used successfully to calculate the competitive binding between protons and metal ions for HA and FA (Christensen *et al.*, 1998;

Pinheiro *et al.*, 1999; Kinniburgh *et al.*, 1999; Berbel *et al.*, 2001). Instead of metal ions, now surface sites compete for the binding sites of the FA. The NICCA equation is combined with the BS model, which accounts for the electrostatics near the surface:

$$S_i = \frac{n_i}{n_H}.S_T.\frac{(\tilde{K}_i c_i X_{0,i} X_{1,i})^{n_i}}{\sum_i (\tilde{K}_i c_i X_{0,i} X_{1,i})^{n_i}} \cdot \frac{\{\sum_i (\tilde{K}_i c_i X_{0,i} X_{1,i})^{n_i}\}^p}{1+\{\sum_i (\tilde{K}_i c_i X_{0,i} X_{1,i})^{n_i}\}^p} \qquad [6.9]$$

in which S_i indicates the amount of inner sphere, outer sphere, and proton complexes formed respectively and S_T represent the total number of sites. $X_{0,i}$ and $X_{1,i}$ indicate the Boltzmann factors (including charge and sign) for complex type *i* in the 0- and 1-plane respectively. Note that in eq. [6.1], Q_i and Q_{max} are expressed in mol/kg. Here, these parameters are expressed per molecule (S_i and S_T). The numbers can be calculated according to:

$$S_i = Q_i.M_{FA} \quad \text{and} \quad S_T = Q_{max}.M_{FA} \qquad [6.10]$$

in which M_{FA} is the averaged molecular mass of the FA molecules (kg/mol). In this equation, subscript *i* indicates the type of reactive group. Van Zomeren and Comans (2001) determined the M_{FA} for SFA to be 0.683 kg/mol.

As S_i and S_T are expressed per mol adsorbed FA, S_i equals the stoichiometry coefficient for each type of complex formed according to the reactions in table 6.1. The subscripts of the stoichiometry coefficients in table 6.1 can be explained as follows. The first subscript index refers to either carboxylic groups (1) or phenolic groups (2). The second index for *b* discerns the two types of outer sphere complexes for phenolic groups. $b_{2,1}$ refers to the situation where the proton is closest to the reactive site of the goethite surface, whereas $b_{2,2}$ refers to the situation where the proton is closest to the phenolic group. The third index refers to the type of surface groups that is complexed, 1 for the singly coordinated sites, and 2 for the triply coordinated sites. Note that $\nu = \sum_i \nu_i = \sum_i \sum_j \nu_{i,j} = \sum_i \sum_j \sum_k \nu_{i,j,k}$, in which ν is stoichiometry coefficient *a*, *b*, or *c* for inner sphere, outer sphere, and proton complexes formed respectively.

Note that the stoichiometry coefficients are not constants, but depend on the pH, ionic strength, surface coverage, etc.

6.4.2 The overall reaction constant

The overall affinity is composed of the constants for the formation of the different complexes weighed by their relative contribution:

$$\begin{aligned}\log K_{overall} = a.\log\tilde{K}_{in} + b_1.\log\tilde{K}_{out,1} + b_2.\log\tilde{K}_{out,2} + \\ (a + b_1 + b_{2,1})\log K_H + c_1.\log\tilde{K}_{H1} + (b_{2,2} + c_2)\log\tilde{K}_{H2}\end{aligned} \quad [6.11]$$

The first three terms of the right hand side (RHS) of equation [6.11] refer to the bonds formed between the FA groups and the surface, in which $\log\tilde{K}_{in}$ is the median affinity constant for the formation of inner sphere complexes and $\log\tilde{K}_{out,1}$ and $\log\tilde{K}_{out,2}$ are the median affinity constants for the formation of outer sphere complexes formed by carboxylic and phenolic groups respectively. The last three terms refer to the protonation reaction of the surface groups ($\log K_H$), the carboxylate groups ($\log\tilde{K}_{H1}$), and the phenolate groups ($\log\tilde{K}_{H2}$) respectively.

Note that the affinity constants of the different outer sphere complexes are assumed to be the same for the reaction with singly and triply co-ordinated groups.

6.4.3 The overall charge distribution

The charge distribution can be calculated as the sum of the charge distributed due to the formation of inner (*a*), outer sphere (*b*), and proton complexes (*c*) with reactive FA groups (see table 6.1) and the charge of the non coordinated ionized groups of the bound FA (z_{nc}) according to:

$$\Delta z_{0,FA} = a.(1 - 0.5) + (b_1 + b_{2,1})(+0.8) + b_{2,2}.(+0.2) \quad [6.12a]$$

$$\Delta z_{d,FA} = a.(-0.5) + (b_1 + b_{2,1})(-0.8) + b_{2,2}.(-0.2) + z_{nc} \quad [6.12b]$$

z_{nc} is the charge of the non coordinated ionized groups of the bound FA and is given by:

$$z_{nc} = -z + a + b + c \quad [6.13]$$

in which *z* is the charge of the fully deprotonated FA molecule.

6.4.4 Speciation of FA in solution

For the calculation of the speciation of FA in solution (III in figure 6.3), the NICCA-Donnan model is used. Under the conditions in solution, the NICCA equation reduces to a simple LF equation because the proton is the only interacting component:

$$Q_H = Q_{max1}\frac{\{\tilde{K}_{H,1}[H]_D\}^{m_1}}{1+\{\tilde{K}_{H,1}[H]_D\}^{m_1}} + Q_{max2}\frac{\{\tilde{K}_{H,2}[H]_D\}^{m_2}}{1+\{\tilde{K}_{H,2}[H]_D\}^{m_2}} \quad [6.14]$$

in which m_i ($m = n_H p$) is a heterogeneity parameter that reflects the combined effect of the intrinsic heterogeneity (p) and the ion specific-heterogeneity (n_H).

Following Filius *et al.* (2001), we assume that the fraction of the dissolved FA molecules of which all carboxylate groups are deprotonated (θ^{fd}_{carb}) can be calculated according to:

$$\theta^{fd}_{carb} = \frac{1}{1+(\tilde{K}_{H,1}[H^+]_D)^{m_1}} \quad [6.15]$$

However, in case of fully deprotonated FA, all phenolate groups should be deprotonated also. The fraction of fully deprotonated FA molecules (θ_{FA^z}) can be calculated according to:

$$\theta_{FA^z} = \theta^{fd}_{carb} * \theta^{fd}_{phen} \quad [6.16]$$

in which θ^{fd}_{phen} is the fraction of the dissolved FA molecules of which all phenolate groups are deprotonated. Note that θ^{fd}_{phen} can be calculated with eq. [6.15] using the constants of the second distribution ($\log\tilde{K}_{H,2}$ and m_2 of table 6.1).

The activity of the fully deprotonated FA molecules can now be calculated according to:

$$[FA^z] = \theta_{FA^z} * [FA_{diss}] \quad [6.17]$$

in which FA_{diss} is the total concentration of FA in solution.

6.5 Materials and Methods

6.5.1 Goethite

The goethite preparation was based on the procedure of Atkinson *et al.* (1967) and is described in more detail by Hiemstra *et al.* (1989). The BET-N_2 surface area of the sample was 94 $m^2\ g^{-1}$.

6.5.2 Fulvic acid extraction

Soil fulvic acid was extracted from a soil using methods based on those recommended by the International Humic Substances Society (Aiken *et al.*, 1979; Swift, 1996). The soil used was a Bs horizon from a peaty podzol (Strichen association). The extraction is described in more detail by Filius *et al.* (2000)

6.5.3 Adsorption experiments

The FA adsorption by goethite was measured in background electrolytes of 0.01 M and 0.1 M $NaNO_3$, using a batch equilibration procedure. The data are obtained from Filius *et al.* (2000).

6.5.4 Proton-ion-titrations at constant pH

Samples of 60 ml of a goethite stock suspension were titrated to pH 4, 5.5, or 7 and left overnight in N_2 atmosphere. The samples have an electrolyte concentration of 0.01 M or 0.1 M $NaNO_3$. The goethite stock solution was titrated with a 5 g/l FA solution having the same pH and ionic strength (and kept under N_2) as the goethite stock solution. After each FA addition, the pH was corrected to the initial pH with acid or base. A reaction time of at least 20 minutes and a maximum drift criterion of 0.002 pH units per minute was used between each addition of FA in order to reach equilibrium. The total amount of added FA was sufficiently small compared to the total surface area of the goethite to have more tan 99% of the FA bound. The acid/base balance can be calculated from the amount of added acid and base because the pH was kept constant and no FA remains in solution.

6.5.5 Data analyses

The ionic strengths were calculated for each data point explicitly taking into account both the background electrolyte ions and free H^+ and OH^-. From the calculated ionic strength (I), the activity coefficients (f) were determined using an adapted Davies equation:

$$-\log f = 0.51 * z^2 * \{\frac{\sqrt{I}}{1+\sqrt{I}} - 0.2 * I\} \qquad [6.18]$$

Blank correction was carried out by calculating, for each data point, the amount of titrant required to increase the pH of an equivalent volume of background electrolyte solution. This was subtracted form the volume of titrant used for the sample.

6.5.6 Model calculations

The model calculations were carried out with the computer program ORCHESTRA (Objects Representing CHEmical Speciation and TRAnsport; Meeussen *et al*, 1997) that is developed specifically to facilitate the implementation of advanced adsorption models. Most chemical equilibrium programs (MINEQL, MINTEQ, PHREEQ, FITEQL, GEOCHEM, ECOSAT) define the equilibrium reactions in terms of components and species, and a matrix that contains the stoichiometric coefficients for the chemical (mass-action and mass-balanced) interactions between components and species. The algorithms that are based on this matrix approach generally allow chemical reactions to be defined in an input file, but model types (adsorption, ion activity correction) have to be predefined in the program source code. This makes it impossible for users to change or add model types without access to the source code.

The most contrasting difference with any of the standard speciation algorithms is that in ORCHESTRA the model type definitions are completely separated from the calculation kernel, and even from the source code. Model types are defined in the form of objects in a separated database. This allows users to freely change or add new model definitions without changing the source code. The object-oriented structure of the model type definitions makes it possible to design a small set of fundamental object classes that can be used as building blocks for specific model implementations. This greatly simplifies the implementation of new chemical models and combination of existing models as done in this study.

6.6 Results and Discussion

6.6.1 Basic charging behavior and FA adsorption

Table 6.2

Basic physical chemical parameters used for the description of the charging behavior of the goethite.

A:	94 m^2/g
C:	0.9 F/m^2
N_s (FeOH):	3.45 sites/nm^2
N_s (Fe_3O):	2.7 sites/nm^2
PPZC:	9.2
Log K_{Na+}	-1
Log K_{NO3-}	-1

The LCD model combines the charging characteristics of the oxide surface and the adsorbed FA. However, the basic charging behavior of the goethite surface and the FA molecules can be described with the CD-MUSIC and NICCA (or LF)-Donnan model, respectively. The basic charging behavior of both components is determined in separate experiments. The charging behavior of goethite is very similar to the reported charging behavior of goethite by Venema *et al.*(1996) and Rietra *et al.* (2000). Table 6.2 gives the parameters used to describe this charging behavior with the CD-MUSIC model.

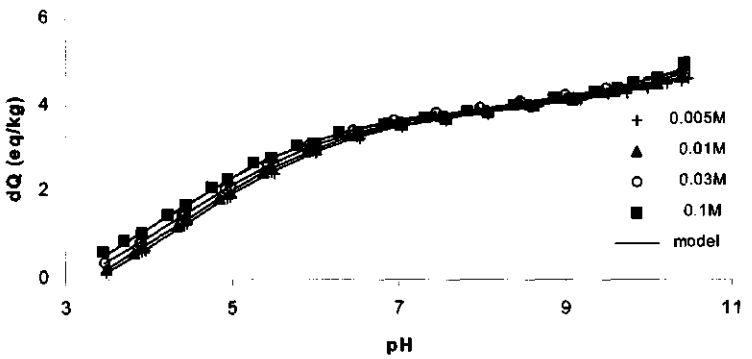

Fig. 6.4 Basic charging behaviour of SFA in solution at four salt levels.

Table 6.3

Basic physical chemical parameters used for the description of the charging behavior of FA with the NICCA-Donnan model.

		$Qmax_i$ (mol/kg FA)	$\log\tilde{K}_{H,i}$	m	$S_{T,i}$ (mol/mol FA)
Carb.(1)		6.11	2.33	0.33	4.17
Phen.(2)		1.91	9.77	0.45	1.30
k	0.57				
M_m (g/mol)*	683				

*Van Zomeren and Comans (2001)

Figure 6.4 shows the charging behavior of SFA in solution for 4 different electrolyte concentrations. The experimental set up is given in detail by Filius *et al.* (2000). The lines in figure 6.4 indicate the model calculations with the LF-Donnan model. The fitting strategy of the experimental data to the LF-Donnan model is described elsewhere (Kinniburgh *et al.*, 1999). The parameters used to describe the charging behavior of SFA with the NICCA-Donnan model are given in table 6.3.

Figure 6.5 shows the adsorption envelops for three different total amounts of FA at constant goethite concentrations as determined in a previous study (Filius *et al.*, 2000). The data show little salt-dependency but are strongly dependent on pH. This type of sorption behavior is commonly found for FA and other fractions of the NOM (Tipping, 1981; Becket and Le, 1990; Wang *et al.*, 1997; Au *et al.*, 1999). The lines in figure 6.5 represent the model description. Table 6.4 lists the parameter values used to describe the adsorption data.

In principal, two parameters are adjustable for each type of defined reaction; *e.g.* the median intrinsic affinity constant of the complex and the n_i parameter. In addition there is the p parameter that determines the width of the carboxylic and phenolic distributions. However the number of adjustable parameters can be reduced by the following assumptions.

We assume a partial correlation between the distribution of the affinity constants of the different complexes. According to Rush *et al.* (1997), the NICCA model can be interpreted to relate to a partial correlation when the n values for the different reactions are equal and smaller than 1. Therefore, we assume $n_i = n_{H,i} = n_{in} = n_{out,i}$. Milne *et al.* (2001) determined the generic NICCA-Donnan model parameters for 25 datasets. Although the m parameter (n * p) used here is obtained from fitting the charging behavior of SFA in solution, the n_H parameters are taken from the generic database. Note that these assumptions fix all n and p values for the carboxylic and phenolic groups. The median affinity constants for each type of

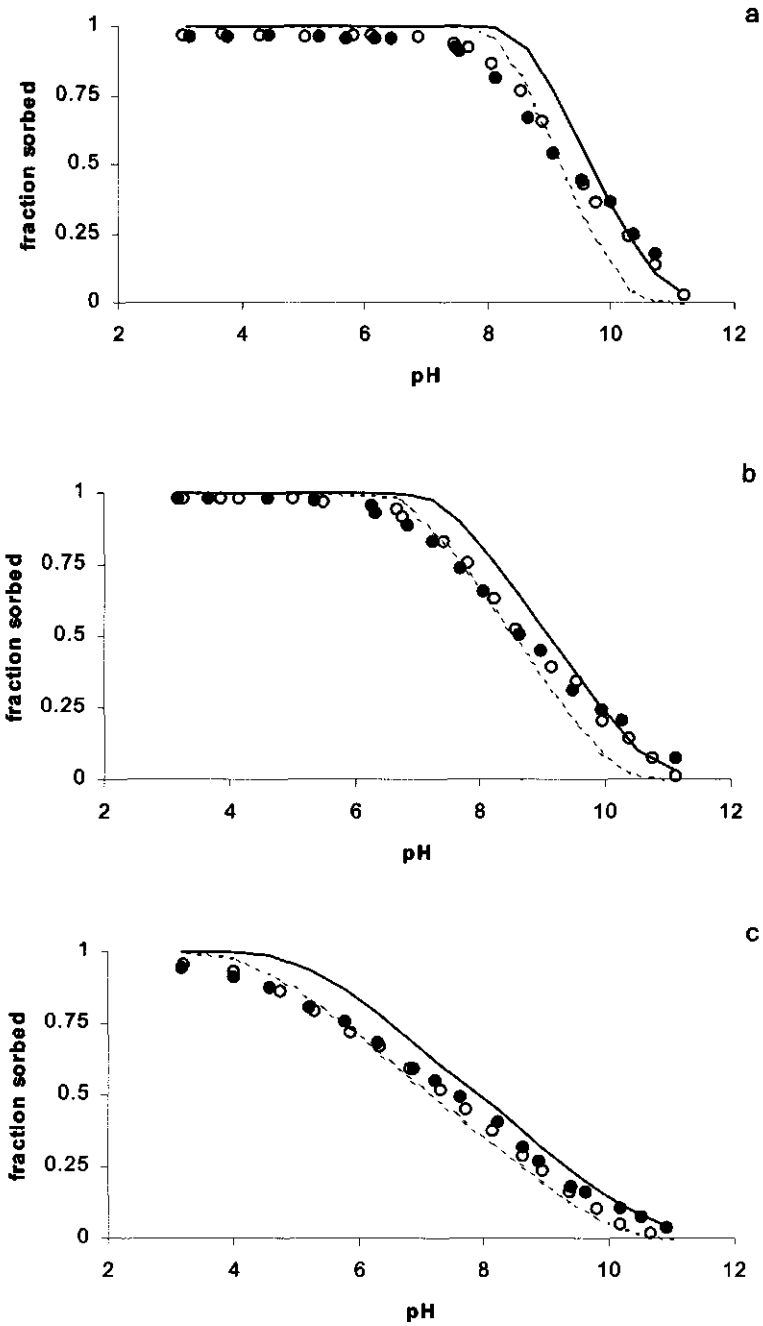

Fig. 6.5 The adsorption envelopes of SFA by goethite in 0.01 M (open symbols and dotted lines) and 0.1 M $NaNO_3$ (solid symboles and full lines). The suspension density of goethite is 5 g/l and three different total FA concentrations: a) 75 mg/l; b) 150 mg/l; c) 300 mg/l.

Table 6.4

Parameters for the NICCA model used for the calculation of the speciation of the adsorbed FA molecules

$\log\tilde{K}_{in}$	-3	Fitted
$\log\tilde{K}_{out,1}$	-1.7	Fitted
$\log\tilde{K}_{out,2}$	3.5	Fitted
n_1	0.66	Generic dataset*
n_2	0.76	Generic dataset*
p_1	0.50	$m = n_H.p$
p_2	0.59	$m = n_H.p$

*Milne *et al.*, 2001

complex formed are the only adjustable parameters.

6.6.2 Number of adjustable parameters

In the application of the LCD model, we assume that the protonation of the adsorbed organic ligands can be described with the same parameters as found for the description of the basic charging behavior of FA in solution. Furthermore, the affinity for the two types of outer sphere complexation of the phenolic groups are assumed to be the same ($\log\tilde{K}_{out,2}$). Therefore, in the model approach used here only three adjustable parameters remain, *e.g.* $\log\tilde{K}_{in}$, $\log\tilde{K}_{out,1}$, and $\log\tilde{K}_{out,2}$. The rest of the parameters presented in table 6.4 are taken from the generic data set (Milne *et al.*, 2001) or independently obtained from curve fitting of solution titration data. Note that in this approach, we can account for a variable speciation of a complex molecule like FA with only three adjustable parameters. This number is comparable to the number of adjustable parameters often needed to describe the adsorption of much simpler anions, like oxyanions (Bowden *et al.*, 1980; Dzombak and Morel, 1990; Manning and Goldberg, 1996). Note that the average number of carboxylic groups per FA molecule is approximately the same as for pyromellitate (Boily *et al.*, 2000b; Filius *et al.*, 2001). The main difference between pyromellitate and FA are the phenolic groups of the FA molecule. In principle, the FA is a mixture of molecules with different number of reactive groups. Due to the differences in chemical composition of the molecules, the reactive groups will have different chemical affinity for surface groups and protons. Although the average number of phenolic groups per FA molecule is close to one, we use a distribution of affinity constants to

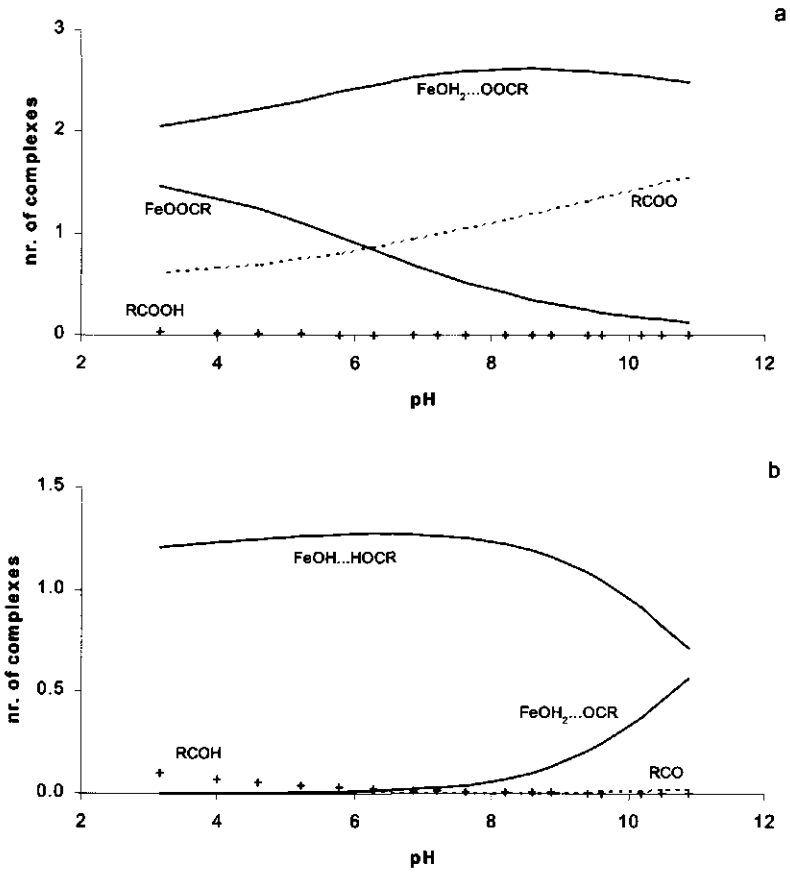

Fig. 6.6 The calculated speciation of adsorbed FA molecules on the goethite surface plotted as function of pH at the highest goethite:FA ratio of fig. 6.5. a) The speciation of the adsorbed carboxylic groups, b) the speciation of the adsorbed phenolic groups.

take this heterogeneity into account. Note that the number of reactive groups is not necessarily an integer as the new model is based on a statistical approach.

6.6.3 Speciation of the adsorbed FA

The adsorption of FA by goethite is largely determined by the speciation of the adsorbed FA molecules. In figure 6.6, the speciation of the adsorbed FA molecules is given for the highest FA:goethite ratio presented in figure 6.5. In a large range of pH values (pH 4-12), figure 6.6 represents the speciation of the bound FA at the "pseudo-plateau" of the

adsorption isotherms. Figure 6.6a shows the speciation of the carboxylic groups. The carboxylic groups react predominantly via outer sphere complexes. With decreasing pH, inner sphere complexes become important whereas the degree of protonated carboxylic groups remains low. Even at low pH, a part of the carboxylic groups is dissociated. This number increases gradually with increasing pH.

Figure 6.6b shows the speciation of the phenolic groups. All phenolic groups are involved in the complexation reactions with the goethite surface over a wide pH range. At low pH, the phenolic groups that are not associated with the surface start to become noticeable. Note that these groups are protonated. The outer sphere complex with the phenolic group as the H bond donor is the most important group over the whole pH range. Above pH 7, the outer sphere complex in which the phenolate group is the H bond acceptor starts to become increasingly important at the expense of the other type of outer sphere complex.

These results indicate that the carboxylic groups are most important for surface coordination at low pH whereas the phenolic groups are more important at high pH. This agrees with the observations of Evanko and Dzombak (1998, 1999) for the binding of small carboxylic and phenolic acids by goethite. They found that the adsorption of carboxylic acids decreases with increasing pH, whereas the binding of phenolic acids increases with increasing pH. Gu *et al.* (1995) found the same when they compared the adsorption of phthalate and catechol by hematite.

In the present model, the main parameters determining the speciation are the median affinity constant, the non-ideality coefficient, and the charge distribution of the different complexes. As was found by Filius *et al.* (2000, 2001), the median affinity constants for the formation of outer sphere complexes are much higher than for the formation of inner sphere complexes. This indicates that the replacement of a water molecule in case of inner sphere complex formation is not necessarily favorable. The higher affinity constant for the formation of outer sphere complexes involving a phenolic group compared to carboxylic groups corresponds with the larger undersaturation of the phenolate oxygen (-1 per O) compared to the carboxylate oxygens (-0.5 per O) of the organic molecule.

The speciation calculations presented in figure 6.6 indicate that at high pH the differences in the charge distribution of the two phenolic outer sphere complexes cause a preferential formation of the complex in which the goethite surface group acts as the H bond donor. With decreasing pH, the complex with the phenolic group as the proton donor becomes more important. For the carboxylate groups, the differences in the charge distribution favors

the formation of inner sphere complexes at low pH. With increasing pH, the electrostatic interactions will favor outer over inner sphere complexation.

This behavior agrees with the findings of Boily *et al.* (2000b) who studied the binding of three carboxylic acids. They inferred from spectroscopic data that outer sphere complexes are important at high pH, whereas inner sphere complex formation becomes significant at low pH.

6.6.4 Co-adsorption of protons

The data in figure 6.5 give little information below pH 5 because the two lowest FA additions are almost fully adsorbed by the goethite. However, recently, Rietra *et al.* (1999) pointed out that proton-ion titrations at constant pH provide additional information under these conditions. Using proton-FA titrations, we measured the macroscopic proton-FA adsorption stoichiometry. Perona and Lecky (1985) and Cernik *et al.* (1996) showed that the macroscopic proton-ion adsorption stoichiometry is related to the pH dependence of ion adsorption via the thermodynamic consistency relationship. Rietra *et al.* (2000) showed how this relationship can be extended to apply for adsorption of species which have a pH dependent variable number of protons bound to the adsorbing species. Their finding can for our case be written as:

$$\left(\frac{\partial(\log[FA_{diss}])}{\partial(pH)}\right)_{\Gamma_{FA}} = \left(\frac{\partial\Gamma_H}{\partial\Gamma_{FA}}\right)_{pH} - d_{pH} \qquad [6.19a]$$

in which Γ_H and Γ_{FA} represent the number of protons and FA molecules bound per unit surface area respectively, and d is the degree of protonation of FA in solution ($[H_{FA}]$ /$[FA_{diss}]$; in which $[H_{FA}]$ is the concentration of protons in solution (mol/l) that are bound by FA molecules). The reference state for the calculations of $\left(\frac{\partial\Gamma_H}{\partial\Gamma_{FA}}\right)_{pH}$ is the fully deprotonated FA molecule, the d-term takes into account that the FA molecules are partly protonated in solution (Rietra *et al.*, 2000). In case the concentration of the mean protonated FA molecule is taken as the reference state for the calculation of $\left(\frac{\partial\Gamma_H}{\partial\Gamma_{FA}}\right)_{pH}$, d in equation [6.19a] equals 0 and the equation reduces to:

$$\left(\frac{\partial(\log[FA_{diss}])}{\partial(pH)}\right)_{\Gamma_{FA}} = \left(\frac{\partial\Gamma_H}{\partial\Gamma_{FA}}\right)_{pH} \qquad [6.19b]$$

The set up of the proton-FA titrations is such that >99% of the FA is adsorbed. In the proton-FA titrations, the pH of the FA solution and goethite suspension are equal and kept constant in order to exclude the change in protonation of non-coordinated FA and goethite groups upon pH changes. The adsorbed amount of FA (x-axis) in such experiments follows directly from the added total amount. The number of protons which co-adsorb/desorb (y-axis) follows from the amount of acid (or base) added in order to maintain a constant pH. The co-adsorption of protons is measured as the extra amount of protons consumed upon the adsorption of FA at constant pH (equation [6.19b]).

In this study, we have measured the proton-FA adsorption stoichiometry for three different pH values and two electrolyte concentrations. Figure 6.7 shows the results of the proton-ion titrations. The lines in the figure indicate model predictions. Note that the model is calibrated on the FA adsorption data of figure 6.5. The FA:goethite ratio used in the proton

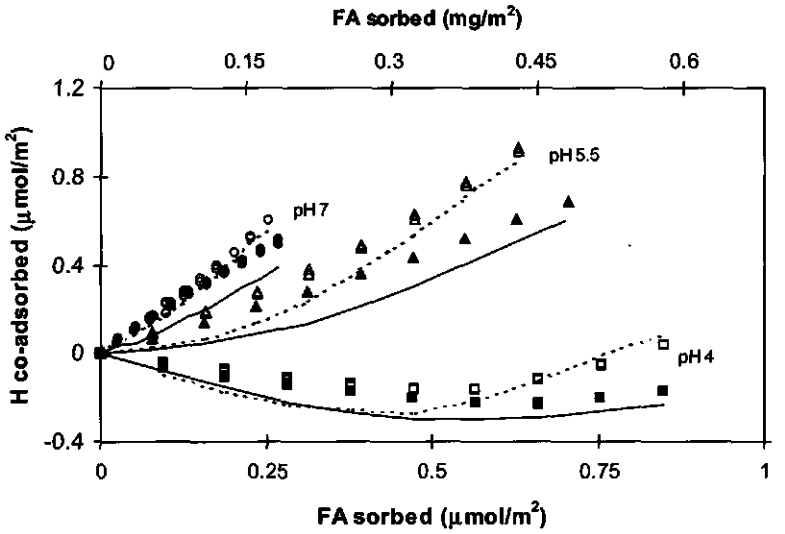

Fig. 6.7 The co-adsorption of protons as function of the adsorbed amount of FA at three pH values and two ionic strengths. The open symbols and dotted lines represent the data at 0.01 M $NaNO_3$ and the solid symbols and solid lines the data at 0.1 M $NaNO_3$. The model lines are pure predictions.

ion titrations is much lower than the ratios used in the adsorption experiments (pH 7: 18-180 μg FA/m^2 and 60-630 μg FA/m^2 respectively). The calculations of the proton co-adsorption are therefore pure predictions for situations which are extrapolations compared to figure 6.5 and not interpolations. The effects of pH, ionic strength, and surface loading on the proton adsorption are predicted quite accurately.

Reaction [6.8] and those given in table 6.1 show that in case of FA adsorption protons are involved in the protonation of the non-coordinated groups of the bound FA (ΔH_{FA}), in protonation of reactive goethite surface groups (ΔH_{goet}), and in the formation of bonds between the reactive groups of both components in case of surface complexation (H_{compl}). Therefore, the co-adsorption of protons is given by:

$$H_{co-ads} = H_{compl} + \Delta H_{goet} + \Delta H_{FA} \qquad [6.20]$$

Note that H_{compl} always has a positive value. ΔH_{goet} is positive because the repulsion of protons near the goethite surface diminishes due to the presence of negatively charged FA. Therefore, the concentration of protons near the surface becomes higher. This results in an enhanced sorption of protons. ΔH_{FA} has a negative value due to the competition between protons and reactive surface groups and due to the increased electrostatic potential near the goethite surface compared to the potential in the Donnan phase in solution. Model calculations show that the potential in the surface region remains positive throughout the whole experiment, whereas the potential of the Donnan phase for the free FA molecules in solution is negative.

According to equation [6.19], the slope of the curves of figure 6.7 directly gives the pH dependence of the adsorption at a particulate pH and surface loading. Note that the slope is for most cases positive, indicating increased adsorption with decreasing pH as is normally observed. However, at low pH and low loading, the slope is negative indicating a decrease of adsorption with decreasing pH.

6.7 Conclusions

The LCD model enables the simultaneous description of the concentration, pH, and salt dependency of adsorption and the related charge phenomena: basic proton charging, co-adsorption of protons upon FA adsorption. The model exhibits different levels of detail. On a microscopic scale, the type of complexes between protons and the reactive groups of FA and

the surface are defined. The structures of the complexes are, if possible, based on information obtained from spectroscopic studies. Protons in solution and reactive surface groups compete for the same reactive groups of the FA molecule. The interactions result in a speciation of the adsorbed FA molecule that depends on pH, ionic strength, surface loading, etc. This level of detail is comparable to the binding of protons and heavy metals by humic materials.

The speciation of the adsorbed FA molecules is calculated using the NICCA model taking protonation and surface complexation of the reactive FA groups, and the electrostatics near the goethite surface into account. The speciation of the adsorbed FA molecule implicitly determines the most important factors for NOM binding by oxide surfaces, *e.g.* the overall binding affinity, the charge distribution near the surface, and the stoichiometry of an adsorbed FA molecule. The macroscopic distribution of FA over the dissolved and adsorbed state is calculated using the CD-MUSIC model using the affinity and charge distribution. The coupling of the NICCA equation and the CD-MUSIC model is self-consistent. This means that the speciation of the bound FA determines the overall affinity constant, the overall charge distribution, and the stoichiometry of the adsorption reaction. For the calculation of the speciation of the bound FA, as well as in the calculation of the overall adsorption of FA by goethite, the electrostatic interactions are taken into account using the BS approach.

Due to the complex nature of the interactions between organic materials and oxide surfaces, spectroscopy studies give little information about the speciation of the adsorbed organic molecules. At best, the spectroscopic data provide quantitative information about the types of complexes formed between the reactive groups of the surface and of the organic molecule. This information corresponds to the microscopic level of detail of the present approach and constraints the types of complexes used in the model. Note that in the discrete models, the speciation of the adsorbed FA molecule is the level with the most detail. Therefore, spectroscopic evidence gives only weak constraints in this type of modeling approach.

Model calculations show that the carboxylic groups are important for the FA binding at low pH, whereas the phenolic groups are important at high pH. This is in agreement with studies determining the sorption of small well-defined weak organic carboxylic and phenolic acids. Inner sphere complexes become important at low pH, outer sphere complexes are important at high pH. This is in agreement with the complex formation inferred from studies using spectroscopy.

The great advantage of the model approach presented here is that it can be applied for a wide range of conditions. Not only variations in pH, ionic strength and FA content are taken

into account accurately, in the new approach the presence of oxyanions and polyvalent ions can be incorporated easily. The speciation of adsorbed oxyanions is relatively simple and has been determined from spectroscopy for a range of ions. The oxyanion adsorption can therefore be calculated with the CD-MUSIC part of the present model. The adsorption of metal ions by goethite can also be described with the CD-MUSIC model, whereas the adsorption of the metal ions by organic material can be described with the NICCA equation. In case the adsorption of metal ions to the individual components is known, the effects of the presence of metal ions on the FA adsorption can be calculated with the present model without any additional parameters.

A lot of work still needs to be done in order to test in how far this approach will give satisfactory results for such complex systems. A further challenge will be to extend the approach for kinetics of ad- and desorption of HA/FA mixtures of natural organic molecules that differ significantly in size.

References

References

Aiken G. R., Thurman E. M., Malcolm R. L., and Walton H. F. (1979) Comparison of XAD macroporous resins for the concentration of fulvic acid from aqueous solution. *Anal. Chim. Acta.* 51, 1799-1803.

Aiken G.R., McKnight D.M.,Wershaw R.L., and MacCarthy P. (1985) *Humic Substances in Soil, Sediment, and Water.* Wiley Interscience: New York.

Ali M.A. and Dzombak D.A. (1996) Competitive sorption of simple organic acids and sulfate on goethite. *Environ. Sci. Technol.* **30**, 1061-1071.

Atkinson R.J., Posner A.M., and Quirk J.P. (1967) Adsorption of potential-determining ions at the ferric oxide-aqueous electrolyte interface. *J. Physic. Chem.* **71**, 550-558.

Au K-K., Penisson A.C., Yang S., and O'Melia C.R. (1999) Natural organic matter at oxide/water interfaces: Complexation and conformation. *Geochim. Cosmochim. Acta* **63**, 2903-2917.

Avena M.J., Vermeer A.W.P., and Koopal L.K. (1999) Volume and structure of humic acids studied by viscometry. pH and electrolyte concentration effects. *Colloids Surfaces A*, **151**, 213-224

Avena M.J., Koopal L.K., and Van Riemsdijk W.H. (1999) Proton binding to humic acids. Electrostatic and specific interactions. *J. Colloid Interface Sci.* **217**, 37-48

Balistrieri L.S. and Murray J.W. (1986) The influence of the major ions of seawater on the adsorption of simple organic acids by goethite. *Geochim. Cosmochim. Acta* **51**, 1151-1160.

Beckett R., and Le N.P., (1990) The role of organic matter and ionic composition in determining the surface charge of suspended particles in natural waters. *Colloids Surfaces* **44**, 35-49

Benedetti M.F., Milne C.J., Kinniburgh D.G., Van Riemsdijk W.H., and Koopal L.K. (1995) Metal-ion binding to humic substances. Application of the nonideal competitive adsorption model. *Environ. Sci. Technol.* **29**, 446-457

Benedetti M.F., Van Riemsdijk W.H., and Koopal L.K. (1996) Humic substances considered as a heterogeneous donnan gel phase. *Environ. Sci. Technol.* **30**, 1805-1813.

Bennett P.C., Melcer M.E., Siegel D.I., and Hassett J.P. (1988) *Geochim. Cosmochim. Acta* **52**, 1521-1530.

Berbel F., Díaz-Cruz J.M., Ariño C., Esteban M., Mas F., Garcés J.L., and Puy J. (2001) Voltammetric Analysis of Heterogeneity in Metal Ion Binding by Humics. *Environ. Sci. Technol* (accepted)

Biber M.V. and Stumm W. (1994) An In-situ ATR-FTIR study: The surface coordination of salicylic acid on aluminum and iron(III) oxides. *Environ. Sci. Technol.* **28**, 763-768.

Boekhold A.E., Temminghoff E., and Vand der Zee S.E.A.T.M (1993) Influence of electrolyte composition and soil pH on Cd sorption by a sandy soil. *J. Soil Sci.*, **44**, 55-96.

Boily J.F., Nilsson N., Persson P., and Sjoberg S. (2000a) Benzenecarboxylate surface complexation at the goethite (a-FeOOH)/water interface: I. A mechanistic description of pyromellitate surface complexes from the combined evidence of infrared spectroscopy, potentiometry, adsorption data, and surface complexation modeling. *Langmuir* **16**, 5719-5729

Boily J.F., Persson P., and Sjoberg S. (2000b) Benzenecarboxylate surface complexation at the goethite (a-FeOOH)/water interface: II. Linking IR spectroscopic observations to mechanistic surface complexation models for phthalate, trimellitate and pyromellitate. *Geochim. Cosmochim. Acta* **64**, 3453-3470

Boily J.F., Lutzenkirchen J., Balmes O., Beattie J., and Sjoberg S. (2001) Modeling proton binding at the goethite (α-FeOOH)-water interface. *Colloids Surfaces A*, **179**, 11-27

Bowden J.W., Nagarajah S., Barrow N.J., Posner A.M., and Quirk J.P. (1980) Describing the adsorption of phosphate, citrate and selenite on a variable-charge mineral surface. *Aus. J. Soil Res.* **18**, 49-60.

Brown I.D. (1978) Bond valences - A simple structural model for inorganic chemistry. *Chem. Soc. Rev.* **7**, 359-376.

Cederberg, A.S., Street, R.L., and Leckie, J.O., *Water Resour. Res.* **21**, 8, 1095 (1985)

Cernick, M., Barmettler, K., Grolimund, D., Rohr, W., Borkovec, M., and Sticher, H., *J. Contam. Hydrol.* **16**, 319-337 (1994)

Cernick M., Borkovec M., and Westall J.C. (1996) Affinity distribution description of competitive ion binding to heterogeneous materials *Langmuir* **12**, 6127-6137.

Christensen J.B., Tipping E., Kinniburgh D.G., Gron C., and Christensen T.H. (1998) Proton binding by groundwater fulvic acids of different age, origin and structure modelled with the Model V and NICA-Donnan model. *Environ. Sci. Technol.* **32**, 3346-3355.

Cornell R.M. and Schindler P.W. (1980) Infrared study of the adsorption of hydroxycarboxylic acids on α-FeOOH and amorphous Fe(III)hydroxide. *Colloid Polymer Sci.* **258**, 1171-1175.

Davis J.A. (1982) Adsorption of natural dissolved organic matter at the oxide/water interface. *Geochim. Cosmochim. Acta* **46**, 2381-2393

De Wit J.C.M., Van Riemsdijk W.H., and Koopal, L.K. (1993a) Proton binding to humic substances: 1. Electrostatic effects. *Environ. Sci. Technol* **27**, 2005-2014.

De Wit J.C.M., Van Riemsdijk W.H., and Koopal, L.K. (1993b) Proton binding to humic substances: 2. Chemical heterogeneity and adsorption models *Environ. Sci. Technol* **27**, 2015-2022.

Dunnivant F.M., Jardine P.M., Taylor D.L., and McCarthy J.F. (1992) Transport of naturally occurring dissolved organic carbon in laboratory columns containing aquifer material. *Soil Sci. Soc. Am. J.* **56**, 437-444

Dzombak D.A. and Morel F.M.M. (1990) *Surface Complexation Modeling: Hydrous Ferric Oxide.* Wiley-Interscience: New York.

Earl K.D., Syers J.K. and McLaughlin J.R. (1979) Origin of the effects of citrate, tartrate, and acetate on phosphate sorption by soils and synthetic gels. *Soil Sci. Soc. Am. J.* **43**, 674-678

Engesgaard, P. and Christensen, T.H. (1988). A review of chemical solute transport models. *Nord. Hydrol.* **19**, 183

Ephraim J., Alegret S., Mathuthu A., Bicking M., Malcolm R.L., and Marinsky J.A. (1986) A united physicochemical description of the protonation and metal ion complexation equilibria of natural organic acids (humic and fulvic acids). 2. Influence of polyelectrolyte properties and functional group heterogeneity on the proton equilibria of fulvic acid. *Environ. Sci. Technol.* **20**, 354-366.

Evanko C.R., and Dzombak D.A. (1998) Influence of structural features on sorption of NOM-analogue organic acids to goethite. *Environ. Sci. Technol.* **32**, 2846-2855.

Evanko C.R. and Dzombak D.A. (1999) Surface complexation modeling of organic acid sorption to goethite. *J. Colloid Inter Sci.* **214**, 189-206

Filius J.D., Hiemstra T., and Van Riemsdijk W.H. (1997) Adsorption of small weak organic acids on goethite: Modeling of mechanisms. *J. Colloid Interface Sci.* **195,** 368-380.

Filius J.D., Lumsdon D.G., Meeussen J.C.L., Hiemstra T., and Van Riemsdijk W.H. (2000) Adsorption of fulvic acid on goethite. *Geochim. Cosmochim. Acta* **64,** 51-60

Filius J.D., Meeussen J.C.L., Hiemstra T., and Van Riemsdijk W.H. (2001) Modeling the binding of benzenecarboxylates by goethite. The ligand and charge distribution (LCD) model. *J. Colloid Inter Sci.* (accepted)

Fokkink L.G.J., de Keizer A., and Lyklema J. (1987) Specific ion adsorption on oxides. *J. Colloid Inter Sci.* **118,** 454-462.

Geelhoed J.S., Hiemstra T., and Van Riemsdijk W.H. (1997) Phosphate and sulphate adsorption on goethite: single anion and competitive adsorption. *Geochim. Cosmochim. Acta* **61,** 2389-2396

Geelhoed J.S., Hiemstra T., and Van Riemsdijk W.H. (1998) Competitive interaction between phosphate and citrate on goethite. *Environ. Sci. Technol.* **32,** 2119-2123

Gerke J. (1992) Phosphate, aluminium and iron in the soil solution of three different soils in relation to varying concentrations of citric acid. *Z. Pflanzenernahr. Bodenk.* **155,** 339-343.

Gu B., Schmitt J., Chem Z., Liang L., and McCarthy J.F. (1994) Adsorption and desorption of natural organic matter on iron oxide: Mechanisms and models. *Environ. Sci. Technol.* **28,** 38-46.

Gu B., Schmitt J., Chem Z., Liang L., and McCarthy J.F. (1995) Adsorption and desorption of different organic matter fractions on iron oxide. *Geochim. Cosmochim. Acta* **59,** 219-229.

Hansen E.H., and Schnitzer M. (1969) Molecular weight measurements of polycarboxylic acids in water by vapor pressure osmometry. *Anal. Chim. Acta* **46,** 247-254.

Hawke D., Carpenter P.D., and Hunter K.A. (1989) Competitive adsorption of phosphate on goethite in marine electrolytes. *Environ. Sci. Technol.* **23,** 187-191

Herzer, J. and Kinzelbach, W. (1989) Coupling of transport and chemical processes in numerical transport models. *Geoderma* **44,** 115

Hiemstra T., Van Riemsdijk W.H. and Bolt G.H. (1989a) Multisite proton modeling at the solid/solution interface of (hydr)oxides: A new approach. I. Model description and evaluation of intrinsic reaction constants. *J. Colloid Interface Sci.* **133,** 91-104

Hiemstra T., De Wit J.C.M., and Van Riemsdijk W.H. (1989b) Multisite proton adsorption modeling at the solid/solution interface of (hydr)oxides: A new approach, II. Application to various important (hydr)oxides. *J. Colloid Interface Sci.* **133,** 488-508.

Hiemstra T. and Van Riemsdijk W.H. (1996) A surface structural approach to ion adsorption: The charge distribution (CD) model. *J. Colloid Interface Sci.* **179,** 488-508.

Hiemstra T., Venema P., and Van Riemsdijk W.H. (1996) Intrinsic proton affinity of reactive surface groups of metal (hydr)oxides: The bond valence principle. *J. Colloid Interface Sci.* **184,** 680-692.

Hingston F.J., Atkinson R.J., Posner A.M., and Quirk J.P. (1967) Specific adsorption of anions. *Nature* **215,** 1459-1461.

Hue N.V. (1991) Effects of organic acids/anions on P sorption and phytoavailablity in soils with different mineralogies. *Soil. Sci.* **152,** 463-471

Jardine P.M., Weber N.L., McCarthy J.F. (1989) Mechanisms of dissolved organic carbon adsorption on soil. *Soil Sci. Soc. Am. J.* **53,** 1378-1385.

Jardine, P.M., Dunnivant, F.M., Selim, H.M., and McCarthy, J.F. (1992) Transport of naturally-occurring dissolved organic-carbon in laboratory columns containing aquifer material. *Soil Sci. Soc. Am. J.* **56**, 393-401

Jaroniec, M 1983 Adv. Colloid Interface Sci. **18**, 149-225

Kaiser K., Guggenberger G., Haumaier L., and Zech W. (1997) Dissolved organic matter sorption on subsoils and minerals studied by 13C-NMR and DRIFT spectroscopy. *Europ. J. Soil Sci.* **48**, 301-310.

Karltun E. (1998) Modelling SO_4^{2-} surface complexation on variable charge minerals. II. Competition between SO_4^{2-}, oxalate and fulvate. *Europ. J. Soil Sci.* **49**, 113-120.

Keizer M.G. and Van Riemsdijk W.H. (1995) ECOSAT; Technical report of the Department of Soil Science and Plant Nutrition; Wageningen Agricultural University: Wageningen.

Kinniburgh D.G. (1993) Technical Report WD/93/23: FIT User Guide. British Geological Survey.

Kinniburgh D.G., Milne C.J., and Venema P. (1995) Design and construction of a Personal-Computer based automatic titrator. *Soil Sci. Soc. Am. J.* **59**, 417-422.

Kinniburgh D.G., Milne C.J., Benedetti M.F., Pinheiro J.P., Filius J., Koopal L.K., and Van Riemsdijk W.H. (1996) Metal ion binding by humic acid: Application of the NICA-Donnan model. *Environ. Sci. Technol.* **30**, 1687-1698

Kinniburgh D.K., Van Riemsdijk W.H., Koopal L.K., Borkovec M., Benedetti M.F., and Avena M.J. (1999) Ion binding to natural organic matter: competition, heterogeneity, stoichiometry, and thermodynamic consistency. *Colloids Surfaces A*, **151**, 147-166

Koopal L.K., Van Riemsdijk W.H., De Wit J.C.M., and Benedetti M.F. (1994) Analytical isotherm equations for multicomponent adsorption to heterogeneous surfaces. *J. Colloid Interface Sci.* **166**, 51-60

Kummert R. and Stumm W. (1980) The surface complexation of organic acids on hydrous γ-Al_2O_3. *J. Colloid Interface Sci.* **75**, 373-385.

Langford C.H., Gamble D.S., Underdown A.W., and Lee S. In Aquatic and terrestrial humic materials Chsistman R.F., and Gjessing E.T. Eds; Ann Arbor Science. Ann Arbor, 1983. Pp. 219-237

Lead J.R., Wilkinson D.J., Starchev K., Canonica S., and Buffle J. (2000) Determination of diffusion coefficients of humic substances by fluorescence correlation spectroscopy: Role of solution conditions. *Environ. Sci. Technol.* **34**, 1365-1369

Leenheer J.A., Wershaw R.L. and Michael M.R. (1995a) Strong-acid, carboxyl-group structures in fulvic acid from the Suwanee River, Georgia. 1. Minor Structures. *Environ. Sci. Technol.* **29**, 393-398.

Leenheer J.A., Wershaw R.L., and Michael M.R. (1995b) Strong-acid, carboxyl-group structures in fulvic acid from the Suwanee River, Georgia. 2. Major Structures. *Environ. Sci. Technol.* **29**, 399-405.

Lovgren L. (1991) Complexation reactions of phthatlic acid and aluminium(III) with the surface of goethite. *Geochim. Cosmochim. Acta* **55**, 3639-3645.

Manning B.A. and Goldberg S. (1996) Modeling competitive adsorption of arsenate with phosphate and molybdate on oxide minerals. *Soil Sci. Soc. Am. J.* **60**, 121-131

Martell A.E. and Smith R.M. (1977) *Critical stability constants volume 3: Other organic ligands.* Plenum Press, New York. 495p.

McCarthy J.F., and Zachara J.M. (1989) Subsurface transport of contaminants. *Environ. Sci. Technol.* **23**, 496-502

McKnight D.M, Wershaw R.L., Bencala K.E. Zeilweger G.W., and Feder G.L. (1992) Humic substances and trace metals associated with Fe and Al oxides deposited in an acidic mountain stream. *Sci. Total Environ.* **117/118**, 485-498.

Meeussen, J.C.L., Scheidegger, A., Hiemstra, T., Van Riemsdijk, W.H., and Borkovec, M. (1996) Predicting multicomponent adsorption and transport of fluoride at variable pH in a goethite-silica sand system. *Environ. Sci. Technol.* **30**, 481- 488

Meeussen, J.C.L., Meeussen, V.C.S., and Lumsdon, D.G. (1997) In *Hydroinformatics '96.* (ed. A. Mueller) pp.557-564. Balkema: Rotterdam.

Meeussen, J.C.L., Van Riemsdijk, W.H., Paterson, E., Kleikemper, J., Scheidegger, A., and Borkovec, M. (1999) Multicomponent transport of sulfate in a goethite-silica sand system at variable pH and ionic strength. *Environ. Sci. Technol.* **33**, 3443-3450

Mesuere K. and Fish W. (1992) Chromate and oxalate adsorption on goethite. 1. Calibration of surface complexation models. *Environ. Sci. Technol.* **26**, 2357-2364.

Milne C.J., Kinniburgh D.G., De Wit J.C.M., Van Riemsdijk W.H., and Koopal L.K. (1995) Analysis of metal-ion binding by Peat Humic Acid using a simple electrostatic model. *J. Colloid Interface Sci.* **175**, 448-460

Milne C.J., Kinniburgh D.G., and Tipping E. (2001) Generic NICA-Donnan Model Parameters for Proton Binding by Humic Substances. *Environ. Sci. Technol.* (accepted)

Murphy E.M., Zachara J.M., Smith S.C., Philips J.L. and Wietsma T.W. (1994) Interaction of hydrophobic organic compounds with mineral-bound humic substances. *Environ. Sci. Technol.*, **28**, 1291-1299

Nilsson N., Persson P., Lovgren L., and Sjoberg S. (1996) Competitive surface complexation of 0-phthalate and phosphate on goethite (α-FeOOH) particles. *Geochim. Cosmochim. Acta* **60**, 4385-4395.

Nordin J., Persson P., Nordin A., and Sjoberg S. (1998) Inner-sphere and outer-sphere complexation of a polycarboxylic acid at the water-boehmite (γ-AlOOH) interface: A combined potentiometric and IR spectroscopic study. *Langmuir* **14**, 3655-3662.

Novack (1974) Hydrogen bonding in solids. Correlation of spectroscopic and crystallographic data. In *Structure and bonding.* (ed. J. D. Dunitz *et al.*), Vol. 18, pp. 177-216. Springer Verlag.

Parfitt R.L., Farmer V.C., and Russell J.D. (1977a) Adsorption on hydrous oxides. I. Oxalate and benzoate on goethite. *J. Soil Sci.* **28**, 29-39.

Parfitt R.L., Fraser A.R., Russell J.D., and Farmer V.C. (1977b) Adsorption on hydrous oxides. II. Oxalate, benzoate and phosphate on gibbsite. *J. Soil Sci.* **28**, 40-47.

Parfitt R.L., Fraser A.R., and Farmer V.C. (1977c) Adsorption on hydrous oxides. III. Fulvic acid and humic acid on goethite, gibbsite and imogolite. *J. Soil Sci.* **28**, 289-296.

Pauling L. (1929) The principles determining the structure of complex ionic crystals. *J. Am. Chem. Soc.* **51**, 1010-1026.

Perona M.J. and Leckie J.O. (1985) Proton stoichiometry for the adsorption of cations on oxide surfaces. *J. Colloid Interface Sci.* **106**, 64-69

Persson P., Nordin J., Rosenqvist J., Lovgren L., Ohman L.-O., and Sjoberg S. (1998) Comparison of the adsorpion of 0-phthalate on boehmite (γ-AlOOH), aged γ-Al_2O_3, and goethite (α-FeOOH). *J. Colloid Interface Sci.* **206**, 252-266

Pinheiro JP, Mota AM, Benedetti MF (1999) Lead and calcium binding to fulvic acids: Salt effect and competition. *Environ. Sci. Technol* **33**, 3398-3404

Van Riemsdijk W.H., De Wit J.C.M., Koopal L.K., and Bolt G.H. (1986) Metal ions adsorption on heterogeneous surfaces: Adsorption models. *J. Colloid Interface Sci.* **109**, 219-228

Van Riemsdijk W.H., Bolt G.H., Koopal L.K., and Blaakmeer J. (1987) Electrolyte adsorption on heterogeneous surfaces: Adsorption models. *J. Colloid Interface Sci.* **116**, 511-522

Rietra R.P.J.J., Hiemstra T., and Van Riemsdijk W.H. (1999) The relationship between molecular structure and ion adsorption on variable charge minerals. *Geochim. Cosmochim. Acta* **63**, 3009-3015

Rietra R.P.J.J., Hiemstra T., and Van Riemsdijk W.H. (2000). Electrolyte anion affinity and its effect on oxyanion adsorption on goethite. *J. Colloid Interface Sci.* **229**, 199-206

Rusch U., Borkovec M., Daicic J., and Van Riemsdijk W.H. (1997) Interpretation of competitive adsorption isotherms in terms of affinity distributions. *J. Colloid Interface Sci.* **191**, 247-255

Scheidegger, A., Borkovec, M., and Sticher, H. (1993) Coating of silica sand with goethite – Preparation and analytical identification. *Geoderma* **58**, 43-65

Scheidegger, A., Burgisser, C.S., Borkovec, M., Sticher, H., Meeussen, H., and Van Riemsdijk, W. (1994) Convective-transport of acids and bases in porous-media. *Water Resour. Res.* **30**, 11, 2937-2944

Sibanda H.M. and Young S.D. (1986) Competitive adsorption of humus acids and phosphate on goethite, gibbsite and tow tropical soils. *J. Soil Sci.* **37**, 197-204

Sigg L and Stumm W. (1980) The interaction of anions and weak acids with the hydrous goethite (α-FeOOH) surface. *Colloids Surfaces* **2**, 101-117.

Sips R. (1948) *J. Chem. Phys.* **16**, 490

Stern O. (1924) Zür theory der electrolytischen doppelschicht; *Z Elektrochem.* **30**, 508-516

Stevenson F.J. (1994) *Humus Chemistry; Genesis, Composition, Reactions*, 2nd ed.; John Wiley & Sons: New York

Stone A.T. (1987) Microbial metabolites and the reductive dissolution of manganese oxides: Oxalate and pyruvate. *Geochim. Cosmochim. Acta* **51**, 919-925.

Swift R.S. (1996) Organic matter characterization. In *Methods of Soil Analysis. Part 3. Chemical Methods-SSSA Book Series no.5.* pp 1011-1069. Soil Science Society of America and American Society of Agronomy, 677 S. Segoe Rd., Madison WI 53711, U.S.A.

Tejedor-Tejedor M.I., Yost E.C., and Anderson, M.A. (1992) Characterization of benzoic and phenolic complexes at the goethite/aqueous solution interface using cylindrical internal reflection Fourier transform infrared spectroscopy. 2. Bonding structures. *Langmuir* **8**, 525-533.

Tipping E. (1981) The adsorption of aquatic humic substances by iron oxides. *Geochim. Cosmochim. Acta* **45**, 191-199.

Tipping E. and Cook D. (1982) The effects of adsorbed humic substances on the surface charge of goethite in freshwater. *Geochim Cosmochim. Acta* 46, 75-80

Tipping E., Griffith J.R., and Hilton J. (1983) The effect of adsorbed humic substances on the uptake of copper(II) by goethite. *Croat. Chem. Acta.* **56**, 613-621.

Venema P., Hiemstra T., and Van Riemsdijk W.H. (1996) Multi site adsorption of cadmium on goethite. *J. Colloid Interface Sci.* **183**, 515-527.

Vermeer A.W.P., Van Riemsdijk W.H., and Koopal L.K. (1998) Adsorption of Humic Acid to Mineral Particles. 1. Specific and Electrostatic Interactions. *Langmuir* **14**, 2810-2819.

Wang L., Chin Y.P., and Traina S.J. (1997) Adsorption of (poly)maleic acid and an aquatic fulvic acid by goethite. *Geochim. Cosmochim. Acta* **61**, 5313-5324

Van de Weerd H., Leijnse A., and Van Riemsdijk W.H. (1999) Modeling the dynamic adsorption/desorption of a NOM mixture: Effects of physical and chemical heterogeneity. *Environ. Sci. Technol.* **33**, 1675-1681

Van de Weerd H., Van Riemsdijk W.H., and Leijnse A. (2001) Modelling transport of a mixture of natural organic molecules (NOM): effect of dynamic competitive sorption from particle to aquifer scale. *Water Resour. Res.* (accepted).

Wershaw R. L., Leenheer J.A., Sperline R.P., Song Y., Noll L.A., Melvin R.L., Rigatti G.P. (1995) Mechanisms of formation of humus coatings on mineral surfaces 3. Composition of adsorbed organic acids from compost leachate on alumina. *Colloids Surf.* **96,** 93-104.

Xu H., Ephraim J., Ledin A., and Allard B. (1989) Effects of fulvic acid on the adsorption of Cd(II) on aluminal. *Sci. Total Environ.* **81/82**, 653-660.

Yates D.E. and Healy T.W. (1975) Mechanism of anion adsorption at the ferric and chromic oxide water interfaces. *J. Colloid Interface Sci.* **52**, 222-228.

Yost E.C., Tejedor-Tejedor M.I., and Anderson M.A. (1990) In situ CIR-FTIR characterization of salicylate complexes at the goethite/aqueous solution interface. *Environ. Sci. Technol.* **24**, 822-828.

Zinder B., Furrer G., and Stumm W. (1986) The coordination chemistry of weathering: II. Dissolution of Fe(III) oxides. *Geochim. Cosmochim. Acta* **50**, 1861-1869.

Zhang Y, Kallay N., and Matijevic E. (1984) Interactions of metal hydrous oxides with chelating agents. 7. Hematite-oxalic acid and -citric acid systems. *Langmuir* **1**, 201-206.

Van Zomeren A. and Comans R.N.J. Characterisation of dissolved organic carbon in leachates from MSWI bottom ash, (*in preparation*)

Summary and concluding remarks

Introduction

The sorption of organic substances by metal (hydr)oxide surfaces strongly influences the mobility and bioavailability of contaminants and nutrients in the soil. Metal(hydr)oxide surfaces can adsorb the organic molecules. For both soil fertility and soil pollution problems, it is important to have an accurate qualitative and quantitative insight in the transport and availability of organic molecules that are sorbed by the metal(hydr)oxide surfaces.

In order to develop a model that can describe the binding of organic molecules by metal(hydr)oxide surfaces accurately, the adsorption of a series of well-defined weak organic acids is determined. Further, the adsorption of an ill-defined weak natural organic acid, *e.g.* FA, is determined. The data are described with two types of model approaches; *e.g.*, a discrete and a continuous modeling approach.

Experimental results

In this thesis, the adsorption of lactic acid, oxalic acid, malonic acid, phthalic acid, citric acid, and fulvic acid (FA) by goethite is experimentally determined at different pH values and two background electrolyte concentrations. The adsorption of the organic acids decreases with increasing pH. The pH dependency is less pronounced for the organic acid with an increased number of reactive groups. The data can be plotted as isotherms, in which the adsorption of the organic acid is plotted as function of the organic acid concentration in solution at a constant pH and background electrolyte level. The adsorption increases with increasing solution concentration. The initial slope of these isotherms is related to the number of reactive groups present in the organic molecule. At constant pH, the initial slope is smallest for the molecules with the smallest number of reactive groups (lactic acid) and is highest for the molecules with the highest number of reactive groups (FA).

Chapter 3 discusses the transport of malonic acid in a column packed with goethite-coated sand. The interaction of malonic acid with protons, both in solution and on the goethite surface, results in a simultaneous breakthrough of malonic acid and protons. The rise in pH upon the initial breakthrough of malonate indicates a co-adsorption of protons upon malonate adsorption. In chapter 6, the co-adsorption of protons upon the adsorption of FA by goethite is studied using proton-ion-titrations. The results show that at low pH and low surface loadings, there is a release of protons upon FA binding. At higher pH and/or high

surface loadings there is an uptake, or co-adsorption, of protons. The release of protons indicates that the FA adsorption increases with increasing pH, whereas the uptake of protons indicates a decrease in FA adsorption with increasing pH.

Proper modeling of the adsorption data should result in an accurate prediction of the co-adsorption of protons.

Modeling

Discrete modeling approach

In chapter 2, the adsorption of lactic acid, oxalic acid, malonic acid, phthalic acid, and citric acid is described with a discrete modeling approach. Starting point in the model development is the CD-MUSIC model with the three-plane (TP) option (Hiemstra and van Riemsdijk, 1996) to account for the spatial distribution of the charge of the adsorbed organic molecule over the solid/water interface. Furthermore, it is assumed that only singly coordinated groups of the goethite surface participate in the complexation reactions between surface and the organic molecule. The ion binding to the organic acids in solution and the complexation of the organic acids with the goethite surface groups are represented by discrete reactions assuming several solution and surface species. The organic acid adsorption data can be described well assuming a limited number of surface species. From the adsorption modeling, the distribution of charge for the inner and outer sphere complexes is found to be constant. Note that in this chapter, the overall affinity constants of the surface species formed are found by curve fitting.

In chapter 4, we describe the binding of FA by goethite using the discrete approach. As for the well-defined organic molecules, the protonation of the reactive groups is described with discrete reactions. The charging behavior of FA in solution is described assuming FA molecules with 5 carboxylic groups and 3 hydroxyl groups. As FA is less well-defined as the simple organic acids studied in chapter 2, it is not realistic to describe the FA adsorption with the same level of detail as the adsorption of the small, well-defined weak organic acids. The charge of the adsorbed organic molecules is located in only 2 planes, *e.g.*, the surface plane and the head end of the diffuse double layer (ddl). Therefore, the electrostatic interactions of the FA adsorption are described using the basic Stern (BS) option of the CD-MUSIC model. The use of the BS option reduces the number of possible charge distributions considerably.

Due to the relatively large size of the FA molecules, the interaction between the reactive FA groups and both singly and triply coordinated groups of the goethite surface becomes more likely. In chapter 4, we include the formation of H-bonds between reactive groups of the FA molecule and triply coordinated groups of the oxide surface. We abstain from the formation of inner sphere complexes with triply coordinated surface groups. The hydroxyl group of the protonated triply coordinated surface site is very difficult to exchange because of the large local over-saturation of charge during the exchange reaction. The triply coordinated surface groups are thus supposed to form outer sphere complexes only.

In chapter 4, the overall affinity constant for the formation of the four FA surface species are based on the contribution in chemical energy of the individual complexes (inner sphere, outer sphere, proton) formed with all reactive groups of the FA molecule.

We found that the use of the BS option and the inclusion of the H bond formation with triply coordinated surface sites also simplifies the description of the adsorption of the well-defined weak organic acids by goethite (results are not shown in this thesis). The adsorption data of the small acids can be described with the same number of surface species or less. Furthermore, the questionable assumptions of ion pair formation between sodium and the non-coordinated reactive groups of the bound organic molecule, and the formation of an outer sphere complex in which the hydroxylate group of the bound citrate molecule is the H bond acceptor (species 12 in table 4.5), can now be omitted.

The discrete modeling approach has several disadvantages when it is applied to organic molecules with a large number of reactive groups. In principle, the adsorbed FA molecules can bind in > 5000 different configurations (see introduction and chapter 4). In the discrete modeling approach, we only use four different surface species for the description of the adsorption of FA by goethite. This leads to a strongly reduced speciation of the adsorbed FA molecules, which is chemically and physically not very realistic. Furthermore, the formation of the different individual complexes (inner and outer sphere complexation for the carboxyl groups and outer sphere complexation for the hydroxyl groups) are characterized by one affinity constant per type of complex for all carboxyl or hydroxyl groups of the FA molecule. Although the addition of chemical energy of the complexation reactions of the individual reactive groups reduces the number of adjustable parameters, it may not be realistic to assume the same affinity constants for the all carboxyl or hydroxyl groups. For example, the binding of protons and metal ions by large organic molecules can only be described assuming a distribution of affinity constants.

Continuous modeling approach

In chapters 5 and 6, the ligand and charge distribution (LCD) model is developed. In the model, the full possible speciation of the adsorbed organic molecules is taken into account using a distribution of affinity constants for the different complexes formed with the carboxyl and hydroxyl groups of the organic molecules. The model can describe the adsorption of large organic molecules. The essence of the model is the calculation of the mean mode of an adsorbed organic molecule, defined by an overall affinity, charge distribution, and reaction stoichiometry. The calculation of the mean mode of the adsorbed organic molecule is based on the pH dependent interaction of a functional group for binding a proton or forming an inner or outer sphere complex with specific surface sites. Note that we assume the same charge distributions for the individual complexes as used in the discrete modeling approach in chapter 4. The combination of the CD-MUSIC and the NICCA model results in the new model with a large number of parameters. A lot of parameters are fixed by additional experiments (charging behavior of goethite and FA) or for structural reasons.

The affinity distributions for the formation of inner sphere, outer sphere and proton complexes with carboxyl and hydroxyl groups are characterized by two parameters, *e.g.* the median affinity constant and a parameter n that accounts for the specific heterogeneity or non-linearity of the complex formation. Furthermore, the distributions of the carboxylic and phenolic groups are characterized by a parameter p_i that accounts for the intrinsic chemical heterogeneity.

The number of adjustable parameters is reduced considerably by the assumption that the distribution for the proton affinity of the dissolved and adsorbed organic molecules is the same. The degrees of freedom are reduced further by the assumption that the distributions of the affinity constants of the different complexes are partially correlated. According to Rush *et al.* (1997), this leads to one constant n-parameter for the different complexes formed. The parameter n is related to the degree of correlation of the different distributions (n=1, full correlation)

In chapter 5, we describe literature data of Boily *et al.* (2000) who determined the adsorption of several benzenecarboxylic acids by goethite. As these organic acids only contain carboxylic groups that are reactive for the surface groups and protons, only three affinity distributions are used (inner sphere, outer sphere, and protonation of the carboxylic groups). Boily *et al.* (2000) also determined the infrared (IR) spectra of the bound organic

molecules. From their data, the relative proportion of each type of binding mode can be derived. The LCD model predicts these data reasonably when it is calibrated on the adsorption data.

In chapter 6, we describe the FA adsorption data determined in chapter 4 with the LCD modeling approach. The model used in this chapter is an extension of the model used in chapter 5 for two reasons: 1) In the description of the charging behavior of FA in solution, electrostatic effects are taken into account explicitly by calculating the proton concentration near/in the organic molecules with a simple Donnan model. 2) FA contains both carboxylic and phenolic groups. Therefore, the distributions of the proton affinity and the affinity of the two types of outer sphere complexes of the hydroxyl groups of the FA are taken into account in addition to the affinity distributions of the carboxylic groups. In case of FA adsorption by goethite, the *n*-values for the distributions of carboxyl and phenolic groups are obtained from the charging behavior of FA in solution, taking the *p*-value from the generic data set presented by Milne *et al.* (2001). The median affinity constants for the different types complexes are the only adjustable parameters (three in total; see chapter 6).

Modeling results

Comparison of the two model approaches shows similar trends for the surface speciation of the adsorbed organic molecules. With increasing pH, the relative importance of the different surface complexes increases in the order of: inner sphere complexation < outer sphere complexation of carboxylic groups < outer sphere complexation in which the phenolic group of the organic molecule is the H-bond donor < outer sphere complexation of the phenolic groups of the organic molecule in which the surface site is the H-bond donor (only for continuous model). Furthermore, in both models, the (median) affinity constants for the different complexes increase in the order inner sphere complexes < outer sphere complexes with carboxylic groups < outer sphere complexes with phenolic groups.

Both models are used to describe the same data set of FA adsorption by goethite. The most important feature in the FA adsorption is the pH dependency of the binding. The pH dependency is determined by the proton exchange ratio of the acid adsorption. The exchange ratio is determined by the charge of the adsorbed ion and the location of its charge at a finite distance from the surface. In both model approaches, the number of inner and outer sphere complexes formed and the protonation of non-coordinated reactive groups of the adsorbed

molecule determine the charge and charge distribution of the adsorbed organic molecules. In the discrete modeling approach, the number of inner and outer sphere complexes and the number of bound protons of each surface species and the relative contribution of each surface species to the total adsorption determines the proton exchange ratio and the pH dependence of the FA adsorption. In the LCD modeling approach, the average number of inner and outer sphere complexes and the average number of bound protons follow directly from the speciation calculations with the NICCA model. As both model approaches describe the same data with the same pH dependency, the calculated overall exchange ratio should be the same for the region where the models are calibrated. The differences in the molar mass used for FA in both model approaches complicate the comparison of the model results. When the discrete modeling approach was applied, the molar mass was not known and was therefore estimated to be 1000 g/mol. When the continuous modeling approach was applied, the molar mass was determined at 683 g/mol (Van Zomeren and Comans, 2001). Consequently, the FA molecules in the continuous modeling approach have a lower charge, as the number of reactive groups is considerably lower. This also implies a different overall charge distribution of the adsorbed FA molecules in both approaches in order to obtain a similar pH dependency of the FA adsorption.

The description of the co-adsorption of protons upon FA adsorption with the discrete model is not shown in this thesis. However, the comparison of both model descriptions of the proton co-adsorption upon FA binding shows that the extrapolations of the LCD model predict the data better than the discrete model. This observation indicates that the speciation of the bound FA in the discrete model approach may be too limited to extrapolate the model to a different range of experimental conditions than used for the calibration of the model. The use of the full possible speciation of the adsorbed molecules in the LCD model gives better results and allows for model calculations outside the range of experimental conditions used in the model calibration.

Concluding remarks

Both the discrete and LCD modeling approaches enable the simultaneous description of the concentration, pH, and salt dependency of organic acid adsorption and the related charge phenomena: basic proton charging, co-adsorption of protons upon organic acid

adsorption. The discrete model exhibits four degrees of freedom, whereas the LCD model exhibits only three. In order to reduce the number of adjustable parameters in the discrete model, several assumptions are made that are not very realistic (*e.g.*, one affinity constant for the complex formation of all carboxylic and phenolic groups; the order of the type of complex that the reactive FA groups will form with protons or reactive surface groups). Furthermore, due to the limited speciation that is taken into account for the adsorbed organic molecules, the discrete model can only be used accurately in the range of experimental conditions at which the model is calibrated.

The use of the LCD modeling approach has several advantages when applied to the adsorption of larger, ill-defined weak organic acids, like FA. The model takes the full speciation of the adsorbed organic molecule into account. Furthermore, the LCD model can deal with the strong competitive and heterogeneous nature of the binding characteristics of the large organic molecules. Due to the complex nature of the interactions between organic materials and oxide surfaces, spectroscopy studies give little information about the speciation of the adsorbed organic molecules. At best, the spectroscopic data provide information about the types of complexes formed between the reactive groups of the surface and of the organic molecule. However, the information obtained from IR spectroscopy studies corresponds directly to the level of detail that is present in the LCD modeling approach. Therefore, IR-data can to some extent constrain the continuous model for the used type of complexes.

The great advantage of the LCD modeling approach is that it can be applied for a wide range of conditions. Not only variations in pH, ionic strength, and organic acid content are taken into account accurately, also the presence of oxyanions and metal ions can be incorporated easily. The speciation of adsorbed oxyanions is relatively simple and has been determined by spectroscopy for a range of ions. The oxyanion adsorption can be calculated with the CD-MUSIC model. Note that this is possible in both types of modeling approaches. However, the cooperative adsorption of organic acids and metal ions cannot be described easily with the discrete model approach. The adsorption of metal ions by goethite in the absence of organic molecules can be described with the CD-MUSIC model. However, in the presence of organic molecules, the metal ions can form ternary complexes with adsorbed organic molecules. In the discrete model, the formation of such ternary complexes requires additional surface species. This increases the number of adjustable parameters. In the LCD model, the adsorption of the metal ions by the goethite is described by the CD-MUSIC part of the model, whereas the adsorption of the metal ions by organic material can be described with

the NICCA equation. In case the adsorption of metal ions to the individual components is known and when it is assumed that the dissolved and adsorbed organic molecules have the same affinity distributions for the metal binding, the effects of the presence of metal ions on the FA adsorption can be calculated with the LCD model without any additional adjustable parameters.

A lot of work still needs to be done in order to test in how far the LCD modeling approach will give satisfactory results for such complex systems. A further challenge will be to extend the approach for kinetics of ad- and desorption of HA/FA mixtures of natural organic molecules that differ significantly in size.

Samenvatting

Samenvatting

De mobiliteit en biobeschikbaarheid van verontreinigingen en nutriënten in de bodem worden sterk beïnvloed door de binding van stoffen aan organische materiaal. De organische moleculen worden op hun beurt sterk gebonden door de in de bodem aanwezige metaal(hydr)oxiden. Om een juiste inschatting te kunnen maken van het gedrag van stoffen in de bodem in relatie tot bodemvruchtbaarheid en bodemverontreiniging is het belangrijk een goed inzicht te hebben in het transport en biobeschikbaarheid van organische moleculen in de bodem.

Om een model te ontwikkelen dat de binding van organische stof aan oxide oppervlakken adequaat kan beschrijven is de adsorptie van een serie organische moleculen met een bekende structuur en een bekend ladingsgedrag bestudeerd. Daarnaast is de adsorptie van fulvozuur aan goethiet bepaald. De data zijn beschreven met twee type modellen, namelijk een "discreet" model en een "continu" model. Teneinde de data met een "continu" model te kunnen beschrijven is in deze studie het Ligand and Charge Distribution (LCD) model ontwikkeld.

Experimentele resultaten

In dit promotieonderzoek hebben we de adsorptie van melkzuur, oxaalzuur, malonzuur, phthaalzuur, citroenzuur en fulvozuur aan goethiet gemeten bij verschillende pH en twee concentraties van het achtergrondelektrolyt. De metingen laten zien dat de adsorptie van de organische zuren daalt met toenemende pH. De daling is het sterkst voor adsorptie van de organische zuren met een klein aantal reactieve groepen. De pH afhankelijkheid van de binding is minder duidelijk voor de zuren met een groter aantal reactieve groepen.

De adsorptie van de organische zuren is naast pH ook afhankelijk van de concentratie organisch zuur in oplossing. Deze concentratie afhankelijkheid kan bij constante pH en constant zoutniveau worden weergegeven met behulp van adsorptie isothermen. De initiële helling van deze isothermen is gerelateerd aan het aantal reactieve groepen per molecuul. Bij eenzelfde pH is de initiële helling het kleinst voor de moleculen met een klein aantal reactieve groepen (melkzuur) en het grootst voor moleculen met een groot aantal reactieve groepen (fulvozuur).

In hoofdstuk 3 wordt het transport van malonzuur door een, met goethiet gecoat zand gevulde kolom, besproken. De interactie van protonen met het opgeloste en geadsorbeerde

malonzuur resulteert in een gelijktijdige doorbraak van malonzuur en protonen. De stijging van de pH bij de doorbraak van malonzuur duidt op een co-adsorptie van protonen wanneer malonzuur wordt gebonden.

In hoofdstuk 6 is de co-adsorptie van protonen gemeten tijdens de adsorptie van fulvozuur. Ditmaal is de co-adsorptie bepaald met behulp van proton-ion-titraties. De resultaten laten zien dat er bij de adsorptie van fulvozuur protonen vrijkomen bij lage pH en lage oppervlakte bezettingen. Bij hogere pH en/of hogere oppervlakte bezettingen is er een opname van protonen. Het vrijkomen van protonen duidt op een toename van de fulvozuur adsorptie bij toenemende pH, terwijl een opname van protonen duidt op een afname van de fulvozuur adsorptie met toenemende pH. Met een thermodynamisch consistent model kan de co-adsorptie van protonen voorspeld worden op basis van de beschrijving van de adsorptie van het organisch zuur.

Modellen

Het discrete model

Het CD-MUSIC model is vertrekpunt in de modelontwikkeling in dit promotie-onderzoek. In hoofdstuk 2 wordt de adsorptie van melkzuur, oxaalzuur, malonzuur, phthaalzuur en citroenzuur beschreven met het CD-MUSIC model, waarbij de ruimtelijke verdeling van de lading van het geadsorbeerde molecuul nabij het oppervlak wordt beschreven met het three plane (TP) model. In de modelering wordt de protonering van de organische zuren in oplossing en de complexatie van de zuren door het goethiet oppervlak beschreven met discrete reactievergelijkingen. In hoofdstuk 2 wordt verondersteld dat alleen de enkelvoudige groepen van het goethiet oppervlak kunnen reageren met de reactieve groepen van de organische zuren. Er is een discreet aantal oppervlakte species nodig om de adsorptie van deze goed gedefinieerde organische zuren te beschrijven wanneer er een constante verdeling van lading voor inner en outer sphere complexen wordt aangenomen. Het aantal inner en outer sphere complexen en het aantal gebonden protonen verschilt echter per oppervlaktespecies, waardoor de overall ladingsverdeling van de oppervlaktespecies varieert. De chemische affiniteit voor de binding van het gehele organische molecuul wordt in hoofdstuk 2 gebruikt als aanpasbare parameter die verschilt per oppervlaktespecies.

In hoofdstuk 4 gebruiken we het discrete model voor de beschrijving van de binding van fulvozuur aan goethiet. Fulvozuur is een relatief groot molecuul waarvan de structuur

slecht bekend is. Voor de beschrijving van het ladingsgedrag van het fulvozuur in oplossing nemen we aan dat het fulvozuur molecuul bestaat uit 5 carboxylgroepen en 3 hydroxylgroepen. De protonering van deze groepen wordt beschreven met discrete reactievergelijkingen. In dit hoofdstuk hebben we de verdeling van de lading van het geadsorbeerde molecuul versimpeld. De lading kan slechts in twee vlakken worden geplaatst; in het oppervlak of aan het hoofdeinde van de ddl. Het gebruik van deze basic stern (BS) optie voor de beschrijving van de electrostatische interacties reduceert de vrijheid in de verdeling van de lading van de geadsorbeerde moleculen aanzienlijk.

In hoofdstuk 4 nemen we aan dat de reactieve groepen van het relatief grote fulvozuur molecuul kunnen binden met zowel enkelvoudig als drievoudig gecoördineerde groepen van het goethiet oppervlak. De drievoudig gecoördineerde groepen kunnen H-bruggen vormen met de carboxyl- en hydroxylgroepen van het organische molecuul. We laten het uitwisselen van liganden (inner sphere binding) met deze groepen buiten beschouwing. De hydroxylgroepen van de drievoudig gecoördineerde oppervlaktesites wisselen slecht uit wegens de grote mate van plaatselijke oververzadiging van lading tijdens de uitwisselreactie.

Het gebruik van de BS optie in combinatie van de vorming van H-bruggen met drievoudig gecoördineerde oppervlakte groepen versimpelt de beschrijving van de adsorptie van de goed gedefinieerde moleculen eveneens aanzienlijk. De adsorptie van deze kleinere zuren kan met hetzelfde aantal of minder oppervlakte species worden beschreven. Tevens vervallen twee twijfelachtige aannames omtrent ionpaarvorming van natrium ionen met de reactieve groepen van het gebonden organisch molecuul die niet gecomplexeerd zijn met het oppervlak, en de vorming van een H-brug waarin de hydroxylaat groep van het citroenzuur de H-brug is (species 12 in tabel 4.5). De beschrijving van de adsorptie van de kleine zuren met deze modelaanpassingen wordt echter niet in dit proefschrift gegeven.

De overall affiniteit die gebruikt wordt voor de beschrijving van de fulvozuur adsorptie aan goethiet met het discrete model is het resultaat van the gezamenlijke energie van de complexeringsreacties van alle reactieve groepen van het gebonden fulvozuurmolecuul. De vorming van de verschillende complexen met de individuele reactieve groepen van het fulvozuurmolecuul (protonering, inner en outer sphere binding voor carboxylgroepen en outer sphere binding voor hydroxylgroepen) hebben in het discrete model 1 affiniteitconstante per type complex voor alle carboxyl- of hydroxylgroepen van het fulvozuurmolecuul. Deze aanname leidt tot een kleiner aantal aanpasbare parameters in vergelijk met de aanpak die we in hoofdstuk 2 hebben gebruikt.

Het discrete model heeft een aantal nadelen wanneer het wordt gebruikt voor de beschrijving van de adsorptie van moleculen met een groot aantal reactieve groepen. Theoretisch kunnen de gebonden fulvozuurmoleculen op > 5000 verschillende manieren binden (voor de berekening zie introductie en hoofdstuk 4). In het discrete model gebruiken we slechts 4 verschillende oppervlakte species voor de binding van fulvozuur aan het goethiet. Deze zeer beperkte speciatie van het gebonden fulvozuur is fysisch/chemisch niet erg realistisch.

De aanname dat alle reactieve groepen van het fulvozuurmolecuul dezelfde affiniteit hebben voor de vorming van inner en outer sphere complexen ligt niet erg voor de hand. Immers, de binding van protonen en zware metalen aan natuurlijk organische materiaal kan slechts goed beschreven worden met een verdeling van affiniteitconstanten.

Het ligand and charge distribution model

In de hoofdstukken 5 en 6 wordt er een modelconcept gepresenteerd waarin alle mogelijke speciaties van het geadsorbeerde organische molecuul kunnen worden berekend onder aanname van een continue verdeling van affiniteitconstanten voor de verschillende complexen die worden gevormd met de hydroxyl en carboxyl groepen van het organische molecuul. In dit modelconcept wordt het CD-MUSIC model wederom gebruikt voor de beschrijving van de verdeling van de organische moleculen over de vaste fase en de oplossing. De belangrijkste input parameters van het model (affiniteitsconstante, ladingsverdeling, aantal oppervlakte groepen en protonen die betrokken zijn in de reactie) worden berekend op basis van alle interacties van de reactieve groepen van het organische molecuul met protonen en oppervlakte groepen. In het ligand distribution (LD) gedeelte van het model wordt met behulp van het NICCA model, of een versimpelde afgeleide daarvan, de competitieve binding van protonen en oppervlakte groepen aan het organische molecuul berekend voor de actuele experimentele condities. De elektrostatische interacties worden berekend met het BS model op basis van de ladingsverdelingen voor inner en outer sphere complexen zoals die zijn gebruikt in het discrete model.

De verdelingen van de affiniteitconstanten van inner sphere, outer sphere en proton complexen worden gekarakteriseerd door 2 parameters, de mediaan van de affiniteitconstanten en de parameter n die de specifieke heterogeniteit of de niet-lineariteit van de complexeringsreactie weergeeft. Verder wordt de intrinsieke chemische heterogeniteit van de reactieve groepen bepaald door de parameter p.

De koppeling van het CD-MUSIC en het NICCA model leidt tot een nieuw model met een aanzienlijk aantal parameters. Veel van die parameters kunnen worden bepaald met behulp van aanvullende experimenten of worden vastgelegd op basis van structurele eigenschappen van het goethiet. Het aantal aanpasbare parameters in het LCD model wordt sterk beperkt door de aanname dat de verdeling van de protonaffiniteitconstanten voor de opgeloste en geadsorbeerde organische moleculen hetzelfde is. Het ladingsgedrag van de opgeloste organische moleculen kan onafhankelijk worden bepaald met behulp van proton titraties. Het aantal aanpasbare parameters wordt verder gereduceerd door de aanname dat de affiniteiten verdelingen van de verschillende complexen partieel gecorreleerd zijn. Volgens Rush et al. (1997) leidt dit tot één constante n voor de verschillende complexen. De n-parameter geeft de mate van de correlatie van de verschillende verdelingen weer.

In hoofdstuk 5 worden data van Boily et al. (2000) beschreven met het LCD model. Boily et al. (2000) bepaalden de adsorptie van benzeencarboxylaten door goethiet. Daarnaast bepaalden ze de infrarood spectra van de gebonden organische moleculen onder uiteenlopende omstandigheden. Op basis van infrarood data kan de relatieve bijdrage van elk type complex worden uitgerekend. Het continue model voorspelt deze relatieve bijdrage goed wanneer het model gekalibreerd is met de adsorptie gegevens.

In hoofdstuk 6 beschrijven we de fulvozuur adsorptie data zoals die bepaald zijn in hoofdstuk 4 met het continue model. Het LCD model is hiertoe op twee punten uitgebreid ten opzichte van het model in hoofdstuk 5. 1) In de beschrijving van het ladingsgedrag van opgelost fulvozuur worden de elektrostatische effecten expliciet meegenomen door middel van de koppeling van het Donnan model aan de NICCA vergelijking. 2) Omdat fulvozuur zowel carboxyl- als hydroxylgroepen bevat, moeten de distributies van de affiniteitconstanten van hydroxylgroepen van het fulvozuur voor protonen en twee type outer sphere complexen aan het model toegevoegd. In het geval van fulvozuuradsorptie door goethiet wordt de n-waarden van de distributies verkregen uit het ladingsgedrag van het fulvozuur in oplossing, waarbij de p-waarden uit een basis data set voor fulvozuur is genomen (Milne et al., 2001). De medianen van de verschillende affiniteitverdelingen zijn de enige aanpasbare parameters (drie in totaal, zie hoofdstuk 6).

Model resultaten

Het discrete model en het LCD model laten vergelijkbare trends zien voor de mate waarin inner sphere-, outer sphere- en protoncomplexen voorkomen. Bij lage pH vormen

carboxylgroepen van het gebonden organisch zuur voornamelijk complexen met protonen en oppervlakte groepen via inner sphere complexen. Als de pH stijgt worden de outer sphere complexen belangrijker voor de carboxylgroepen. De hydroxylgroepen zijn voornamelijk geprotoneerd bij lage pH. Naarmate de pH stijgt worden eerst de outer sphere complexen waarin de organische hydroxylgroep de H-brug donor is en daarna de outer sphere complexen waarin de oppervlakte groepen de H-brug donor is belangrijk (alleen voor het LCD model). In beide modellen neemt de (mediaan) affiniteitconstante voor de verschillende oppervlakte complexen toe in de volgorde: inner sphere complexes < outer sphere complexes met carboxyl groepen < outer sphere complexes met hydroxyl groepen.

Beide modellen kunnen worden gebruikt voor het beschrijven van dezelfde set data van fulvozuuradsorptie aan goethiet. Een van de belangrijkste aspecten van de fulvozuuradsorptie is de pH afhankelijkheid van de binding. Deze pH afhankelijkheid wordt bepaald door de proton uitwisselcoëfficiënt. Verschillende auteurs laten zien dat de proton uitwisselcoëfficiënt wordt bepaald door de lading van het adsorberende ion en de ladingsverdeling van dat ion over interface van de oplossing en het goethiet. In beide modelconcepten worden de lading en de ladingsverdeling van de adsorberende organische moleculen bepaald door het aantal inner en outer sphere complexen dat wordt gevormd en de mate van protonering van de reactieve groepen van het fulvozuur die naar de oplossing zijn gericht. In het discrete model bepalen het aantal inner sphere, outer sphere en proton complexen van elk oppervlakte species, alsmede de relatieve bijdrage van elk oppervlakte species aan de totale speciatie van het fulvozuur, de protonen uitwisseling en daarmee de pH afhankelijkheid. In het LCD model volgt het gemiddelde aantal complexen en protonen direct uit de speciatie van het geadsorbeerde fulvozuurmolecuul die wordt berekend met het NICCA model. De berekende protonen omwisselcoëfficiënt moet hetzelfde zijn voor beide modellen omdat ze dezelfde data met dezelfde pH afhankelijkheid moeten beschrijven. Echter, het vergelijk van de twee modelbeschrijvingen wordt bemoeilijkt doordat er in de twee modellen een verschillende molmassa voor het fulvozuur is gebruikt. De molmassa van het fulvozuur was tijdens het modeleren van de data met het discrete model nog niet bekend. De molmassa is toen geschat op 1000 g/mol. Tijdens het modeleren met het continue model was de molmassa bekend (683 g/mol). In de beschrijving met het LCD model hebben de fulvozuurmoleculen een kleinere lading omdat de moleculen een kleiner aantal reactieve groepen hebben. Om tot de juiste pH afhankelijkheid te komen moet er een andere ladingsverdeling worden aangenomen. Wanneer de ladingsverdeling van de inner sphere,

outer sphere en protoncomplexen niet wordt gewijzigd, betekent dit dat de onderlinge verhouding van het aantal complexen verandert.

In dit proefschrift wordt de co-adsorptie van protonen tijdens de fulvozuurbinding niet beschreven met het discrete model. Wanneer de proton co-adsorptie voorspellingen van beide modellen echter worden vergeleken blijkt dat de extrapolaties van het LCD model de data beter beschrijven dan het discrete model. Dit suggereert dat in het discrete model de speciatie van het gebonden fulvozuur te beperkt is om goede voorspellingen te doen voor experimentele omstandigheden die sterk afwijken van de omstandigheden waarmee het model gekalibreerd is. Het LCD model voorspelt data buiten de range waarvoor het model gekalibreerd is beter omdat de volledige speciatie van het geadsorbeerde organische molecuul in dit model wordt meegenomen.

Afsluitende opmerkingen

Zowel het discrete als het continue model kunnen de concentratie-, pH- en zoutafhankelijkheid van de organische zuren adsorptie goed beschrijven. Het discrete model heeft 4 vrijheidsgraden, terwijl het LCD model er 3 heeft. In het discrete model zijn er verschillende minder realistische aannames gemaakt om het aantal aanpasbare parameters te minimaliseren (1 affiniteitconstante voor de complexvorming van alle carboxyl- en hydroxylgroepen; de volgorde in complexvorming van de carboxyl- en hydroxylgroepen met protonen en reactieve oppervlaktegroepen). Hoewel het discrete model een grotere vrijheid kent kan het slechts gebruikt worden in de range van experimentele omstandigheden waaronder het model gekalibreerd is. Reden hiervoor is de beperkte speciatie van gebonden organische moleculen die wordt meegenomen in het discrete model.

Het gebruik van het LCD model biedt verschillende voordelen wanneer het wordt toegepast voor de beschrijving van de adsorptie van groter, slecht gedefinieerde organische zuren, zoals fulvozuur. Het model berekent de volledige speciatie van het geadsorbeerde molecuul. Tevens houdt het continue model rekening met het sterk competitieve en heterogene karakter van de binding van de grote organische moleculen.

De informatie die wordt verkregen met infrarood spectroscopie komt direct overeen met het detailniveau waarop de diverse complexen worden gedefinieerd in het continue model. Door de ingewikkelde structuren van de organische stof geeft infrarood spectroscopie weinig informatie over de speciatie van de gebonden organische moleculen. Idealiter geeft

infrarood spectroscopie informatie over de type complexen die worden gevormd tussen de reactieve groepen van de organische stof, protonen en de reactieve oppervlakte groepen.

Een groot voordeel van het LCD model is dat het kan worden toegepast voor een scala aan omgevingsomstandigheden. Naast veranderingen in pH, ionsterkte en organische stof gehalte, kan de aanwezigheid van oxyanionen en meerwaardige kationen gemakkelijk worden meegenomen in de modelering. De adsorptie van oxyanionen kan in beide modelconcepten worden meegenomen. De coöperatieve adsorptie van organische zuren en metaalionen kan echter niet zo gemakkelijk worden meegenomen in het discrete model. Metalen kunnen ternaire complexen vormen met geadsorbeerde organische moleculen. Hoewel de adsorptie van metaalionen aan goethiet goed kan worden beschreven met het CD-MUSIC model wanneer er geen organische stof aanwezig is, kan het discrete model de vorming van ternaire complexen met organische stof moleculen slechts meenemen wanneer er nieuwe oppervlakte species worden verondersteld. Hierdoor neemt het aantal vrijheidsgraden van het discrete model toe. De binding van metaalionen aan opgelost en geadsorbeerd organisch materiaal kan goed worden beschreven met de NICCA vergelijking. Met behulp van het LCD model kan het effect van de aanwezigheid van metaalionen op de adsorptie van organische stof aan oxiden worden berekend zonder enige nieuwe aanpasbare parameters. Vervolgstudies zullen moeten uitwijzen of het LCD model in staat is goede resultaten te geven voor de speciatieberekeningen van zulke complexe systemen.

Nawoord

Het boekje dat voor u ligt is voor mij de afsluiting van een periode van 6 jaar waarin ik met veel plezier en soms een vloek en een zucht, heb gewerkt aan de koppeling van twee modellen waarmee de binding van organisch moleculen aan oxide oppervlakken kan worden beschreven. Vanaf de eerste experimenten op het lab van Rein tot en met het schrijven van dit nawoord heb ik ontzettend veel geleerd over de chemische aspecten van bodemkwaliteit, maar veel belangrijker, ook over de kwaliteitsaspecten van een goede werkomgeving. Ik heb het geluk gehad met veel mensen te mogen samenwerken binnen de vakgroep (of tegenwoordig sectie), maar ook daarbuiten. Graag wil ik hier de gelegenheid gebruiken om iedereen te bedanken.

In de eerste plaats wil ik Willem, m'n prof en dagelijks begeleider, bedanken. Je gaf me de ruimte om zelfstandig te werken, maar was altijd bereid mee te denken over interessante wetenschappelijke vraagstukken. Naast de vele inhoudelijke discussies was er veel tijd voor meer persoonlijke gesprekken. We gingen 6 weken naar Aberdeen om de contacten met Hans en David te leggen c.q. te onderhouden. Het weekendje met David, Jane en Trudie was erg bijzonder. De beklimming van de Ben Venu zal ik niet snel vergeten.

The collaboration with Hans and David was very pleasant. I have enjoyed the two visits to the Macauley Institute very much! Hans, je programmatuur geeft dit boekje meer muzikaal volume. Zonder Orchestra had dit boekje er niet gelegen, zonder de dirigent had ik de muziek nooit leren spelen! David's enthusiasm for the modeling of the organic acid adsorption has motivated me strongly. The hill walks at lunchtime and at midnight I will always remember. Thanks!

Op de vakgroep was het Tjisse die me altijd op de hoogte wist te brengen van de laatste ontwikkelingen op oxide gebied. Er waren echter ook minder plezierige zaken. Elke keer wanneer je een stuk voor me gecorrigeerd had schrok ik me rot. Alle lege stukken stonden vol met rode of blauwe inkt en soms waren er zelfs extra blaadjes toegevoegd vol met correcties en suggesties. Toch wil ik je daarvoor bedanken. De verhalen werden altijd stukken beter!

Zoals gezegd, het experimenteel werk heb ik met veel plezier gedaan op het lab van Rein. Ik kreeg daarbij veel hulp van Rein, Gerdien, Erik, Arie en Monique. Bedankt voor alle hulp en de leuke tijd op het lab! Daarnaast hebben een aantal studenten veel van het praktisch

werk van me overgenomen. Graag wil ik Joanne, Joris, Stefan, Maria, Tom en Ellen heel hartelijk bedanken voor de prettige en leerzame samenwerking.

Last but not least ben ik in de kelder aangekomen. Het is al door veel AIO's gezegd en voor mij ook zeer zeker waar; jullie hebben een belangrijke rol gespeeld in het plezier waarmee ik bij de vakgroep heb gewerkt!! Het gezamenlijke lunchen, de keren dat we na het werken in de kroeg belandden en niet te vergeten de zeilweekendjes en de trip naar Berlijn zal ik nog lang herinneren. Peter, Jeanine, Wendela, Henriette, Chris, Lipeng, Irene, Bart, Renske, Jacqueline, Eduardo, Romulo, Dirkje, Johan, Peter, Arie, Anke, Paul, Louise, Annemiek, Ram, Maria, Nicole, Rasoul, Maurits, Laura en Thomas bedankt voor de leuke tijd! Een aantal kelderbewoners wil ik nog even speciaal noemen. Allereerst m'n kamergenote Rikje. Het was leuk om een tijd met jou de kamer te delen. De wandelingen die er uit voortgekomen zijn hebben me veel aan het nadenken gezet! René, bedankt voor alle nuttige en onzinnige discussies die we hebben gevoerd! Ik durf te zeggen dat zonder jou inbreng de ins en outs van het CD-MUSIC model en ook de tv programma's van gisteravond me veel minder duidelijk waren geworden. Tot slot Leonard. Het was simpelweg erg leuk om een goede vriend te hebben rondlopen op het werk!

Ik heb lang genoeg rondgelopen in het scheikundegebouw. Tijd om de laatste woorden uit te spreken:

Hartstikke bedankt en tot ziens!

Jeroen

Levensloop

Jeroen Filius werd geboren op 12 maart 1971 in Putten. In 1989 haalde hij zijn VWO diploma aan het Christelijk College Groevenbeek in Ermelo. Daarna studeerde hij Milieuhygiëne met de specialisatie Bodem aan de Landbouwuniversiteit in Wageningen.
Tijdens zijn studie liep hij stage bij de British Geological Survey in Walingford, Engeland. Hij ronde zijn studie af in september 1995 met de afstudeervakken bodemhygiene en bodemscheikunde. Vanaf juni 1995 tot april 2001 werkte hij als assistent in opleiding bij de vakgroep Bodemkunde en Plantenvoeding van de Landbouwuniversiteit Wageningen (tegenwoordig sectie Bodemkwaliteit van de Wageningen Universiteit). Tijdens deze periode deed hij onderzoek naar de binding van organische stof aan metaal(hydr)oxiden. De belangrijkste resultaten van dit onderzoek zijn weergegeven in dit proefschrift.